A review on self-assembly of colloidal nanoparticles into clusters, patterns, and films : emerging synthesis techniques and applications

A Review on Self-Assembly of Colloidal Nanoparticles into Clusters, Patterns and Films: Emerging Synthesis Techniques and Applications

Rituraj Borah[1,2]✉, Karthick Raj AG[1,2], Antony Charles Minja[1,2], Sammy W. Verbruggen[1,2]

[1]Sustainable Energy, Air & Water Technology (DuEL), Department of Bioscience Engineering, University of Antwerp, Groenenborgerlaan 171, 2020 Antwerp (Belgium)

[2]NANOlab Center of Excellence, University of Antwerp, Groenenborgerlaan 171, 2020 Antwerp (Belgium)

✉Email: rituraj.borah@uantwerpen.be

Abstract

The colloidal synthesis of functional nanoparticles has gained tremendous scientific attention in the last decades. In parallel to these advancements, another rapidly growing area is the self-assembly of these colloidal nanoparticles into greater periodic arrangements. Firstly, the organization of nanoparticles into ordered structures is important for obtaining functional interfaces that extend or even amplify the intrinsic properties of the constituting nanoparticles at a larger scale. The synthesis of large-scale interfaces using complex or intricately designed nanostructures as building blocks, requires highly controllable self-assembly techniques down to the nanoscale. In certain cases, for example, when dealing with plasmonic nanoparticles, the assembly of the nanoparticles further enhances their properties by coupling phenomena. In other cases, the process of self-assembly itself is useful in the final application such as in sensing and drug delivery, amongst others. In view of the growing importance of this field, this review provides a comprehensive overview of the recent developments in the field of self-assembly of different nanostructures and their applications. For clarity, the self-assembled nanostructures are classified into two broad categories: finite clusters/patterns, and infinite films. Different state-of-the-art techniques to obtain these nanostructures are discussed in detail, before discussing the applications where the self-assembly significantly enhances the performance of the process.

1. Introduction

As the term itself suggests, self-assembly is a process of the autonomous organization of components into larger periodic structures without direct mechanical intervention. While self-organization is a ubiquitous phenomenon in nature at different length scales, in nanotechnology, self-assembly is a promising technique to build functional structures and interfaces from nanomaterials, molecules, and so on. The growing interest on self-assembly stems from the fact that it enables self-organization down to the nanoscale, whereas mechanical intervention is simply not possible. Thus, apart from the feasibility of unique spontaneously evolving structures that other synthesis/nanofabrication techniques cannot realize, self-assembly also promises an alternative economical nanofabrication technology.

While the thin-film techniques are the most technologically developed routes for the fabrication of nanostructures and nanostructured interfaces, there lie several challenges and intrinsic deficiencies in those methods. For instance, geometries that can be fabricated by atomic or molecular deposition followed by etching processes are typically limited to primitive planar geometries of a single element.[1] [2]. Thus, the applications that require complex geometries, facet-dependent chemistry, hybrid metal/metal and metal/metal oxide coupling, metal/metal oxide and organic coupling, etc., are not easily feasible with those techniques. In some fields, such as plasmonics, complex shapes such as 3D nanostars, helical nanostructures, nanocages, etc., are difficult to synthesize with conventional thin-film techniques.[3] Moreover, the fabrication of sub-30 nm structures with lithographic techniques is still a challenge. The self-assembly technique, on the other hand, is intrinsically free from these drawbacks. With the rapid advancement in the field of wet-chemical synthesis processes, nanostructures of complex geometry and composition with sizes going down to <5 nm (for instance, quantum dots) can be synthesized with relative ease and low cost.[4] [5] Self-assembly of such nanostructures as building blocks

to form functional interfaces provides greater flexibility to obtain complex structures inaccessible by lithographic techniques.

While self-assembly is a broad topic even within the field of functional materials, this review is particularly focused on the self-assembly of nanostructures (primarily nanoparticles of different shapes and sizes) and their applications. The primary criterion for a method to qualify as self-assembly in this article is straightforward: individual colloidal nanoparticles or nanostructures have to assemble collectively without direct mechanical intervention. In fact, mechanical assembly at nanoscale is an extremely difficult task. Thus, most nanoscale assemblies are either driven by an external driving force such as magnetic fields, thermal convection, electromagnetic irradiation, etc., or interparticle interactions such as electrostatic, van der Waal interaction etc., or a combination thereof. This review covers self-assembly of colloidal nanoparticles in general to broadly categorize two main classes of self-assembled structures: clusters and films. The synthesis/fabrication procedures of these two classes are discussed in different sub-sections categorized based on the primary driving mechanism of the assembly method. This review particularly focuses on the applications of self-assembled structures in different fields as well as the outlook on developing trends. Particular attention has been paid towards addressing the shortcomings in the existing reviews dealing with self-assembled nanostructures.[6] [7] Deng *et al*. covers self-assembled structures of anisotropic nanoparticles and their properties.[6] In the recent review by Rao *et al*., while the fundamental principles of self-assembly methods are discussed in depth, a critical discussion on the specific experimental procedures could not fit in the scope.[7] In this review, a comparative picture encompassing different well-established methods to obtain nanoparticle films and clusters are discussed with specific details of the experimental procedures to guide experimentalists in the lab. Next, the emerging applications of self-assembled clusters and films in presently important fields are discussed. Importantly, the term supraparticle has also been used by many for self-assembled clusters of nanoparticles. Some reviews have covered these supraparticle structures, with a focus narrowed down to specific structures and applications. [8] [9] [10] For example, Li *et al*. focuses on self-assembled structures formed due to inter-particle interactions and their biological applications.[8] While the article discusses the interparticle forces in details (also discussed briefly in section 2.1), the more advanced emerging techniques like light induced assembly, lithography assisted self-assembly and DNA origami have not been covered. In the end, all self-assembly processes are driven by interparticle forces or external force fields or a combination of both. However, discussing the experimental methods in details is important for researchers trying to explore them in the lab. Similarly, the mini-review by Piccinini *et al*. only covers simpler structures, leaving out the advanced techniques.[9] This review presents a holistic picture comparing different self-assembly techniques and the application of the self-assembled structures or the self-assembly process itself.

Classification of self-assembly. Generally, self-assembly of nanoparticles can enable the formation of countless complex structures, all the way from nano to macro scale. However, based on the present state of literature, one can divide self-assembled structures broadly into two classes. The first one encompasses finite clusters and patterns, or superlattices of such clusters. Self-assembled nanoparticle clusters of up to a few hundred nanometres in size are included in this class. Other patterns such as chains of nanoparticles or superlattices of nanoparticle clusters are also included here. In any case, the number of constituting nanoparticles or nanostructures should not be more than several hundreds. The second class of structures includes primarily nanoparticle films that are extended to “infinity” in two dimensions. In our general terminology, if the area of the nanoparticle array is infinitely larger than the thickness, it can be considered a film. In the specific context of photoactive nanoparticles such as semiconductor photocatalyst nanoparticles and plasmonic nanoparticles, an additional complementary definition of “infinitely large” area may be provided: if one of the dimensions extends to a length scale that is much larger than the incident light wavelength, then that dimension can be defined as the extension to infinity. For instance, a self-assembled 20 nm Au nanoparticle film of 1x1 cm^2 area irradiated by green light is perceived to extend to “infinity” in two dimensions in the sense that the size of the film in the order of 1 cm is much larger than the visible wavelength range in the order of 500 nm,

where the film finds its applications. While they are both obtained by self-assembly of nanoparticles, clearly, clusters (or patterns) and films are fundamentally different kinds of nanostructures. Films are nanostructured periodically, but they extend to macroscale. However, clusters are smaller structures that form from the assembly of individually well-defined pre-formed nanoparticles/nanostructures. Thus, clusters or patterns are still nano- or micro-structures. Due to this difference, the self-assembly methods and setups for clusters and films have significant differences. For instance, the formation of a nanoparticle film by self-assembly happens mostly at an interface. It may be a liquid-liquid, gas-liquid, solid-liquid or solid-gas interface. In contrast, self-assembled clusters may form both in the bulk colloidal phase or at an interface depending upon the technique. Similarly, in applications, the two kinds of self-assembled structures play fundamentally different roles. In biological applications, clusters may be useful even in intercellular functions due to their small size, whereas films may be more suitable for sensing or external therapeutic applications. Generally, the function of the individual nanoparticles is enhanced in individual clusters or nanoparticles of different functions can be combined in individual clusters for a synergistic effect. In nanoparticle films, the periodic arrangement may lead to the enhancement of the individual functionalities of the nanoparticles. These aspects are discussed in details later in the application section. In what follows, the synthesis methods of these two classes, clusters and films, are discussed in sub-classes defined based on the general synthetic procedures. First, the classification of self-assembled structures, their synthesis and application are summarized in **Figure 1** for a complete overview.

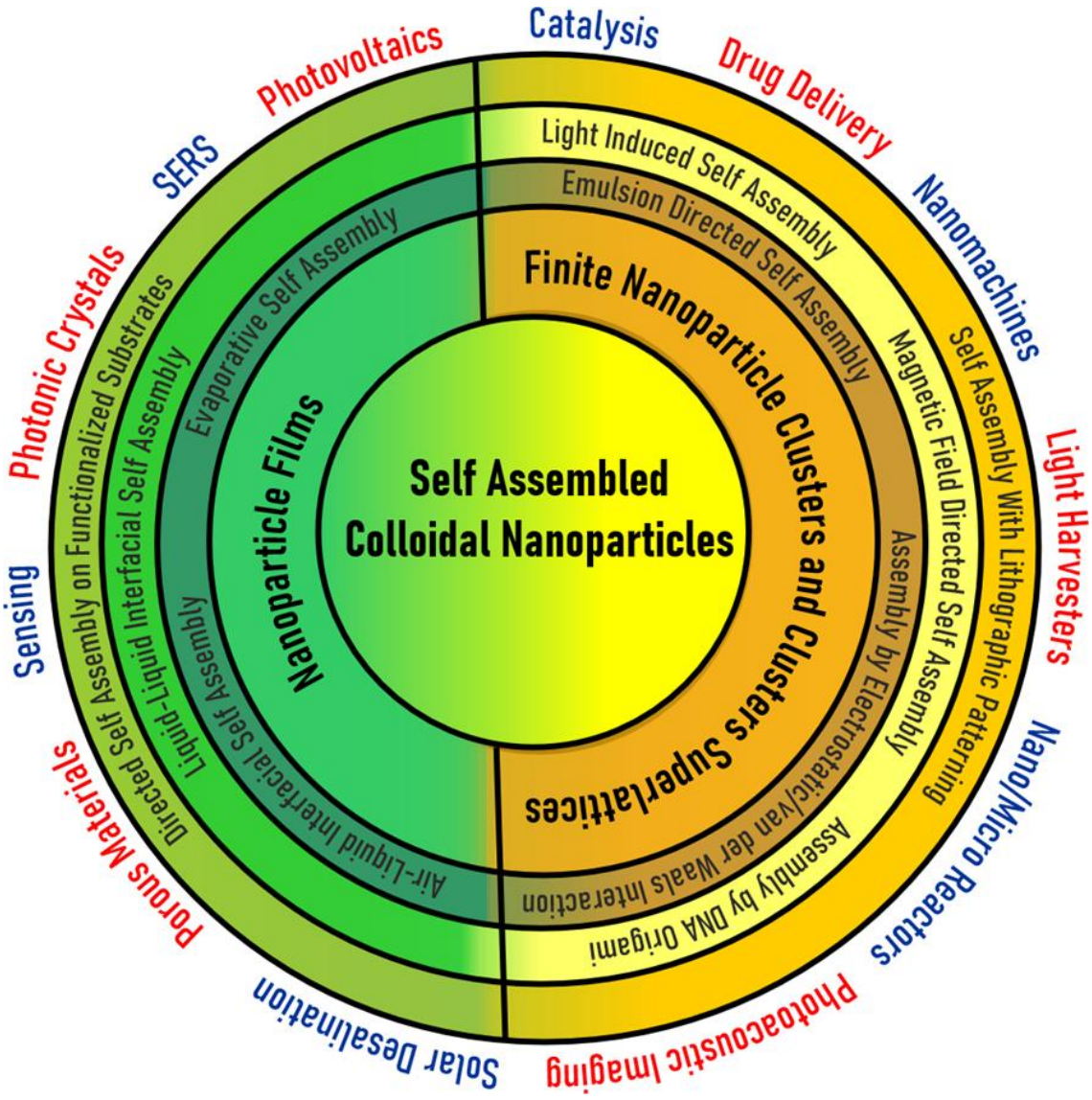

Figure 1. An overview of the classification of self-assembled nanoparticle structures. Broadly, self-assembled structures are divided into two categories: nanoparticle films and, nanoparticle clusters and clusters superlattices. For each category, the well-established synthesis techniques are highlighted. Different applications that are enhanced by self-assembly or self-assembled structures are highlighted at the outer boundary.

2. Emerging methods of self-assembly

2.1 Finite clusters and clusters superlattices

Self-assembled clusters of nanoparticles constitute a class of hybrid nanostructures that exhibit novel functionalities. The clustering often results in an enhancement of the functionalities or combination of different functionalities. For instance, clustering of plasmonic nanoparticles facilitate coupling of the individual plasmon modes of the nanoparticles to result in an enhancement in the light-nanoparticle interactions.[11] Similarly, the combination of a plasmonic nanoparticle with a catalytic nanoparticle results in clusters with photocatalytic functionality which is enhanced by the plasmonic component.[12] [13] However, uncontrolled aggregation of nanoparticles may lead to precipitation or polydisperse clusters, which is not desirable in most cases. In a colloid, as nanoparticles have high surface energy due to the small size, they tend to aggregate by Van der Waals attractive interactions. On the other hand, the surface charge repulsion or steric hindrance due to stabilizing surface molecules prevent the aggregation of the nanoparticles[14]. The DLVO (Derjaguin-Landau-Verwey-Overbeak) theory combines Van der Waals attractive force and electrostatic repulsive force due to the electric double layer (EDL) to predict the overall force between particles. The repulsive forces pose a barrier as electrical repulsive forces drop exponentially, while the Van der Waals forces decrease are inversely related to the square of the interparticle distance. It is the height of the energy barrier that determines if the collision energy can exceed it to promote aggregation.[15] The variation of pH and dissolved ionic solutes can thus easily lead to the point of zero charge (PZC) or zero zeta potential, which leads to fast aggregation of nanoparticles without requiring large supply of external energy.[16] This kind of clustering is perhaps the simplest assembly process as citrate (or even ligand stabilized) stabilized nanoparticles can be assembled by the addition of normal salt that neutralizes the zeta potential.[17] [18] [19] The field of self-assembly has evolved with different strategies to obtain more complex nanostructures with greater control. In what follows, different self-assembly methods to synthesize finite clusters of nanoparticles and cluster arrays are discussed.

2.1.1 ***Emulsion directed self-assembly.*** Emulsions can sustain micro-droplets of an oil-in-aqueous phase or the vice-versa (i.e. reverse emulsion). Thus, if the dispersed phase hosts colloidal nanoparticles, these nanoparticles can also be trapped in the microdroplets in colloidal phase, which upon drying can result in clusters or 3D assemblies of nanoparticles. Naturally, the main condition here is that the surfactant molecules can efficiently emulsify the two phases by assembling at the oil-water interface of the droplets, so that the nanoparticles remain inside the droplets. As shown in **Figure 2 (a)**, depending upon the nanoparticle concentration in the dispersed phase *i.e*. oil phase and the size of the dispersed phase droplet, the size of the nanoparticle clusters is determined. Similarly, for nanoparticles dispersed in an aqueous medium (or another polar medium), a reverse emulsion strategy needs to be adopted in order to trap the aqueous colloidal droplets in a hydrophobic (e.g. oil) phase.[20] [21] Usually, emulsion directed self-assembly can be quite straightforward. For example, Schmitt *et al*. demonstrated the formation of 3D dimensional clusters of small Au nanoparticles (~2 nm) through oil-in-water emulsions in a straightforward way, by simply mixing a thiol stabilized nanoparticle colloid in a non-polar medium (toluene, cyclohexane, dodecane, or hexadecane) with an aqueous solution of nonionic copolymer surfactant P123 (EO20PO70EO20, Pluronic BASF), **Figure 2 (b)**.[22] The role of the surfactant should be emphasized here, as Lacava *et al*. demonstrated that for Au nanoparticles and hexane-in-water systems, SDS and Triton X-100 were better than others in forming stable emulsions with the nanoparticles encapsulated in the dispersed phase. While Span 20 and Tween 85 resulted in

reasonably stable emulsions and significant entrapment of the nanoparticles at the oil-water interface was observed. In other cases, the formation of so-called Pickering emulsions can also result in ring-like assemblies upon drying.[23] Interestingly, the organization of colloidal particles in an emulsion droplet while forming a cluster is largely driven by thermodynamics, resulting in precisely defined shell structures for a certain number of particles. As demonstrated by Wang *et al*. using free energy calculations, colloidal clusters with specific "magic numbers" possess higher thermodynamic favourability than those without it, **Figure 2 (c)**.[24] The system finds it free energy minimum configuration, which is a icosahedral structure, through a complex pathway. A molecular dynamic simulation study for tens of thousands of nanoparticles shows that the icosahedral structure is unique to the packing at this length scale in contrast to long range FCC structures.[25]

Another possibility in the emulsion formation is that instead of nanoparticles being stable as a colloid in the micro-droplets, the nanoparticles can assemble at the oil-water interface taking the role of the emulsifier. The formation of such nanoparticle stabilized Pickering emulsions naturally leads to the formation of hollow nanoparticle assemblies, **Figure 2 (d)**.[26] Even ligand stabilized nanoparticles dispersed in oil (or water) phase can also get trapped in the interfacial barriers for the formation of the Pickering emulsions as the most thermodynamically favourable system, **Figure 2 (e)**.[27] Interestingly, with large particles, relatively small droplets of water can be permanently stabilized by Pickering emulsion of water in oil, **Figure 2 (f)** by careful control of the quantity of water. For a clear comparison, **Table 1** summarizes emulsion directed self-assembly procedures from different significant literature reports and the resulting structures. Ordinary emulsions normally result in closed packed 3D nanoparticle assemblies. Usually, hollow assemblies can be obtained from Pickering emulsions, if the dispersed phase is rapidly removed so that the nanoparticles at the interface do not gradually converge towards the centre during drying. Also, with larger Pickering emulsion droplets, keeping the hollow structure is easier. Naturally, obtaining a hollow structure also requires the encapsulated emulsion droplet to be free of other nanoparticles or nanostructures. Lin *et al*. showed that Pickering emulsion formation in the presence of nanoparticles of two different sizes (*i.e*. 2.8 and 4.6 nm CdSe nanoparticles) leads to the assembly of larger nanoparticles at the interface, while the smaller nanoparticles are encapsulated in the droplet.[28] In such a situation, core-shell kind of self-assembled structures are obtained. For a comparative overview, **Table 1** summarizes the methods reported in different important works in the past.

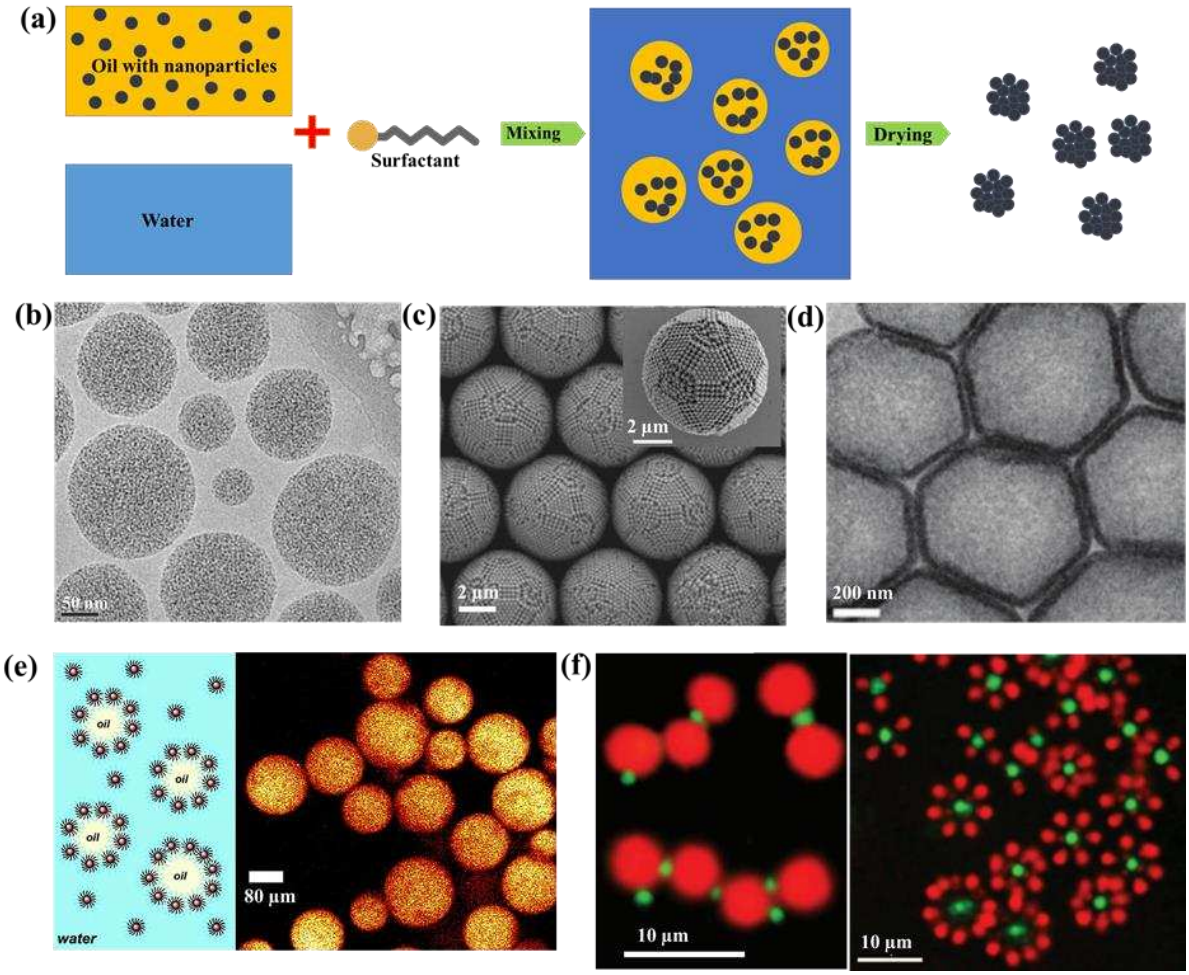

Figure 2. (a) General schematic representation of the emulsion-directed self-assembly of nanoparticles where the nanoparticles are assembled in the dispersed phase droplets. (b) Emulsion-directed self-assembled clusters of 2 nm small Au nanoparticles. Reprinted with permission[22] ©2016, American chemical society. (c) Formation of icosahedral clusters by polystyrene nanoparticles[24] ©2018 CC-BY 4.0. (d) Hollow assembly of 5.8 nm iron-oxide nanoparticles due to the formation of oil-water Pickering emulsion. Reprinted with permission[26] ©2016 John Wiley & Sons. (e) Pickering emulsion stabilized PEGylated Au nanoparticles. Reprinted with permission[27] ©2007, American chemical society. (f) Permanently assembled PMMA particles (radius 1.08 µm) in CHB-decalin at the oil-water interface in various configurations: free-floating spherical water droplets (green) surrounded by particles in hexagonal packing (left), and small water droplets (green) linking together PMMA particles (right).[29] © 2007, National Academy of Science.

Table 1. Summary of emulsion directed nanoparticle clustering or self-assembly procedures reported in selected literature.

Literature	Cont. phase/dispersed phase	Nanoparticle/shape/size/capping ligand	surfactant	Emulsion type	Unique feature
Lin *et al.*[28] (2005)	Toluene/water	CdSe/nanospheres/2.8 nm and 4.6 nm/Tri-n-octyl-phosphine-oxide (TOPO)	None	Pickering type, water-in-oil	Large nanoparticles at the interface, smaller ones encapsulated
Glogowski *et al.*[27] (2006)	Water/ethyl acetate or perfluorodecal	Au/nanospheres/5-8 nm/thiolated poly(ethylene glycol)	None	Pickering type, oil-in-water	Hollow clusters encapsulating

	in or 1,2,4-trichlorobenzene (TCB) or toluene				the organic phase
Leunissen *et al.*[29] (2007)	CHB-decalin/water	PMMA/microspheres/1.08 µm/poly(12-hydroxystearic acid	None	Pickering type, water-in-oil	Hollow assemblies encapsulating water.
Jiang *et al.* [30] (2008)	Water/paraffin wax	SiO_2/microspheres/3 µm/none	Didodecyldimethylammonium bromide	Pickering type, water-in-oil	Colloidosome structures
Cho *et al.*[31] (2009)	Both Water/toluene and toluene/water	Polystyrene/nanospheres/230 nm/none	Pluronic F108	Oil-in-water and water-in-oil	Closed packed clusters on drying
Qiu *et al.*[32] (2010)	Water/hexane	Fe3O4, CdS, and Au Nanoparticles/nanospheres/(3-15), 3 and 6 nm/oleylamine	CTAB and polymers such as poly(acrylic acid) (PAA), polyethyleneimine (PEI), poly(styrenesulfonate) (PSS)	Surfactant stabilized, oil-in-water	Closed packed clusters on drying
Wagner et al.[33] (2012)	Water/toluene	Polystyrene and SiO_2/nanospheres/154 and 33 nm/none	none	Pickering type Oil-in-water	Hollow clusters after calcination of polystyrene
Liu *et al.*[34] (2015)	n-butanol/water	Au/nanospheres/ 98 nm/ Poly(diallyldimethylammonium) chloride	None	Pickering type water-in-oil	Hollow closed packed colloidosomes
Park *et al.*[26] (2016)	Water/chloroform	Iron oxide, CdSe, Au/nanospheres/5.8, 4.4, 6 nm/oleic acid, oleylamine	CTAB	Pickering type, oil-in-water	Hollow assemblies
Koike et al.[35] (2018)	n-dodecane/ Water	Au-SU8 negative photoresist (amphiphilic Janus particles)/microtriangles/10 µm/none	None	Pickering type, water-in-oil	Hollow assemblies
Wang *et al.* [36] (2020)	Water/cyclohexane	CdSe, PbSe/nanospheres/7.7, 9.9 nm/oleyl amine	SDS	Oil-in-water	Binary icosahedral clusters

The obvious advantage of emulsion directed self-assembly is the scalability. Firstly, large volumes of nanoparticle colloids can be self-assembled into controlled clusters by the emulsification process, even in continuous operation. Secondly, large number of nanoparticles (e.g. hundreds) can be self-assembled into solid or hollow clusters by this methods. Also, for the combination of two or more types of nanoparticles, this method is more convenient than others . One important limitation of this method, however, is that the clusters can only have closed packed structures that are thermodynamically favourable. This limits the applicability of this method to more sophisticated or complex structures such as linear assemblies, helical assemblies etc., that are discussed in the following sections. Another important aspect which is relevant to such colloidal systems in general is the presence of excess ligands after self-assembly that are not useful in their applications. The removal of the ligands at the end is often an important step. With metal oxides, a calcination step or plasma treatment may be sufficient. While plasma etching is generally quite effective[37], calcination may not always be able to remove all the ligands especially in the case of self-assembled systems.[38] With non-noble metals or organic nanoparticles, selective etching or non-oxidizing plasma treatment is more useful to prevent oxidative/chemical degradation of the nanoparticles.[39] Similarly, electrochemical removal of the ligands can be quite promising in the cases where atmospheric exposure is to be avoided.[40] In the

specific case of photocatalytic nanoparticles, the ligands can be removed just by illumination of light as the ligands can be degraded by photocatalytic oxidation.[41]

2.1.2 ***Magnetic field directed self-assembly*****.** The primary criterion for nanostructures to be assembled under the influence of a magnetic field is that, obviously, the nanostructures should be responsive to magnetic forces. Thus, magnetic nanoparticles such as Fe_3O_4, Ni and Co, or hybrid nanoparticles with a magnetic component can be directed by magnetic fields towards self-assemblies with much ease, **Figure 3 (a)**.[42] As shown by Singh *et al.* in **Figure 3 (b)**, by applying an external magnetic field, a self-assembled monolayer of nanoparticles over diethylene glycol can be turned into an array of helical superstructures by the interplay of van der Waals and magnetic dipole-dipole interactions, Zeeman coupling, and entropic forces.[43] Taheri *et al.* demonstrated a similar approach for the self-assembly of iron oxide nanoparticles induced by an external magnetic field to form 1D nano-chains, monolayer sheets in 2D, and large 3D cuboids with internal ordering.[44] The self-assembly of the nanocubes can be elucidated considering the dipole–dipole interaction of small superparamagnetic particles. The importance of this work stems from the fact that the assembled iron oxide nanocubes are very small (~8.2 nm), which demonstrates the feasibility of the magnetic field directed self-assembly method even for such small nanostructures. Linear structures of magnetic nanoparticles are also interesting for various applications, as will be discussed later in the application section. Chong *et al.* showed the linear assembly of Fe_3O_4 nanoparticles and their protection by a silica shell that makes the assemblies mechanically robust and chemically resistant, **Figure 3 (c)**.[45] Another approach towards microscopic control of nanostructure assemblies by an external magnetic field is by microscopic variation of the magnetic field. As shown in **Figure 3 (d**), Demirörs *et al.* showed that periodic (periodicity 10 micron) magnetic moulds with Ni (~2 micron) islands over PDMS can selectively assemble magnetic microparticles with high efficiency (fidelity of the assembly ~97 %). A similar approach can be implemented with smaller magnetic nanoparticles for nanoscale assemblies in desired applications.[46] As demonstrated by Erb *et al.*, application of a magnetic field on a colloidal mixture of diamagnetic and paramagnetic particles in a magnetized ferrofluid results in the spontaneous formation of fractal clusters, **Figure 3 (e, f)**. While the particles in this work are of mm sizes, a similar phenomenon at nanoscale with nanoparticles remains as an interesting aspect to be investigated in the future. The primary advantage of magnetic field directed self-assembly is that the external field can be easily modulated to control the assembled structure. Also, in many applications, hybrid nanoparticles with a magnetic component can be easily separated after a process simply by a magnetic field.

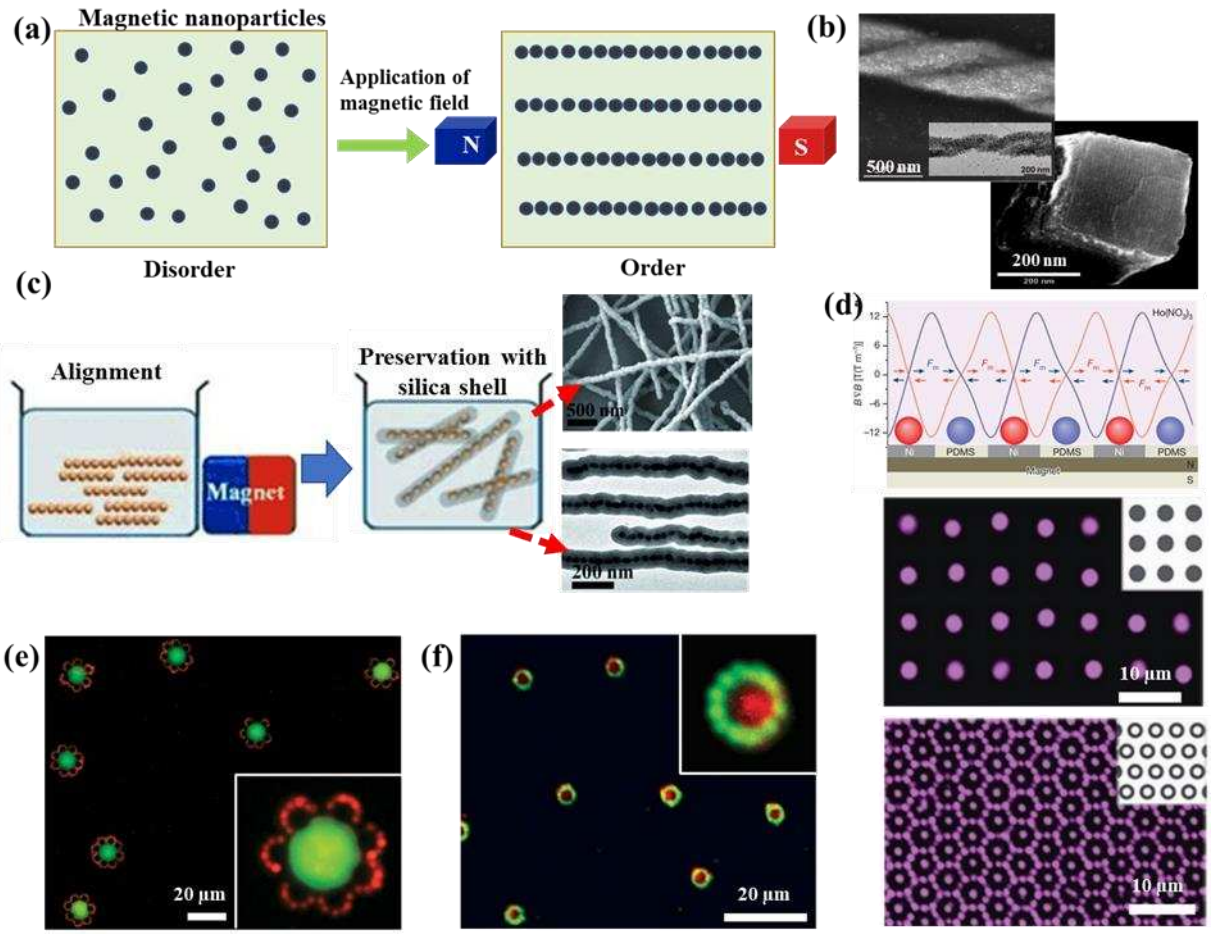

Figure 3. (a) General schematic representation of the magnetic-field directed self-assembly of nanoparticles. (b) Helical ribbons formed by the application of an external magnetic field on Fe_3O_4 nanocubes assembled on the DEG surface. Reprinted with permission[43] ©2014, AAAS. Magnetic-field-induced self-assembled 3D cuboid which consists of more than 10,000 iron oxide nanocubes. Reprinted with permission[44] © 2015, National Academy of Sciences. (c) Magnetic-field-induced linear assembly of Fe_3O_4 nanoparticles and protection by silica shell for stability. Reprinted with permission[45] © 2013 John Wiley & Sons. (d) Magnetic moulds with Ni and PDMS islands for variable magnetic field for directed assembly of particles (top), 2.85 mm magnetic particles in size assembled on a square grid of nickel islands (middle), 1.2 mm diamagnetic particles arrange in the PDMS voids of a hexagonal grid of nickel rings. Reprinted with permission[47] © 2013 Nature Publishing Group. (e,f) Rotationally symmetric fractal clusters form from non-magnetic particles (red and green) and paramagnetic core particles by the application of a magnetic field. Reprinted with permission[48] © 2009 Nature publishing group.

2.1.3 ***Assembly directed by DNA origami.*** Nanoparticle assembly mediated by DNA is inspired by the remarkable programmability of DNA molecules. The formation of nanostructures by DNA molecules itself is a vast field of research in itself.[49] The use of DNA molecules for nanoscale patterning was foreseen by Seeman back in 1982 when he presented the criteria for the formation of nucleic acid junctions by the maximization of Watson-Crick base pairing and the lack of sequence symmetry customarily found in living systems.[50] These junctions can be treated as the building blocks covalently linked together by linear DNA to form complex structures that can be templates for the organization of metal nanoparticles.[51] At the molecular level, the DNA-nanoparticle interaction occurs through functional groups that strongly interacts with the nanoparticles through ligand–receptor binding, physical grafting or covalent attachment.[52] For example, it was shown by Mirkin *et al.* that the

interaction of Au nanoparticles with DNA takes place through imine groups, as the electrons of the imine group are more available as compared to those from the amino group due to the delocalization of the electrons in the aromatic ring.[53] Then, by the use of thiolated oligonucleotides, Au nanoparticles are bound by a thiol-Au bond[54]. DNA directed self-assembly of nanoparticles into various sophisticated structures like oligomers[55], helix[56] [57], honeycomb[58], nanoparticle polymer[59], etc., has already been reported. Also, a number of reviews has covered these works that gained significant attention from the scientific community.[60] [61] Recently, Liu *et al.* showed a 2D supramolecular assembly of gold nanorods guided by DNA triangles and hexamers, **Figure 4 (a)** First, truncated-triangular DNA origami with edges of 80 nm and a thickness of 2.5 nm are obtained by self-assembly. Then, arbitrary edges of the DNA triangle can be stitched together through base pairings with a set of sequence-encoded DNA connectors to form hexamers. The assembly of the nanorods at deterministic locations on the origami then occurs through DNA base-pairing interactions. Another interesting work towards nanomotor applications is on the assembly of Au nanoparticles on DNA origami rings as shown in **Figure 4 (b)**.[62] The planetary nano-gearsets are formed by connecting two DNA origami rings and cross-linking two Au nanoparticles in between. Kim *et al*. demonstrated that photopatterning of DNA-directed Au nanorod self-assembled films is possible by the photothermal effect when illuminated by a laser[63]. As the illuminated spots heat up due to the photothermal effect, the disentanglement of the nanoparticles from the DNA linkage is possible by the application of a laser of sufficient intensity and suitable wavelength, **Figure 4 (c)**. DNA-directed large scale self-assembly also facilitates high structural control and porosity for catalytic applications.[64] While DNA facilitates the formation of sophisticated structures, the DNA itself does not have remarkable electrical, optical or thermal properties. Another important challenge of DNA directed self-assembly in commercial applications is the high price of DNA-based materials. Still, for certain niche applications, DNA-directed assembly can still be promising in view of the state-of-the-art.

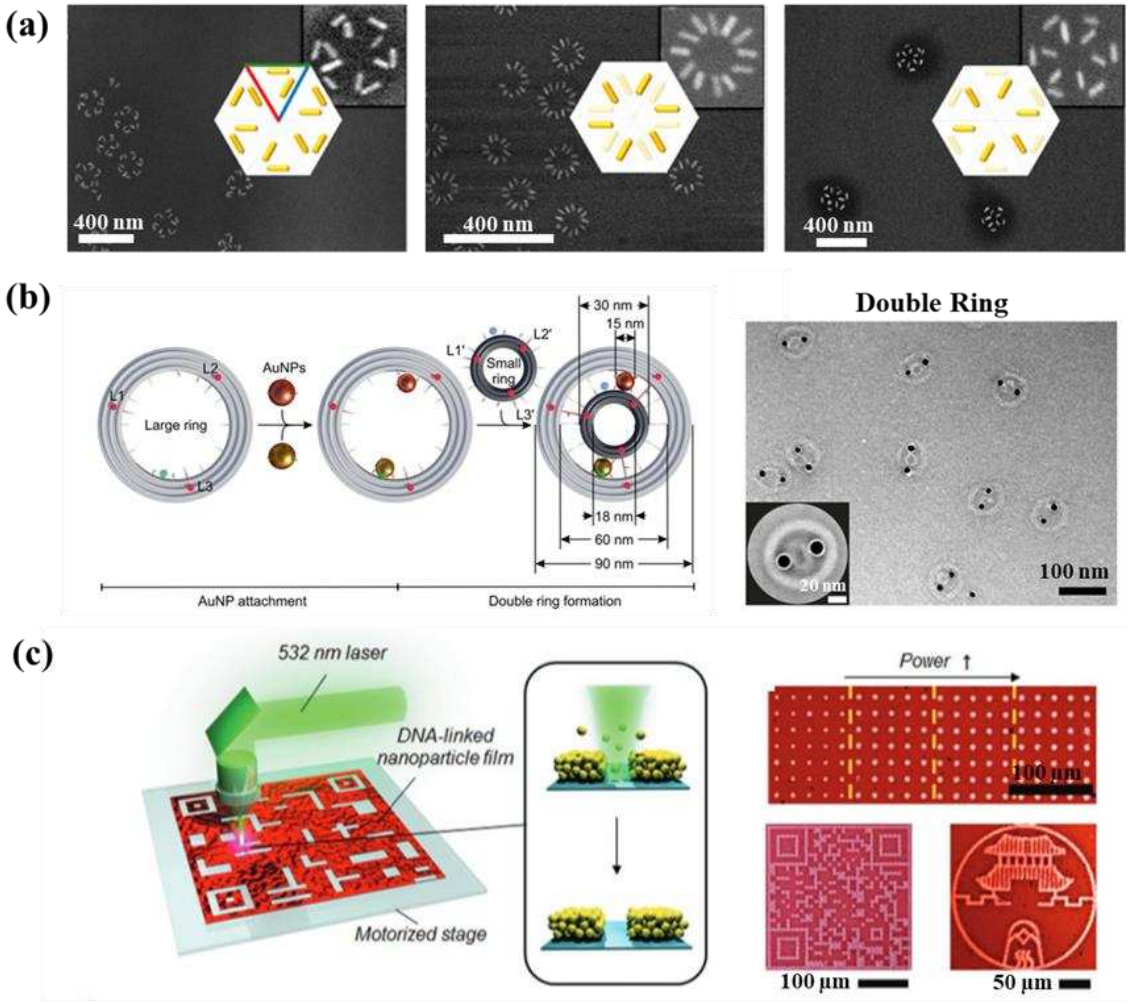

Figure 4. (a) Self-assembly of Au nanorods into deterministic patterns on DNA hexamer origamis. Reprinted with permission[65] © 2021, American Chemical Society. (b) Nano-gearsets by the self-assembly of two Au nanoparticles by cross-linking in between two concentric DNA origami nano-rings.[62]© 2022 CC-BY 4.0 (c) Photothermal nano-pattering of Au nanoparticle films obtained by DNA assembly. Photothermal heating of the illuminated spots facilitates unlinking of the nanoparticles. Reprinted with permission[63] © 2022 John Wiley & Sons.

2.1.4 ***Lithography assisted self-assembly*****.** The nanoscale fabrication of modern nanotechnology is mostly based on photolithographic techniques due to its versatility to produce a wide variety of patterns. Incorporation of lithographic techniques into self-assembly processes provides great flexibility in the variability of the nanoscale organization. Lithography can be used to fabricate patterned templates of nanoscale architectures for colloidal nanoparticle assembly.[66] The patterns for self-assembly can be composed of a soft mold (such as PDMS) or they can also be engraved onto the substrate. As shown in **Figure 5 (a)**, the fabrication of a soft PDMS template first requires the fabrication of a topographically structured Si master template.[67] The inverted pyramid patterned Si template in this case was produced by a direct laser writing lithography technique. The final soft PDMS mold facilitates the assembly of the colloidal Au nanoparticles into pyramidal clusters on a glass substrate. A concentrated Au nanoparticle colloid was drop-casted on the mold before covering with the glass substrate for the drying of the solvent phase. Similarly, Matricardi *et al.* prepared 2D Au nanoparticle assemblies by a similar procedure using PDMS soft molds, **Figure 5 (b)**.[68] Importantly, since the nanoparticles are well-dispersed in an aqueous phase, the substrate required hydrophilization by plasma treatment in order to enhance the nanoparticle-substrate affinity. Instead of using soft molds, the substrate itself can also be

patterned. Flauraud *et al*. showed that nanorods can be trapped in trenches patterned on a Si substrate during a capillary self-assembly procedure.[69] As shown in **Figure 5 (c)**, a concentrated control volume of Au nanorod colloidal solution was confined between a top plate and the low wetting patterned substrate so that a receding solvent/vapor interface is formed upon sliding the top plate. By heating of the substrate, solvent evaporation is induced at the wedge-shaped receding interface which also results in convective flow that drags the nanoparticles from the bulk to the interface. The flow induces concentration of nanoparticles in the wedge-shaped region and dynamically sustains the concentration against nanoparticle back-diffusion. The receding contact line drags the concentrated colloid zone over the substrate, and the nanoparticles escape the colloidal meniscus to get trapped in the trenches as shown in the inset. As shown in **Figure 5 (d)**, this technique is quite efficient in producing complex patterns of nanoparticles. In the assembly of anisotropic nanoparticles such as nanorods, the orientation of the particles is also important, especially in the case of plasmonic nanoparticles. As shown by Hanske *et al*., colloidal destabilization by varying the solvent composition leads to enhanced surface activity and partial aggregation of gold nanoparticles, which can be advantageous for creating homogeneous AuNR arrays. In the formation of nanorod clusters in soft PDMS molds, the presence of ethanol in the solvent promoted horizontal orientation of the nanorods in the clusters, **Figure 5 (e)**. Also, the average cluster height increases with an increasing concentration of the surfactant CTAB. Complete filling of the PDMA mold voids could be possible only above a minimum surfactant concentration.[70] Interestingly, the height of the assembly could also be controlled by the variation of the surfactant concentration. As shown in **Figure 5 (f)**, by increasing the CTAB concentration from 20 µM to 500 µM, the height of the assembly could be increased from 40 to 120 nm. An alternative approach can also be through photolithographic patterning on a self-assembled film. It has been shown that photolithography on a silica nanoparticle film followed by reactive-ion etching can produce different patterns[71]. In the combination of self-assembly and lithography, one is complimentary to the other as each technique has its merits and drawbacks. While self-assembly provides access to small and complex colloidal nanostructures, lithography enables the formation of complex patterns with a high degree of control.

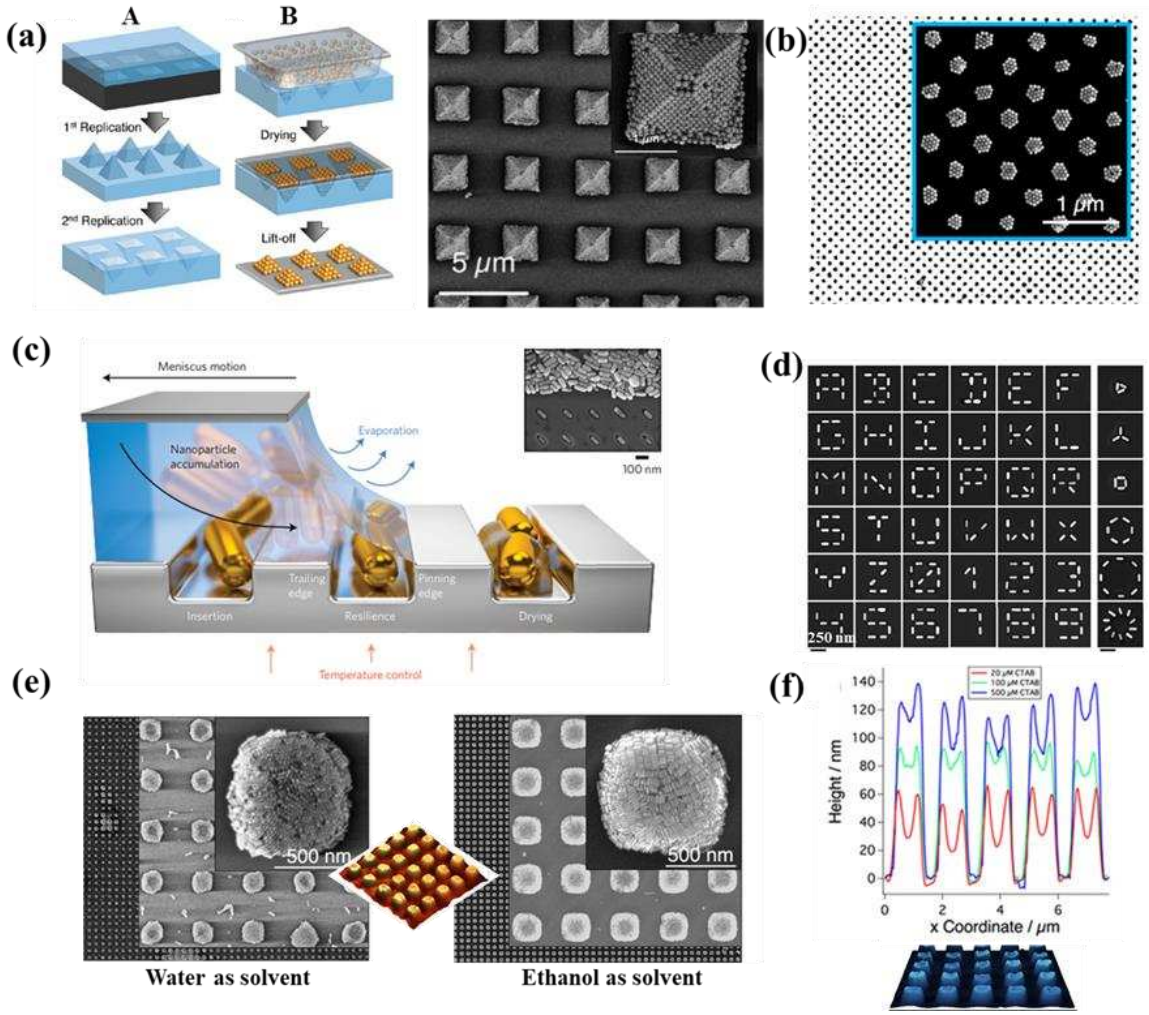

Figure 5. (a) Fabrication procedure of the PDMS soft mold from the Si master (A) and self-assembly procedure on substrate (B). The SEM image shows the pyramidal assemblies. Reprinted with permission[67] © 2017, American Chemical Society (b) 2D nanoparticle clusters from a soft PDMS mold. Reprinted with permission[68] © 2018, American Chemical Society (c) Capillary assembly processes of nanoparticles in nanoscale trenches engraved on substrate.[69] (d) Accuracy of the capillary assembly process in obtaining complex structures.(c-d) Reprinted with permission[69] ©2017 Nature publishing group (e) Presence of ethanol in the colloid resulted in more ordered clustering of nanorods in a soft PDMS mold.[70] (f) Increasing surfactant (CTAB) concentration increases the cluster height (red: 20 μM, green: 100 μM, blue: 500 μM of CTAB).(e-f)[70] © 2019 CC-BY 4.0.

2.1.5 ***Light induced self-assembly.*** In light-induced self-assembly, light is the energy input driving a certain chemical and physical process that results in the assembly of nanoparticles, **Figure 5 (a)**. If the nanoparticles themselves are not photoactive, the light driven processes affect the surface functionalizing molecules, solvent phase or separate photoactive entities present in the solution.

A simple example is light-induced zeta potential neutralization that can lead to the self-assembly of nanoparticles into clusters due to the absence of electrostatic stabilization.[72] Interestingly, hybridization in nanostructures has also led to both photo- and magneto-responsive nanostructures.[73] Similarly, if the solvent medium is photo-responsive, a light induced processes can lead to the assembly of nanoparticles that are stably dispersed. Kundu *et al*. demonstrated that the reversible light induced modulation of acidity (pH) of a medium is possible by photoconversion of a photo-responsive molecule. This change of pH results in zeta potential reduction by H^+ removal from the nanoparticle surfaces with COOH terminated ligands, thereby leading to clustering the nanoparticles, **Figure 6 (b)**.[74] Similar pH

sensitive Au nanoparticle clustering triggered by light was demonstrated by He *et al*. where Au nanoparticles functionalized with guanidiniocarbonyl pyrrole carboxylate zwitterion (GCPZ) molecules reversibly assemble at neutral pH due to surface charge minimization.[75] Naturally, light induced self-assembly can also be driven by just photosensitive surface ligands on the nanoparticles without any role of the solvent medium. When the particles are trapped at the air-liquid interface, re-arrangement of the particles can be induced by cis-trans photo-isomerization of photo-responsive surfactants. Shown for microparticles in **Figure 6 (c)**, such photosensitive surfactants allow dynamic switching of the particle organization between a highly crystalline (under light) and a disordered (in the dark) phase with a fast response time (crystallization in ~10 s, disassembly in ~1 min)[76]. Such an assembly-disassembly method can be applied for particles regardless of the size if they are trapped at the interface. Apart from the chemical routes, light induced assembly can also be driven by physical effects such as photothermal, Marangoni convection, optofluidic convection, near-field optical force, etc., because of the illumination.

Jaquay *et al*. have shown that the excitation of the resonance modes of photonic crystal arrays results in near-field patterns that give rise to optical forces that can drive colloidal nanoparticles to assemble into well-ordered patterns, **Figure 6 (d)**.[77] The resonantly-enhanced attractive optical force that drives the nanoparticles towards the photonic crystal interface is stronger than the inter-particle forces.[78] Alternatively, Jin *et al*. demonstrated that illumination on plasmonic colloidal nanoparticles (Au nanorods, nanostars, and nanospheres) results in photothermal convection that drives the nanoparticles to assemble at the point of illumination.[79] The size of the assembly can be increased by either increasing the intensity of light or the illumination time, **Figure 6 (e)**. Another photothermal route towards reversible self-assembly of nanoparticles is by the integration of a thermo-responsive component. For instance, poly-n-isopropylacrylamide (PNIPAM) -capped Ag–Fe_3O_4 heterodimers are thermally responsive as the PNIPAM chains above its low critical solution temperature (LCST) of 32 ^oC collapse due to immiscibility. Thus, the Ag–Fe_3O_4 heterodimers can be reversibly assembled and disassembled by changing the temperature with illumination that heats up the Ag part photothermally, **Figure 6 (f)**.[80]

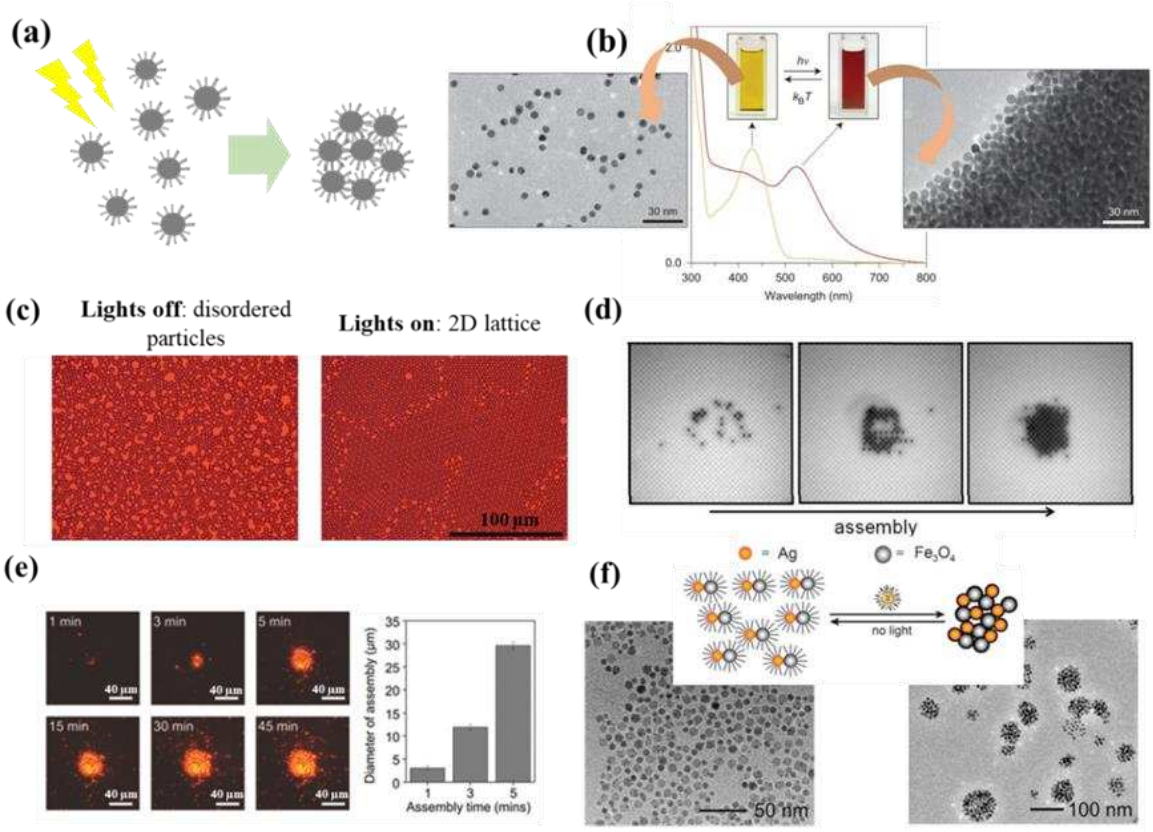

Figure 6. (a) Schematic of light assisted nanoparticle self-assembly by surface photo-chemistry (b) Self-assembly of COOH surface terminated nanoparticles by light-induced acidity regulation (pH). The acidity is regulated by merocyanine molecules (MCH^+) in the solvent that transform to spiropyran under visible light. Reprinted with permission[74] © 2015, Nature Publishing Group (c) Light induced self-organization of nanoparticles trapped at the air-liquid interface is also possible by cis-trans switching of a photosensitive surfactants (Trans-AzoTAB to cis-AzoTAB) at the interface. Reprinted with permission[76] © 2019 John Wiley & Sons. (d) Excitation of the resonance modes of photonic crystals gives rise to optical forces due to strong near-field gradients that induce nanoparticle clustering. Reprinted with permission[77] © 2013, American Chemical Society. (e) Intense illumination of nanoparticle colloids leads to photothermal convective currents that assemble the nanoparticles at single spot. Reprinted with permission[79] © 2018 John Wiley & Sons. (f) Thermo-responsive PNIPAM capped nanoparticles for assemblies when the temperature reaches the low critical solution temperature (LCST) of 32 ºC by photothermal heating, leading to immiscibility of the ligands and hence colloidal instability. The self-assembly process is reversible. Reprinted with permission[80] © 2013 Royal Society of Chemistry.

In conclusion of this section of self-assembled clusters and superlattices, we can state that colloidal self-assembled clusters are a unique class of materials that can be obtained through unique synthesis techniques. Thus, for similar structures, the techniques can differ from material to material depending upon the chemistry involved in the synthesis of the nanoparticles. Thus, only a subjective comparison can be drawn among the different techniques as shown in **Table 2**. For example, emulsion directed self-assembly generally cannot yield complex chiral structures from a few nanoparticles like DNA origami techniques. However, emulsion directed assembly is generally economical, scalable and easy. With regard to economy, both DNA directed assembly and lithography assisted assembly are expensive techniques due to the high price of DNA and conventional thin-film techniques. These aspects need to be taken into consideration while choosing any of these techniques for a certain application.

Table 2. A comparative summary of self-assembly methods to obtain finite clusters and cluster superlattices from colloidal nanostructures.

Self-assembly method	Accessibility to complex structures	Ease of the self-assembly procedure	Economy of the process	Scalability of the process
Emulsion directed self-assembly.	low	high	high	high
Magnetic field directed self-assembly.	low	high	high	high
Self-assembly directed by DNA origami.	high	medium	low	low
Lithography assisted self-assembly.	high	medium	low	medium
Light induced self-assembly.	low	high	high	high

2.2 Nanoparticle films

To obtain a film from colloidal nanoparticles, the intuitive and common method is naturally to drop-cast a concentrated solution of the nanoparticles on the desired substrate or to make a paste of the nanoparticles by adding binders. However, as will be discussed in **section 2.2.3**, drop casting inherently results in non-uniform distribution of nanoparticles. The preparation of a paste from a nanoparticle colloid also often results in random distribution of the nanoparticles and loss of functionality due to the presence of extra substances. On the other hand, in many applications such as photonic applications,

precise nanoscale order of nanoparticles is highly important as the functionalities are strongly dependent on the arrangement. Thus, well-controlled self-assembly techniques as discussed below had to be developed over the years and these techniques are under continuous improvement.

2.2.1 ***Air-liquid interfacial self-assembly***. Among different self-assembly based techniques that have been developed for the fabrication of nanoparticle thin films, air-liquid interfacial assembly has been the most widely investigated approach based on which commercial technologies have also been developed. These developments have been inspired by the original Langmuir-Blodgett technique for organic molecules which is extended to nanoparticles to obtain nanoparticle films.[81] This technique simply involves trapping of nanoparticles at the liquid-air interface which form a closed packed film when there are enough nanoparticles to cover the interfacial area available. As this technique is highly sensitive to the surface properties of the nanoparticles and the physicochemical properties of the subphase (the liquid used for the self-assembly), the process needs to be tailored for different nanoparticles synthesized by different methods. Thus, this technique is still being explored for further development towards more complex nanoscale arrangements and large scale applications.[82]

The common Langmuir-Blodgett trough design has a large area container (or trough) (for example, Kibron Microtrough G4 has a surface area of 930 cm^2) where the sub-phase (mostly water) is filled up to the top. The nanoparticles are introduced on the surface of this liquid to be trapped at the interface as shown in **Figure 7 (a)**.[83] The surface area over the liquid is then reduced by a movable barrier so that the surface area is exactly what is needed for the nanoparticles to form a closed packed monolayer film. The movable barrier in this design is very important for using water as the subphase as this allows surface pressure regulation. Due to the high surface tension of water, introduction of nanoparticles at the air-water interface of a fixed area results in increasing surface pressure that hinders free movement of the nanoparticles to form a continuous closed packed film. Thus, the barrier allows a large surface area in the beginning for a limited number of nanoparticles to move around freely in two dimensions and are gradually packed into a smaller area by the barrier sliding over the water surface. Also, the barrier allows for different packing densities in the film, **Figure 7 (a)**. Further, the barrier regulates the surface pressure during the transfer of the film to a substrate by vertical dipping. An alternative simpler setup for the air-liquid interfacial assembly consists of a low surface tension liquid (e.g., ethylene glycol, diethylene glycol, etc.) contained in a container so that the liquid surface, which is of fixed area unlike the setup discussed above, acts as the interface. This method has been used extensively by Murray *et al*., amongst others, to obtain self-assembled films over relatively smaller areas (up to a few cm^2) but also for more complex arrays such as multilayer films, binary nanoparticle films and so on.[84] [85] [86] The low surface tension liquid facilitates easier movement of the nanoparticles at the interface in the formation of the film without requiring external arrangements for the regulation of the surface area, **Figure 7 (b)**. Naturally, this method offers less control over the monolayer or multilayer formation. When the number of nanoparticles introduced over the subphase is exactly equal to what is needed to cover the entire surface, the film tends to be monolayer. With increasing number of nanoparticles over this limit, bi-layer or multilayers form at different locations of the films.[87] [88] Regardless of the subphase used, in air-liquid interfacial assembly procedures, nanoparticles that are synthesized in an aqueous medium have to functionalized with organic ligands to be dispersed in a volatile organic solvent. It stands to reason that the use of a non-polar solvent (e.g., hexane, toluene, chloroform, etc.) as the solvent of the nanoparticle colloid is convenient as the solvent stays separated from the polar subphase (water or glycols) due to the immiscibility. This requires the nanoparticles to be made dispersible in a non-polar phase, for instance via ligand exchange procedures. Usually, all the excess ligands present in the non-polar phase are removed before self-assembly. Griesemer *et al.* systematically investigated the effect of the excess ligands on film formation to show that a certain excess ligand concentration inhibits the wrinkling and folding of the film during compression, which is beneficial to the film quality. Also, the interparticle distance slightly increases with increasing excess ligand concentration, **Figure 7 (c)**.[89] For nanoparticles stably dispersed only in polar solvents, Nie *et al*. provided a solution by demonstrating that nanoparticles dispersed even in a polar phase (PVP coated

Au nanoparticles in ethanol) can spread over a water surface without mixing when the nanoparticles are introduced as an aerosol by electro-spraying, **Figure 7 (d)**.[90] After nebulization, the solvent in the tiny colloid droplets evaporates rapidly resulting in trapping of the nanoparticles at the air-water interface. In fact, complete hydrophobization of the nanoparticles is not a requirement to trap the nanoparticles at the interface. As Moon *et al*. showed, nanoparticles can be trapped at the interface by reducing the compatibility of the colloidal dispersion phase to water, increasing the particle concentration in the colloid, reducing the zeta potential of the colloidal particles, adding a salt (NaCl) in the suspension, and utilizing soft particles. Morag *et al*. showed another interesting possibility by adding elaidic acid and myristyl alcohol to thiol-coated Au nanoparticles to obtain network-like Au nanoparticle films with polygonal myristyl alcohol domains, **Figure 7 (e)**.[91] Elaidic acid, on the other hand, is added for solubilizing Au NPs at the air/water inter-face at the operating temperature.

As the air-liquid interfacial assembly can yield well-ordered nanoparticle layers, this high control over the arrangement also facilitates the formation of more complex structures. For example, a layer-by-layer approach to stack nanoparticle films can result in multilayer films, **Figure 7 (f)** and **(g)**. Also, multi-layered structures can be obtained with desired structural properties in each layer.[92] Similarly, mixing different nanoparticles in the colloidal phase results in a well-ordered distribution of the nanoparticles in the films. For example, mixing nanoparticles of two different sizes in different ratios leads to the formation of different binary lattices, **Figure 7 (h)**. Again, mixing nanoparticles of different shapes and materials can make more compositional and structural complexities possible. For a quick overview, **Table 3** summarizes the setups used for air-liquid interfacial self-assemblies in a selection of representative studies.

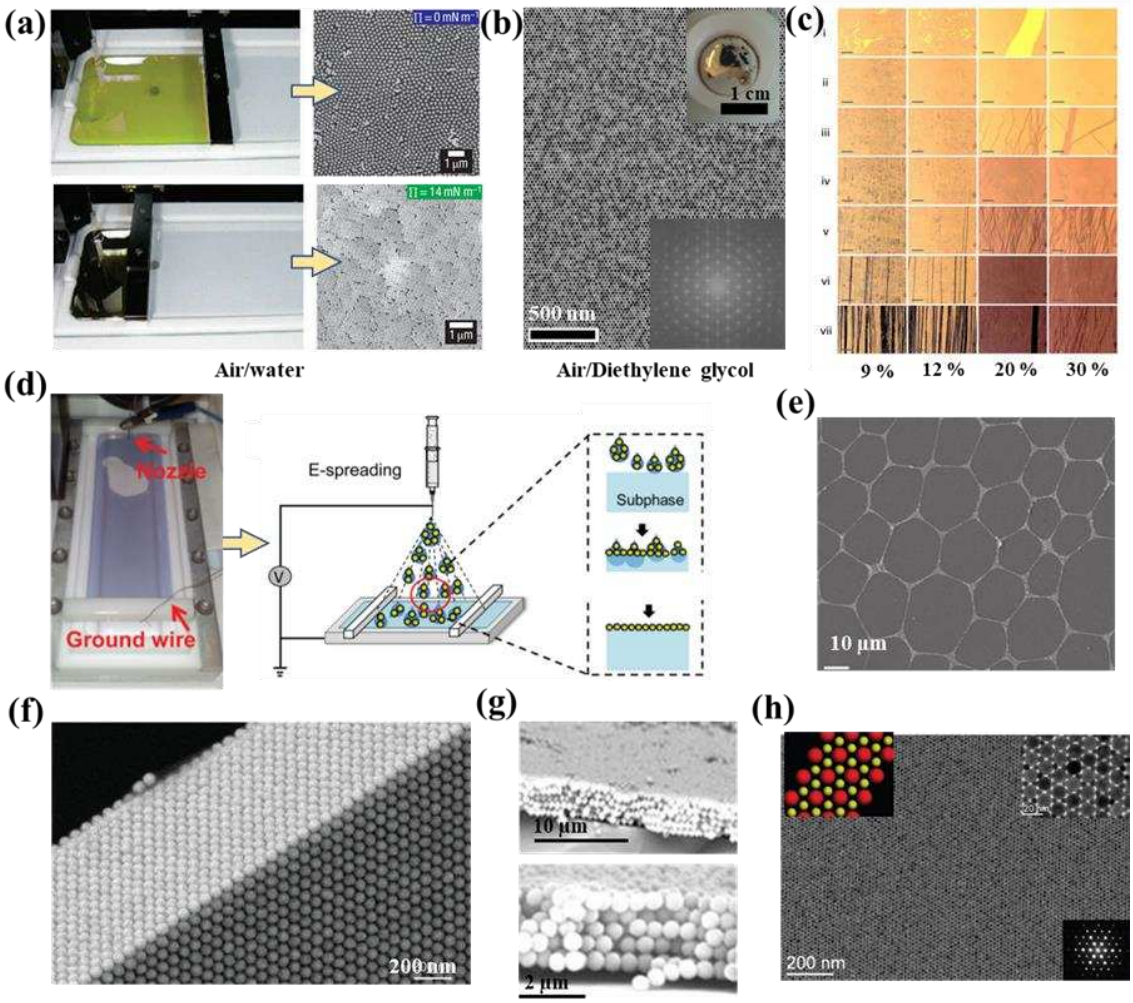

Figure 7. (a) Ag nanoparticles self-assembled at the air-water interface using a Langmuir-Blodgett trough setup, the movable barrier can compress the film towards higher packing density. Reprinted with permission[83] © 2007, Nature Publishing Group (b) Au nanoparticles self-assembled at a fixed air-diethylene glycol interface[93] © 2020 CC-BY 4.0. (c) The presence of excess ligands at the interface inhibits wrinkling and folding of the nanoparticle film during compression. Reprinted with permission[89] © 2017 Royal Society of Chemistry (i-vii: different stages of compression for different ligand concentrations) (scale bar: 40 μm). (d) Nie *et al*. showed that nanoparticles dispersed in polar solvents (e.g. ethanol) can also be trapped at the air-water interface by nebulization with electro-spreading. Reprinted with permission[90] © 2015, American Chemical Society (e) Network-like assemblies can be obtained by adding myristyl alcohol that forms polygonal domains. Reprinted with permission[91] © 2011 John Wiley & Sons. (f) Multilayer Au nanoparticle film obtained at the air-liquid interface. Reprinted with permission[87] © 2020 Nature Publishing Group (g) Multilayer 300 nm silica nanoparticle film obtained by layer-by-layer deposition of air-liquid self-assembled nanoparticle monolayers[92] © 2016 Optica Publishing Group (h) Self-assembly of a mixture of 15-nm Fe_3O_4 and 6-nm FePt nanocrystals at the air-liquid interface results in binary assemblies. Reprinted with permission[85] © 2010, Nature Publishing Group.

Table 3. Summary of air-liquid interfacial self-assembly procedures reported in selected literature.

Literature	**Subphase**	**Nanoparticle/shape/Approx. size/capping ligand**	**Nanoparticle solvent**	**Set-up description/unique feature**	**Film quality**
Kim *et al*.[94] (2001)	water	$BaCrO_4$/nanorod/20 nm length, 5 nm dia./dioctyl sodium sulfosuccinate (AOT or Aerosol-OT)	isooctane	Commercial Nima Technology M611 LB trough with surface pressure regulation.	Nanorod monolayer with unidirectional alignment
Song *et al*.[95] (2005)	water	Pt/nanocubes, cuboctahedra, and octahedra/9-10 nm/	Chloroform	Commercial Nima Technology M611 LB trough	Randomly packed monolayer
Tao *et al*.[83] (2007)	water	Ag/truncated cubes, cuboctahedra, and octahedra/120, 150 and 250 nm/PVP	Ethanol-chloroform (1:100 ratio)	Commercial KSV Nima 611 LB trough	Several cm^2 closed packed film
Dong *et al*.[85] (2010)	Diethylene glycol	Binary mixture of Fe3O4 and FePt/ nanospheres/15 and 6 nm/oleylamine	Hexane	A Teflon well with glass cover for slow evaporation	Binary nanocrystal superlattices.
Martin *et al*.[96] (2010)	Toluene (droplet)	Au/nanospheres/3.2 to 5.2 nm/1-dodecanethiol	Hexane	A droplet of Toluene on substrate was used as a subphase.	Closed packed monolayers of several mm^2 area.
Moon *et al*.[97] (2011)	Water	Polystyrene, SiO2, pNIPAm, Ag, Au /nanospheres/ 500, 700, 45,40/PS, SiO2, pNIPAM: no ligand, Ag, Au: PVP	Ethanol, Butanol, Isopropanol	Water contained in a petri dish was used as an interface. The nanoparticles were introduced carefully on the surface.	Closed packed large area (several cm^2) films
Xiong *et al*.[98] (2013)	Water	Au and Fe_2O_3 binary mixture/nanospheres/ 5 nm and 13.4 nm/1-dodecanethiol	Toluene with dissolved PMMA	A PMMA polymer layer over water induces contact line pinning for the formation of closed packed assembly.	Closed packed binary lattice.
Nie *et al*.[90](2015)	Water	Au/nanosphere/50 nm/PVP	Ethanol	Nebulization of nanoparticle colloid by electrospraying on water surface (LB trough).	Several cm2 monolayer films.

Schulz *et al.*[93]	Diethylene glycol	Au nanoparticles/spheres/25 nm/Thiolated polystyrenes (PSSH)	Toluene	A HDPE well (ID ~1.1 cm, max. vol 1.0 ml) to containing the subphase and glass cover for slow evaporation.	

*The content in the third column separated by / is the respective order in the cases two or more kinds of nanoparticles are included.

2.2.2 ***Liquid-Liquid interfacial self-assembly***. Since Yogev and Efrima[99] first reported on solid-like Ag films at the interface between two immiscible liquids, liquid-liquid interfacial self-assembly has become a well-established robust procedure. The main advantage of the liquid-liquid interfacial assembly is that hydrophilic nanoparticles dispersed in a polar phase can be directly self-assembled without the requirement of any ligand functionalization.[100] Conversely, as shown by Lin *et al*., hydrophobic nanoparticles like CdSe can also be directed to self-assemble at the water/toluene interface.[28] In liquid-liquid interfacial assembly, the two liquids should have sufficient difference in polarity to remain immiscible, like water and oil. As shown in **Figure 8 (a)**, the contact angle, *i.e*., the wettability, of the nanoparticles with respect to the oil and water determines whether self-assembly is possible or not. Normally, an intermediate contact angle (θ ~ 90^o) results in the assembly of the nanoparticles at the interface. The intermediate conditions between hydrophilic and hydrophobic limits characterized by θ in **Figure 8 (a)** can in fact be measured if the particles are not too closely packed. Isa *et al*. demonstrated that the contact angle for a single nanoparticle at the interface can be measured using freeze fracture shadow-casting cryo-scanning electron microscopy, **Figure 8 (b)**.[101] Reincke *et al*. showed that by gradually varying the surface charge density of the nanoparticles, the contact angle can be varied, **Figure 8 (c)**.[102] Without adding ethanol, the nanoparticles remained in the water phase, due to their high surface charge, when a separate heptane phase was added and vigorously mixed. They showed despite being a stable colloid after ethanol addition, when the non-polar heptane phase was introduced on the top of the water-ethanol surface, the nanoparticles immediately assembled as a film at the interface. A similar approach was also adopted by the same authors via pH reduction from 9 to 2 by 1 M HCl addition to water that induced migration of Au nanoparticles to the liquid-liquid interface.[103] Interestingly, upon the restoration of the pH by NaOH addition, large 16 nm nanoparticles dissolved back to the water phase but the smaller 9 nm particles remained at the interface. It was proposed that 4-mercaptobenzoic acid capped nanoparticles smaller than 10 nm stably attach to the oil-water interface while larger nanoparticles attach reversibly. When the hydrophobization of the nanoparticles by surface ligands is not strong enough for the nanoparticles to be able to cross the barrier from polar to non-polar medium, the nanoparticles get trapped at the interface. Thus, alkanethiol coated Au nanoparticles can also be self-assembled at the oil-water interface with a high packing density, **Figure 8 (d)**.[104] With anisotropic nanoparticles, the liquid-liquid interfacial assembly can yield an ordered assembly as shown by Mao *et al*. for PVP coated Au nanorods, **Figure 8 (e)**. As PVP is a water soluble polymeric stabilizer, it creates an intermediary surface potential required for interfacial trapping.[105] Other materials, for instance sulphonated graphene sheets (GSs) can be self-assembled at the hexane/water interface in-spite of their thin sheet-like structure, **Figure 8 (f)**.[106] While nanoparticles spontaneously migrate from the bulk to the liquid-liquid interface, the direct injection of nanoparticles at the interface has been shown to yield more efficient trapping of nanoparticles. As shown in **Figure 8 (g)**, this requires the free end of the capillary carrying the nanoparticles only to touch the interface by capillary forces. [107] [108] This direct injection makes the self-assembly of nanoparticles irrespective of size. As larger nanoparticles have larger energy barriers to cross to get trapped at the interface, direct injection gets past the barrier by introducing the nanoparticles directly at the interface. While it is a promising technique, the main challenge faced by experimentalists while performing liquid-liquid interfacial assembly is the difficulty to transfer the self-assembled film onto a substrate. The summary of different significant reports on liquid-liquid interfacial assembly is provided in **Table 4**.

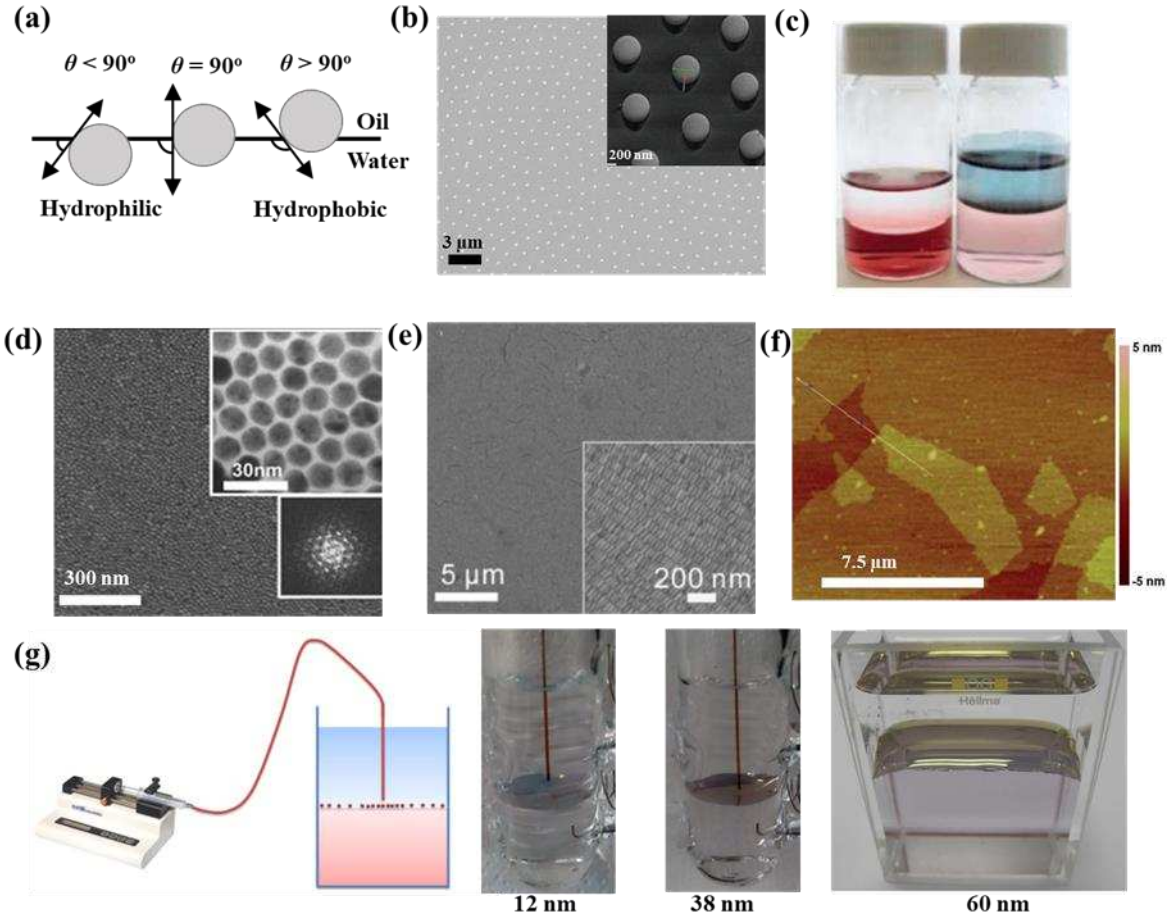

Figure 8. (a) General schematic of nanoparticle entrapment at the liquid-liquid interface according to their wetting properties. The midway between hydrophilic and hydrophobic conditions, $\theta = 90^{o}$ favours the assembly of the nanoparticles at the interface. (b) Spontaneous self-assembly of 16 nm Au nanoparticle film at the heptane/water interface by ethanol addition[101] © 2011 CC-BY-NC-SA. (c) Self-assembled monolayer of alkanethiol coated Au nanoparticles at water-hexane interface. Reprinted with permission[102] © 2004 John Wiley & Sons. (d) Low-magnification image of amidine latex particles at the n-decane/water interface, measured the single nanoparticle contact angle at the interface by freeze fracture shadow-casting cryo-scanning electron microscopy. Reprinted with permission[104] © 2007, American Chemical Society. (e) cyclohexane/water Interfacial self-assembly of PVP coated Au nanorods. Reprinted with permission[105] © 2018 John Wiley & Sons. (f) AFM image of sulphonated graphene sheets (GSs) self-assembled at the hexane/water interface. Reprinted with permission[106] © 2011 Royal Society of Chemistry. (g) Girault *et al* showed that direct injection of the nanoparticles by a capillary tube at the interface leads to efficient trapping of the nanoparticles. The free end of the capillary only touched the interface by capillary forces. The Figure shows assembly of nanoparticles of three different sizes by this method. Reprinted with permission[107] © 2015, American Chemical Society.

Table 4. Summary of Liquid-Liquid interfacial self-assembly procedures reported in selected literature.

Literature	Liquid phases (top/bottom)	Nanoparticle/shape/size/ capping ligand	Colloid solvent	Set-up description	Film quality
Reincke *et al.*[103]	Heptane/water	CdTe and Au/nanospheres/(2.8-4) and (6 and 16) nm/ mercaptocarboxylic acids	water	1 M HCl was gradually added to induce migration of the nanoparticles to the interface by the	Not known.

		and 4-mercaptobenzoic acid		reduction of the pH from 9.	
Park *et al*.[104] (2007)	Hexane/water	Au/nanospheres and nanorods/13 nm and Length:40/ dia:9.6/citrate and CTAB	Water + ethanol	Upon ethanol addition to the water phase, the nanoparticles migrate to the interface to attach to thiol ligands in the hexane phase.	Closed packed with metallic appearance.
Ren *et al*.[109] (2012)	Chloroform/water	NaYF4:Yb,Er/nanoplatelets/78 nm wide and 37 nm thick/ oleic acid	Chloroform	Ethanol was added to chloroform to induce the migration of the nanoparticles to the chloroform/water interface.	Closed packed films.
Fang et al.[108] (2013)	Heptane + 1,2-dichloroethane/water	Au/nanospheres/nanosphere/60 nm/none	Ethanol + water	Nanoparticles were introduced close to the interface by a syringe pump.	Closed packed film with metallic appearance.
Jia *et al*.[106] (2014)	Hexane/water	Sulphonated Graphene/nanosheets/NA/ none	Water + ethanol	Ethanol dispersed nanosheets were introduced to water for spontaneous migration to the interface.	Continuous films.
Velleman *et al*.[110] (2016)	Water/1,2-dichloroethane (DCE)	Au/nanospheres/12.8 nm/12-mercaptododecanoic acid (MDDA)	Water	Spontaneous Interfacial assembly was induced by changing ionic strength of either the water or DCE phase with NaCl and Tetrabutylammonium (TBA)/ tetraphenylborate (TPB) respectively.	Packing density varied by salt/electrolyte conc.
Chai *et al*.[111] (2017)	Water/toluene (with PDMS-NH_2)	SiO2/nanospheres/13 nm/none (COOH terminated)	water	Spontaneous Interfacial assembly was induced by changing ionic strength of water with NaCl.	
Sebastian *et al*.[112] (2017)	Hexane/water	Ir/nanospheres/1-2 nm/none	Ethanol	Nanoparticles were introduced close to the interface by a syringe pump.	Closed packed film.
Mao et al.[105] (2018)	Cyclohexane/water	Au/nanorod/Length ~ 50, dia ~10 nm/PVP	Ethanol	Nanoparticles were introduced close to the interface.	

2.2.3 ***Evaporative self-assembly***. Although the evaporation process of the solvent is also an important step in other self-assembly processes such as air-liquid and liquid-liquid interfacial assembly, this sub-section targets self-assembly processes where the evaporation of the solvent takes place on the substrate during the actual film formation. It is common knowledge that simple drop casting of nanoparticle colloids to form homogeneous films on horizontal substrates is limited by the so called "coffee ring effect" that spontaneous drives the particles to accumulate at the liquid-solid-air contact line during drying, **Figure 9 (a)**.[113] The higher rate of solvent evaporation at the contact line induces replenishment by capillary flow from the bulk liquid of the droplet resulting in an outward flow that leads to the accumulation the particles at the contact line.[114] As shown in **Figure 9 (b)**, slow droplet evaporation by the control of relative humidity and temperature leads to reduced Marangoni flow and hence to the formation of more uniform assemblies.[115] As summarized by Mampalli *et al*., different strategies such as contact line pinning, disturbing of capillary flow, trapping solute and so on, have been adopted for

the suppression of the coffee ring effect.[116] [117] Interestingly, Bigioni *et al*. could produce Au nanoparticle monolayers as shown in **Figure 9 (c)** even with rapid solvent evaporation and attractive particle-particle interaction.[118] However, the pinning of the contact line at the edge of substrate during the drying process was important in the process. An interesting strategy adopted to avoid the coffee ring effect during drop-let drying is by introducing the nanoparticles on the surface of the drying droplet so that the accumulation from the bulk can be avoided.[96] For stable contact line pinning in such strategies, the substrate can be chemically pre-treated, for instance, with dopamine.[119] Importantly, the coffee ring effect is a dynamic phenomenon particular to droplet drying, especially on a smooth horizontal surface. As shown by Dimitrov and Nagayama, drying of a colloid next to a vertical wall is a simple yet effect evaporative self-assembly process as the liquid-solid contact forms a thin liquid film for fast evaporation and replenishment. Thus, the nanoparticles in the fast-evaporating liquid film spontaneously form a film on the vertical surface while the nanoparticles continuously migrate to the contact line, **Figure 9 (d)**. Miyahara and co-workers have reported extensively on the different parameters governing the nanoparticle assembly from a drying liquid on an adjacent vertical substrate.[120] [121] They showed that only above a certain nanoparticle volume fraction ($\phi > 10^{-3}$) in the colloid, continuous nanoparticle films form at the liquid-solid contact points, while at a lower concentration regime ($\phi < 10^{-4}$), nanoparticles form horizontal strips.[122] Interestingly, controlled evaporative assembly can be used to produce complex structures like binary assemblies as well. As shown in **Figure 9 (e)**, by mixing nanoparticles of two different sizes, complex binary assemblies of different configurations such as superlattices with AB, AB_2, AB_3, AB_4, AB_5, AB_6, and AB_{13} stoichiometry, and cubic, hexagonal, tetragonal, and orthorhombic symmetries could be obtained.[123] Further sophistication by including more nanoparticle sizes and shapes is a promising way forward. Another effective strategy is to create a thin film of the colloidal solution by capillary force so that the evaporation from the thin film region will lead to the formation of a closed packed nanoparticle film while the nanoparticles from the bulk will continuously replenish the evaporating region, **Figure 9 (f)**.[124] This is similar to evaporative self-assembly on a vertical substrate as in this case also the solvent evaporate form the meniscus where the layer of the solvent is thin leaving behind the nanoparticles. The evaporation can also be controlled by microstructures on the substrate. For example, over a substrate with ~300 nm large dome-like structures, a 30 nm nanoparticle colloid dries in a way that the nanoparticles assemble around the domes in satellite-like structures, **Figure 9 (g)**.[125] For comparison and overview, **Table 5** summarizes the main features of evaporative self-assembly techniques reported in important literature.

Table 5. Summary of evaporative self-assembly procedures reported in selected literature.

Literature	**substrate**	**Nanoparticle/shape/size/capping ligand**	**Nanoparticle solvent**	**Set-up description/unique feature**	**Film quality**
Jiang *et al*.[126] (1999)	Glass slide	SiO_2/nanospheres/200 - 700nm/none	ethanol	The substrate glass slides were dipped vertically into an ethanol colloid for slow evaporation.	Monolayer or multiplayer films according to particle size and volume fraction.
Shevchenko *et al*.[123]	TEM grids or silicon nitride	PbS, PbSe, CoPt3, Fe2O3, Au, Ag, and Pd/nanospheres/3.4 to 13.6 nm/thiol, amines and oleic acid	Toluene and mixtures of toluene with tetrachloroethylene or chloroform	The substrates were dipped in the colloidal solutions contained in a tilted vial.	Binary superlattices depending upon the nanoparticle composition in the colloid.
Bigioni *et al*.[118] (2006)	Si_3N_4 substrate (3 mm×4 mm)	Au/nanosphere/6 nm/1-dodecanethiol	Toluene	A nanoparticle colloid droplet is deposited on the substrate so that liquid-solid substrate contact line pinning is fixed at the edge.	Closed packed monolayer films.

Ku *et al.*[127] 2011	400-mesh copper carbon-coated grids	Co/nanospheres/10 nm/oleic acid	1,2-dichlorobenzene	The substrate grid was dipped in a concentrated colloid for slow drying.	Intricate spatial patterns due to magnetic interactions.
Watanb *et al.*[122] (2012)	glass	Au/nanospheres/60,100 nm/not mentioned	Water	The substrate was vertically dipped in a drying colloid in a beaker at elevated temperature.	Linear patterns of Au nanoparticle assemblies.
Mueller *et al.*[128] (2012)	Glass slide	Au/nanostars/150 nm/pNIPAM	Ethanol	On a water droplet, nanopatterned PDMS with nanoparticles was pressed and left to dry.	Linear assemblies according to the PDMS patterns.
Xie et al.[115] (2013)	Silicon wafer	Au/nanorods/length:59.2, diameter:17.3 /CTAB	water	2 stage slow droplet drying near equilibrium and without contact line pinning.	Closed packed vertical assembly
Li et al.[129] (2016)	Si wafer	Au/nanorod/length:58 nm, dia: 16 nm/MUDOL 11-mercaptoundecyl)hexa(ethylene glycol)	water	Drop casting over Si wafer	
Li *et al.*[130] (2016)	Si wafer	Polystyrene/nanosphere/216 and 255 nm/none	water	Drying at 75 °C for coffee ring effect suppression.	
Arai *et al.*[124] (2019)	Glass substrate	SiO_2/nano- and microspheres27,45,90 and 2000 nm/none	water	Horizontal connective assembly	Closed packed Monolayers.

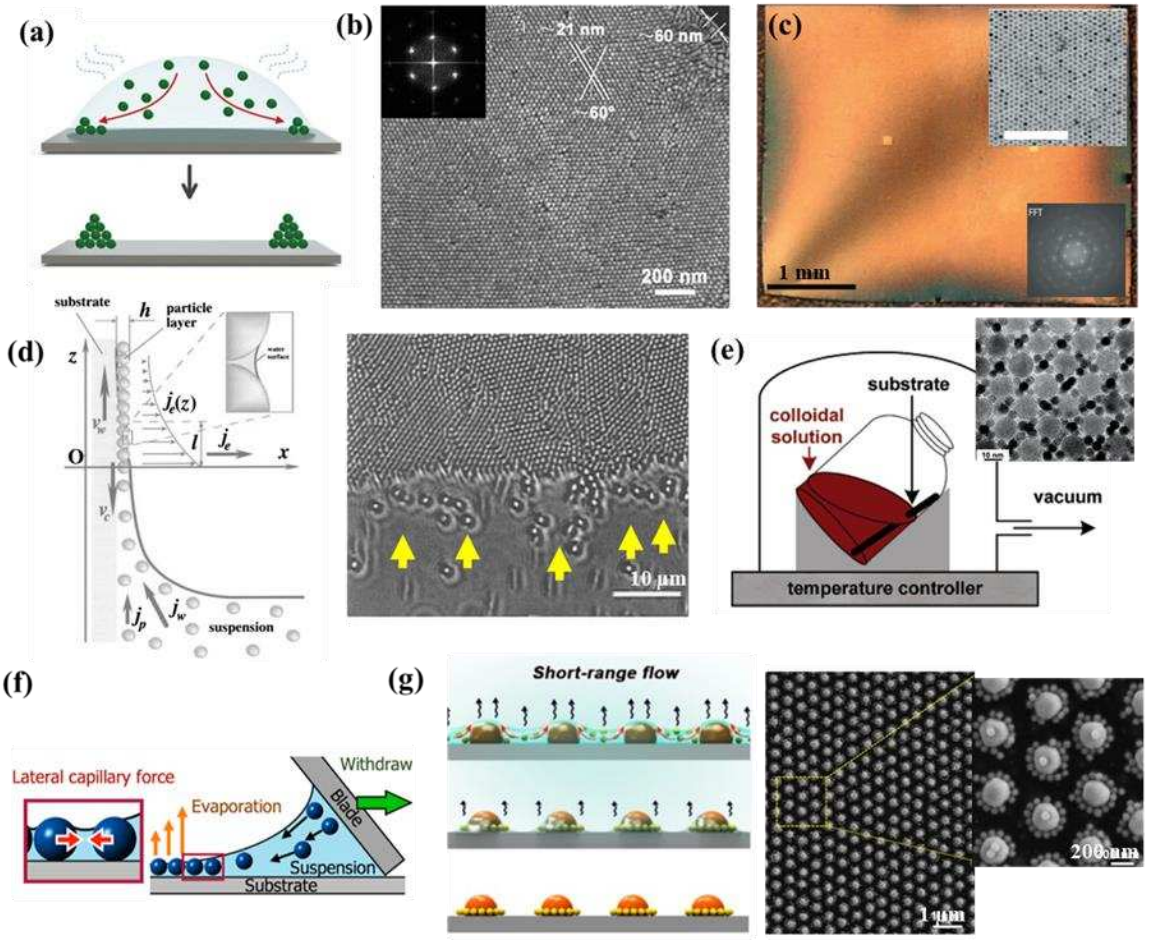

Figure 9. (a) Schematic representation of the Coffee ring effect-driven particle accumulation at the droplet edge during drying. Reprinted with permission[117] © 2019 John Wiley & Sons. (b) Suppression of coffee ring effect by slow droplet evaporation to form Au nanorod vertical assemblies as reported by Xie et al. Reproduced with permission[115] © 2013 American Chemical Society. (c) Bigioni *et al* showed a combination of rapid solvent evaporation and attractive particle-particle interaction results in Au nanoparticle monolayer. Reproduced with permission[118] © 2006 Nature Publishing Group. (d) Drying mechanism near the contact line of a liquid next to a vertical wettable solid substrate that induces particle accumulation near the contact line. Upward migration of particles during drying on vertical substrate as shown by Dimitrov and Nagayama. Reproduced with permission[131] © 1996, American Chemical Society. (e) Simple evaporative assembly can also yield complex binary supercrystals. Reprinted with permission[123] © 2006, American Chemical Society. (f) Horizontal convective self-assembly induced by capillary force. Reprinted with permission[124] © 2019, American Chemical Society. (g) Controlled evaporation of nanoparticle colloid over an array of larger nanostructures lead to the formation of satellite-like binary assemblies. Reprinted with permission[125] © 2021, American Chemical Society.

2.2.4 ***Directed Self-assembly on functionalized substrate***. In contrast to spontaneous self-assembly processes discussed so far, directed self-assembly involves structure directing additives such as organic molecules that facilitate linkage between the nanoparticles and the substrate to form ordered arrays. A common example is to obtain nanoparticle assemblies on silicon substrates using siloxane chemistry where the organic molecule is bound to the substrate through the Si-O-Si bond.[132] A simple procedure as shown by Liu *et al*. is to coat the silicon(111) surface with a aminopropyltriethoxylsilane (APTES) monolayer with the amino groups oriented away from the substrate so that nanoparticles with special affinity towards the amino group (e.g. Au or Ag nanoparticles) get attached, **Figure 10 (a)**.[133] Nanoparticles bound by electrostatic attraction can then be functionalized, for instance thiol functionalization of Au nanoparticles, to weaken the electrostatic forces and form closed packed assemblies by van der Waal interactions. Instead of self-assembled molecular monolayers as templates, Yap *et al*. showed that a spin-coated film of polystyrene-blockpoly(2-vinylpyridine) (PS-b-P2VP) reverse micelles form positive zeta potential nanopatterns that act as templates for the negatively charged particles to attach electrostatically, **Figure 10 (b)**.[134] One interesting aspect of the nanoparticle assembly mediated by molecular monolayers (or multilayers) on a substrate is that it has shown the possibility of using the molecular layer as a resist layer in scanning probe lithography techniques.[132] Scanning probe lithography, where an AFM tip is used for writing nanoscale patterns by some kind of chemical reaction instead of masks used in photolithography, can be a powerful future nanofabrication technique, **Figure 10 (c)**. For instance, Ling *et al*. have shown the use of scanning probe oxidation of a monolayer of n-octadecyltrichlorosilane (OTS) on a silicon substrate into nanopatterns that can be etched and further modified with aminopropyltrimethoxysilane (APS) for Au nanoparticles to assemble into those patterns.[135] Alternatively, nanopatterns can also be created by electrochemical oxidation on the OTS monolayer with an AFM tip to convert $-CH_3$ groups of the base monolayer to -COOH sites. Subsequently, adsorption of Nonadecenyltrichlorosilane (NTS) on the tip-inscribed -COOH sites and chemical conversion of the terminal ethylenic groups of the NTS to $-NH_2$ (amine) facilitates the self-assembly of Au nanoparticles on amines, **Figure 10 (d)**.[136] In addition, *in-situ* generation of CdS nanoparticles is also possible by chemical oxidation of terminal ethylenic groups of the NTS region to -COOH groups which then react with cadmium salt and passing H_2S gas.[137]

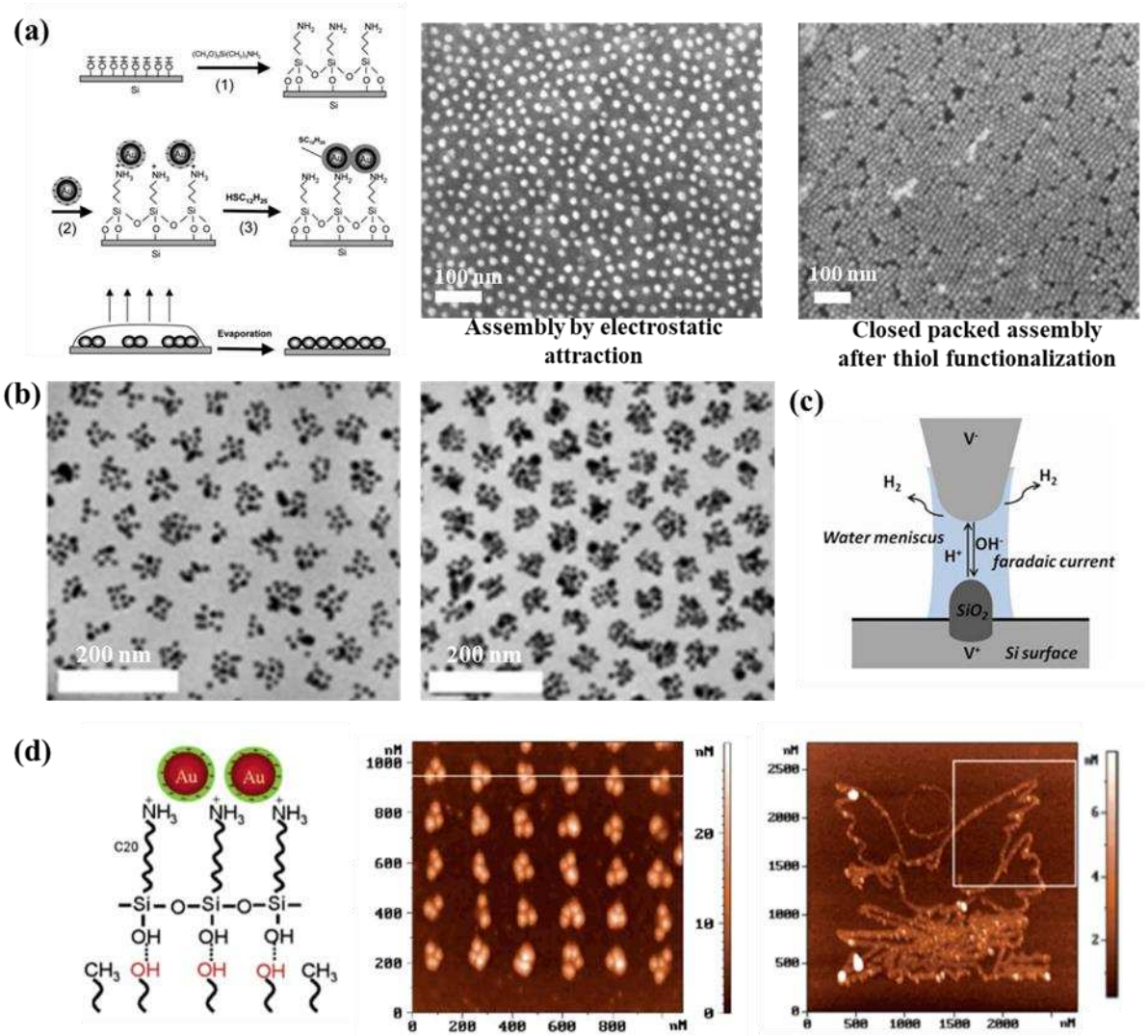

Figure 10. (a) Au nanoparticles assemble electrostatically on APTES monolayer grafted on Si substrate which can be converted to closed packed assemblies by thiol functionalization of nanoparticles. Reprinted with permission[133] © 2002 Royal Society of Chemistry. (b) Au nanoparticle self-assembly on polystyrene-blockpoly(2-vinylpyridine) (PS-b-P2VP) reverse micelle patterns obtained by spincoating. Reprinted with permission[134] © 2012, American Chemical Society. (c) Schematic view of the electrochemical process taking place between the AFM tip and the sample surface in oxidation-scanning probe lithography. Reprinted with permission[138] © 2019 Springer Nature (d) Au nanoparticle self-assembled patterns by oxidative scanning probe lithography on OTS monolayer on Si substrate and subsequent reactions to obtain -NH_2 terminal groups. Reprinted with permission[136] © 2004, American Chemical Society

Concluding this second section on self-assembled nanoparticle films, we have observed that among all different self-assembly techniques discussed above, the air-water interfacial assembly is the most widely explored technique in literature. However, it is the evaporative self-assembly that is the most versatile, compatible with different synthesis chemistry procedures used for the synthesis of the colloidal nanoparticles. This is due to the fact that while the air-water interfacial assembly requires functionalization (often hydrophobic functionalization) of the nanoparticles to be trapped at the interface; in evaporative assembly, the capillary flow driving the nanoparticles towards the drying meniscus is independent of the nanoparticle functionalization. Thus, the evaporative self-assembly has the potential to be more versatile across complex colloidal nanostructures with different surface chemistries. While the liquid-liquid interfacial self-assembly procedures are often easy to re-produce,

the real usefulness of this technique is severely limited by the difficulty in the transferring of the films from the interface to the desired substrate. For a holistic overview, **Table 6** provides a subjective comparison among different techniques to obtain self-assembled films.

Table 6. A comparative summary of self-assembly methods to obtain films from colloidal nanostructures.

Self-assembly method	Accessibility to complex structures	Ease of the self-assembly procedure	Economy of the process	Scalability of the process
2.2.1 Air-liquid interfacial self-assembly.	high	medium	high	high
2.2.2 Liquid-Liquid interfacial self-assembly.	low	low	high	medium
2.2.3 Evaporative self-assembly.	high	high	high	high
2.2.4 Directed Self-assembly on functionalized substrate.	medium	medium	high	high

3. Applications

The growing interest in the self-assembly of nanoparticles is guided by the vast application potential of assembled structures. Broadly, bottom-up construction starting at the nanoscale and using functional nanoparticles can result in complex structures that cannot be obtained with traditional top-down approaches. For instance, the fabrication of thin films of ordered bi-functional core-shell nanoparticles are only possible with a self-assembly process. In fact, otherwise sophisticated thin-film techniques can also be replaced by self-assembly based techniques for certain applications. For an overview, **Figure 11** outlines the known applications of nanoparticle clusters and films. With the multitude of interesting emerging applications, only a broad topical selection is provided here. In the following, interesting applications where self-assembled structures play a significant role are discussed in detail.

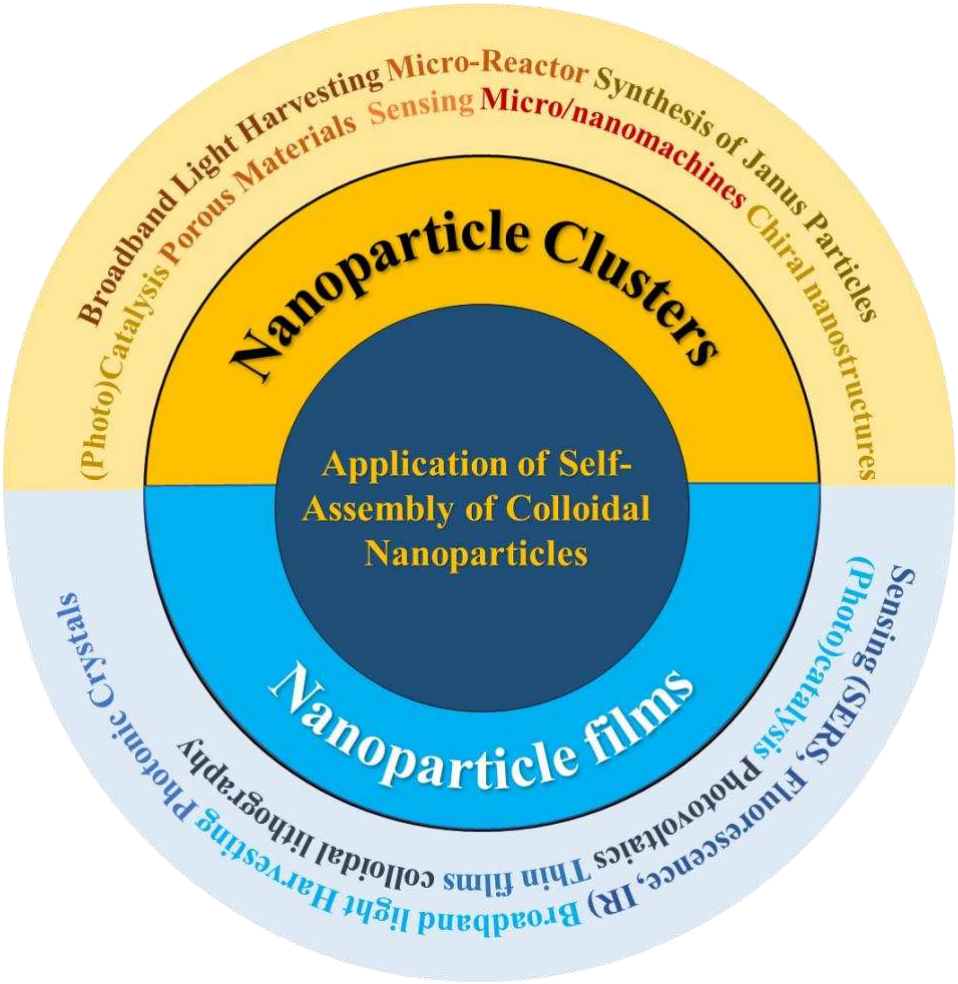

Figure 11. Summary of emerging applications of nanoparticle clusters and films.

3.1.1 ***Photothermal effect mediated applications.*** When the electromagnetic energy (*i.e.*, light) absorbed by nanoparticles is dissipated as heat, the temperature of the nanoparticle and the surrounding medium rises. This phenomenon is known as the photothermal effect. Plasmonic nanoparticles are excellent light absorber with high absorption cross sections. The strong absorption is due to the resonant free electron oscillations (also known as the plasmon resonance) in these nanoparticles driven by the incident light or electromagnetic field.[139] The photothermal effect of plasmonic nanoparticles is promising in many applications such as solar energy harvesting[140], solar desalination[141], thermal catalysis[142], photoacoustic imaging[143], sensing[144] [145], optofluidic tweezers[146] [147], etc. It has been shown that plasmonic coupling in assemblies of nanoparticles results in an enhancement of the individual nanoparticle absorption intensity, which in turn enhances the photothermal properties.[11] For light harvesting applications, high absorption intensity (or absorptance in the case of a film) should also be accompanied by low scattering (or reflectance in the case of a film) for the minimization of the energy loss. 3D and 2D assemblies of plasmonic nanoparticles with small (up to a few nm) interparticle gaps are thus excellent light harvesters.[148] Zhou *et al*. demonstrated hybrid porous structures with assemblies of Al nanoparticles inside for complete absorption of light without scattering (or reflection), **Figure 12 (a**). These structures achieved significant enhancement in the water evaporation rate for the application in solar desalination.[149] Similarly, 3D plasmonic nanoparticle assemblies exhibit broadband absorption for greater coverage of the solar spectrum.[150] Also, strong absorption in the near-infrared and infrared is advantageous for photoacoustic imaging in biological systems.[151] The broadening and the red-shift of the plasmon band in the nanoparticle assemblies is a result of the plasmonic coupling. As shown by Zhu *et al*., nanogap Au nanoparticle assemblies with high infrared

absorptance provide a strong photoacoustic signal for imaging of tumors, **Figure 12 (b)**.[152] The potential of plasmonic nanoparticle assemblies (or clusters) in photoacoustic imaging has also been demonstrated in various other works.[151] [153] [154] [155] [156] Photothermal release of drugs in target cells is another important medical application which can be further enhanced by the clustering effect. Goodman *et al*. showed that DNA release from nanoparticles in gene therapy by laser illumination has two distinctly different mechanisms for continuous wave (CW) laser and pulsed laser. While CW laser illumination drives the release of dehybridized single-stranded DNA though a photothermal process, pulsed-laser illumination results in DNA release by the breakage of the Au−S bond. When Au nanoparticles (or any other plasmonic nanoparticles) form hollow clusters obtained by Pickering emulsion mediated self-assembly, the plasmonic coupling and the hollow structure together lead to extreme broadening of the optical extinction spectra, **Figure 12 (c)**.[34] Such clusters can be excellent broadband solar energy harvesters as the spectrum covers the entire solar energy range. Song *et al*. demonstrated an interesting anticounterfeiting application of self-assembled Au nanorods based on the photothermal effect[157]. Depending on the self-assembly structure as shown in **Figure 12 (d)**, the photothermal effect can activate thermochromic dyes to show encoding patterns in 20 s that again becomes invisible 10 minutes after laser illumination is stopped.

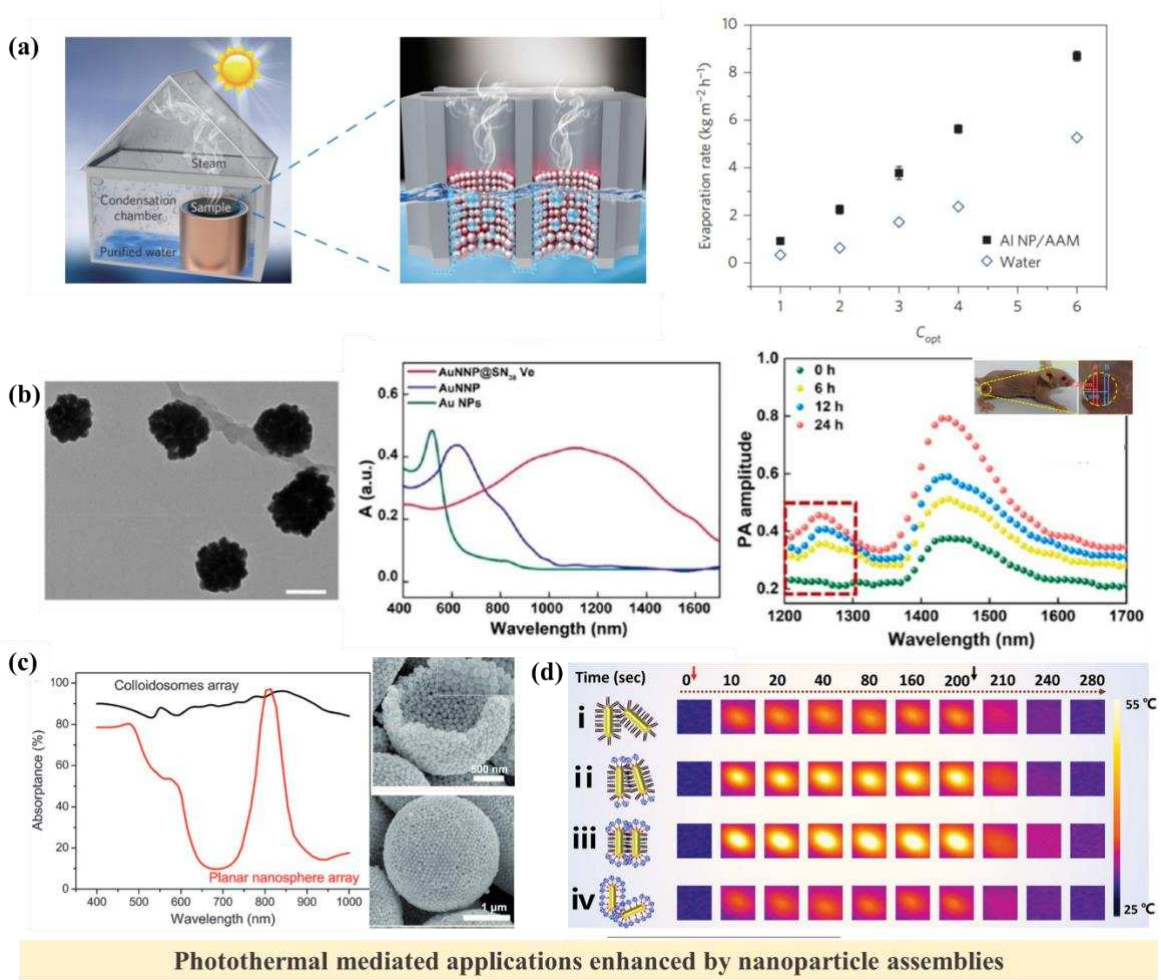

Figure 12. (a) Self-assembly of Al nanoparticles inside porous structures facilitates complete absorption of light without scattering (or reflection) losses, which can be useful for solar desalination. Reprinted with permission[149] © 2007 Nature Publishing Group (b) Au nanoparticle clusters have red-shifted and stronger plasmon bands (absorption) for enhanced photoacoustic imaging. Reprinted with permission[152] © 2020, American Chemical Society (c) Au nanoparticle hollow clusters obtained by Pickering emulsion mediated self-assembly procedure have nearly complete absorption of the visible

spectrum to be used for light harvesting applications. Reprinted with permission[34] © 2015 John Wiley & Sons. (d) Self-assembled Au nanorods of different configurations can be used for photothermal anti-counterfeiting patterns that are activated by laser illumination due to the presence of thermochromic dyes. Reprinted with permission[157] © 2020 John Wiley & Sons.

3.1.2 ***(Photo)catalysis and photo(electro)catalysis.*** In photocatalysis or catalysis in general, self-assembly can be crucial for the positioning of catalytic nanoparticles in an ordered way. This also allows the functionalization of individual nanoparticles towards better activity or selectivity before their self-assembly to form a large-scale interface. For example, hybrid Au core-ZnO shell nanoparticles can be self-assembled into a monolayer or multilayer films that work as photoelectrodes in water-splitting, **Figure 13 (a)**.[158] In such a configuration, the plasmonic cores not only help in enhancing the photocatalytic activity of the ZnO shells, but the individual nanoparticles can also couple among themselves to exhibit lattice resonances that further improve this light-matter interaction[159] [160]. As shown in **Figure 13 (a)**, the enhancement of the hybrid nanoparticle film over pure ZnO is ~6 times. Similarly, Kim *et al*. showed that self-assembly is an effective strategy to obtain uniform catalytic interfaces from nanoparticles. Their self-assembled films of Au-Cu alloy nanoparticles also allowed unambiguous comparisons, **Figure 13 (b)**.[161] In heterogeneous catalysis, self-assembled monolayer (or multilayer) films can form highly active interfaces from more than one constituent nanoparticles that also facilitate comparison between different systems for normalized active surface area. Self-assembly also facilitates facile fabrication of photonic crystal structures of photocatalysts by using assembly of sacrificial templates. As shown in **Figure 13 (c)**, inverse opal crystals of TiO_2 obtained by using polystyrene nanosphere films as sacrificial templates have significantly higher photocatalytic activity than normal TiO_2 due to the slow light or slow photon effect in the photonic crystal.[162] The exploitation of the slow light effect in photocatalytic activity enhancement has also been reported in number of investigations.[163] Self-assembly into 3D clusters provides another strategy to combine two different types of nanoparticles for a specific application. For instance, as shown in **Figure 13 (d)** emulsion directed clustering of Au and CdSe nanoparticles results in clusters with improved activity by plasmonic enhancement. Shi *et al*. showed that such hybrid clusters yielded a multi-fold increase in the H_2 evolution reaction over CdSe nanoparticles[164]. As evident in the synthesis of self-assembled multi-layered films, the void space in-between the nanoparticles inherently renders the structures porous, and the porosity itself can hence be controlled by the nanoparticle size and the inter-particle spacing. Thus, self-assembled structures can be promising as porous materials in applications where high porosity is advantageous. For example, in catalysis, porous self-assembled substrates can be useful for highly dispersed catalyst loading.[165] [166] Similarly, in electrocatalysis, self-assembled nanoparticle films can be effective electrode materials. Wang *et al*. showed that self-assembled electrodes obtained by layer-by-layer assembly of lithium titanate nanoparticles (**Figure 13 (e)**) can deliver a specific capacity of 167 mAh g^{-1} at 0.1 C.[167] The electrodes exhibit comparable performances to conventional slurry-cast electrodes at different current densities with greater flexibility to design advanced multi-layered nanostructures with cationic polyelectrolytes. In electrocatalytic applications, self-assembled nanoparticles can form electrodes with high coverage of active sites[168] [169]. Self-assembly of iron oxide nanoparticle-COOH on the APTES-ITO electrodes for instance facilitates electrochemical detection of ppb level concentration of Cd(II) and Pb(II) ions in seawater, **Figure 13 (f)**[170]. As discussed above, when plasmonic nanoparticles form clusters, the increased optical interaction results in higher photothermal temperatures. In plasmonic photocatalysis, cluster enhanced photothermal temperature or hot-electron generation may significantly enhance catalytic processes[171]. It has been shown by Lee *et al*. that clustering induced the generation of strong electromagnetic hotspots that enhance the light-to-chemical energy conversion process.[172] This is achieved by trimers of Au nanoparticles coated with catalytic Pd and Pt shells, where the plasmonic Au cores couple electromagnetically. Thus, in plasmonic catalysis, self-assembled clusters are especially promising due to the plasmonic coupling among the constituting nanostructures.

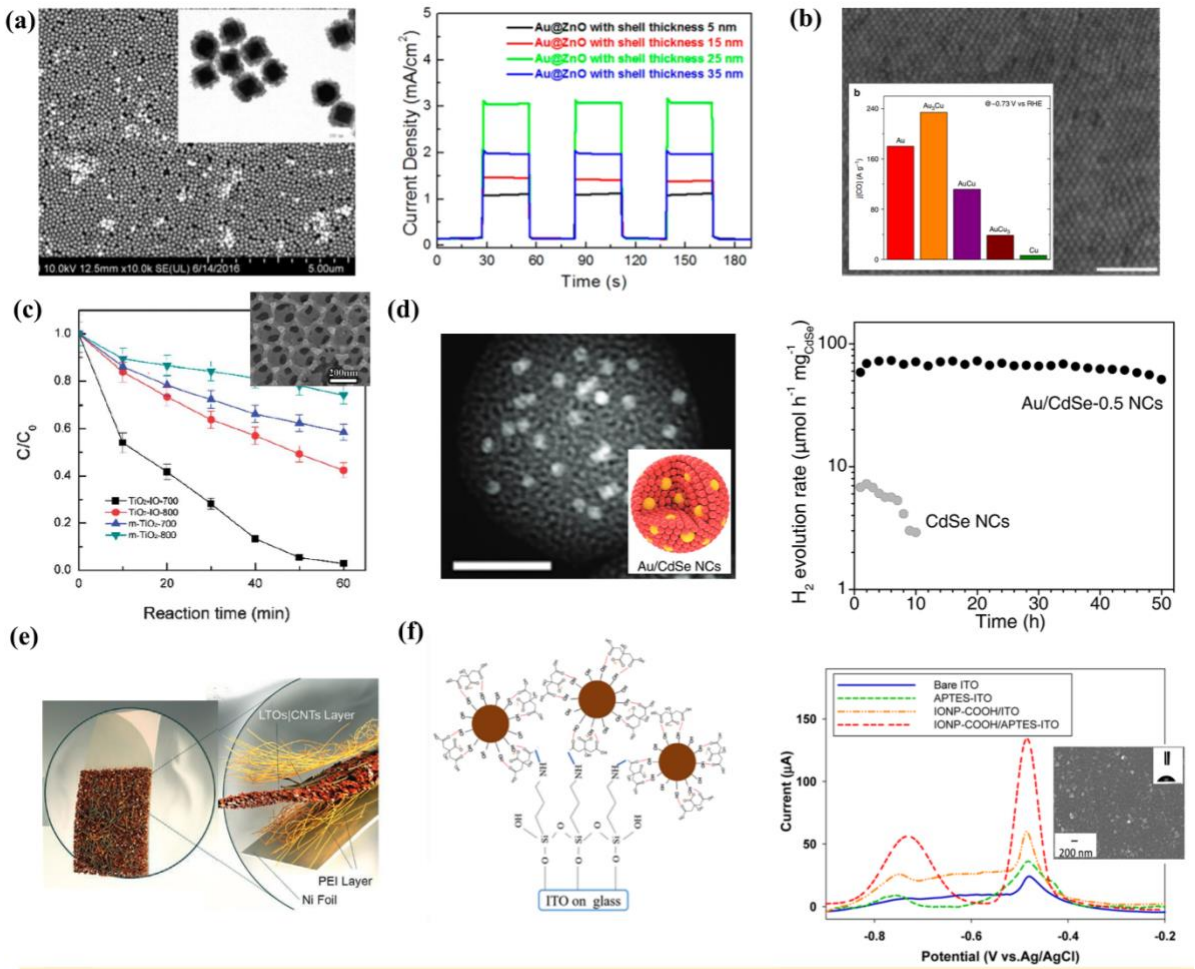

Applications of nanoparticle self-assembly in the fabrication of photo-electro-catalytic nanomaterials/interfaces

Figure 13. (a) Self-assembled Au@ZnO core-shell nanoparticle films for photoelectrochemical water splitting. Reprinted with permission[158] © 2017, American Chemical Society (b) $AuCu_3$ nanoparticles films obtained by the Langmuir–Schaefer technique for CO_2 reduction. Reprinted with permission[161] © 2014 Nature Publishing Group (c) Inverse opal photonic crystal of TiO_2 structures (black line) has significantly higher photocatalytic activity than normal TiO_2 due to the slow light effect in the photonic crystal. Reprinted with permission[162] © 2013 Royal Society of Chemistry (d) Emulsion based self-assembly of CdSe and Au nanoparticles into clusters enhance the photocatalytic H_2 evolution reaction. Reprinted with permission[164] © 2017 John Wiley & Sons. (e) Self-assembled electrode for lithium ion battery can be obtained by layer-by-layer assembly of lithium titanate nanoparticles and carbon nanotube (CNT) on Ni foil. Reprinted with permission[167] © 2021 John Wiley & Sons. (f) Self-assembly of iron oxide nanoparticle-COOH on the APTES-ITO electrodes for the detection of ppb level Cd(II) and Pb(II) ions.[170] © 2022 CC-BY-NC-ND 4.0.

3.1.3 ***Photovoltaics.*** In photovoltaics many efforts are being dedicated towards efficient management of light. As listed by Wang and Qi,[173] different light management strategies have been demonstrated so far, **Figure 14 (a)**, where self-assembly can be quite advantageous for the fabrication process and the required structural complexity. One such strategy is the fabrication of an anti-reflection coating for efficient light trapping before reflection losses. Shimomura *et al*. demonstrated the fabrication of such anti-reflection coating by electrostatic layer-by-layer assembly of 15 nm silica (SiO_2) and 7 nm TiO_2 nanoparticles that showed significant decrease in reflection with an increasing number of layers, **Figure 14 (b)**.[174] Such anti-reflection coating can significantly enhance the photovoltaic efficiency[175].

Efficiency enhancements of 11% to 12.3% have been reported for Si solar cells coated with self-assembled silica nanospheres. Apart from the reduction in surface reflectance in the UV and IR regions, silica nanospheres are also thermal shock resistant and chemically inert.[176] Chang *et al*., on the other hand, showed an efficiency enhancement of 25% by the use of a scattering enhancing coating made of self-assembled polystyrene microspheres, **Figure 14 (c)**.[177] These 2D polystyrene sphere layers were obtained on the top surface of a GaAs solar cell. The scattering of the microspheres enhances the path length of the incident light. Self-assembled layers of other dielectric nanoparticles such as alumina, silica, *etc*., can also enhance the performance of solar cells by scattering of incident light, increasing active layer absorption and photocurrent output.[178] [176] While thin film solar cells usually have a hierarchical structure with stacks of planar films, self-assembly facilitates complex patterning in these films. For instance, self-assembled polystyrene nanosphere multi-layers can be used as a sacrificial template so that the semiconductor material can fill the interstitial voids before the template is removed. This approach was demonstrated by Guldin *et al*. to obtain inverse TiO_2 opal or hollow structures (**Figure 14 (d)**) that result in 10% enhancement in the photocurrent.[179] The slow light effect of photonic crystals is also an important physical aspect that is known to enhance both photovoltaic and photocatalytic processes.[163] In inverse opal structures as shown in **Figure 14 (d)**, the slow light effect can also significantly enhance the photovoltaic efficiency.[179] [180] In thermophotovoltaics, nanostructures for selective thermal emission can also be obtained by self-assembly. As shown by Arpin *et al*., 3D tungsten photonic crystals obtained by self-assembled templates have unprecedented thermal stability up to 1400°C and modified thermal emissions. Also, with self-assembled photonic crystals of hafnium diboride it is demonstrated that refractory metallic ceramic materials are viable candidates for photonic crystal-based solar thermophotovoltaic devices.[181]

In many instances, plasmonic nanoparticles have been shown as the light-trapping components in a line of work often referred to as plasmonic photovoltaics.[182] [183] As plasmonic nanoparticles are intense light absorbers, more light is trapped by such nanoparticles and potentially leading to hot electron generation. It is postulated that the hot electrons from the plasmonic metal are injected into the semiconductor and holes migrate to the counter electrode through the hole transport material. When these plasmonic nanoparticles are obtained as closed packed films, the inter-particle coupling enhances the light-matter interaction even further. Reineck *et al*.[184] showed that self-assembled Au and Ag nanoparticles can be combined with TiO_2 photovoltaic films to get photocurrents that are much higher than those obtained for dye sensitized solar cells, **Figure 14 (e)**. Also, the nanoparticles are much more stable over time compared to organic dyes.

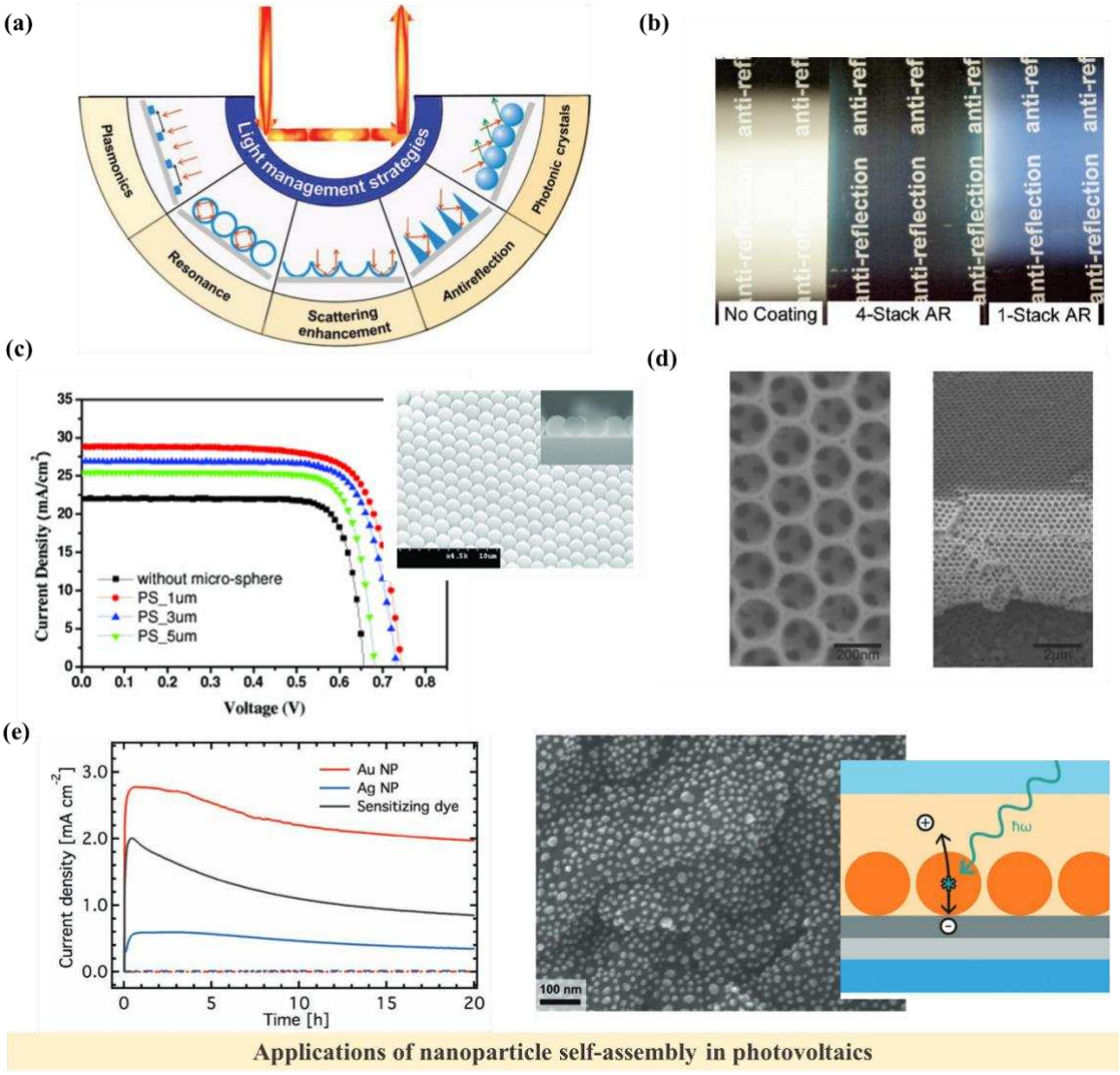

Applications of nanoparticle self-assembly in photovoltaics

Figure 14. (a) Different light-management strategies in photovoltaics by micro and nanopatterning. Reprinted with permission[173] © 2019 John Wiley & Sons. (b) Anti-reflection coatings obtained by layer-by-layer self-assembly of silica and titania nanoparticles. Reprinted with permission[174] © 2010, American Chemical Society (c) Self-assembled polystyrene spheres on GaAs solar cells significantly enhance the current density by multiple scattering and optical path elongation.[177] © 2009 Optica Publishing Group (d) The use of multi-layer self-assembled polystyrene nano/microspheres as sacrificial templates results in porous networks of TiO_2, when TiO_2 is crystallized in the interstitial voids and the polystyrene is removed, Such inverse opal structures have a strong slow light effect. Reprinted with permission[179] © 2010, American Chemical Society (e) The plasmonic enhancement in solar cells can be further improved using self-assembled films of plasmonic nanoparticles that are coupled electrodynamically to result in stronger light-matter interactions. Plasmonic solar cells show higher photocurrents and stability over time than organic dye sensitized cells. Reprinted with permission[184] © 2012 John Wiley & Sons.

3.1.4 ***Sensing.*** In sensing applications, self-assembly can be used to obtain the actual sensing interface. For example, for metal oxide (MOS) based chemo-resistive gas sensing, metal oxide nanoparticles can be self-assembled into thin films or clusters. In self-assembled films, individual metal oxide nanoparticles can at first be subjected to pre-modification or functionalization for sensitivity enhancement[185]. In general, colloidally synthesized high surface area nanoparticles provide a higher contact interface compared to planar thin films, resulting in higher sensitivity given that the other

sources of resistance are eliminated. Miao *et al*. showed that CuO nanosheets obtained by air-water interfacial self-assembly result in excellent sensitivity as such films provide large surface area but small thickness (~30 nm), **Figure 15 (a)**.[186] Indeed, with increasing thickness of the films by multiple layer assembly, the sensitivity decreases. Borah *et al*. showed that different metal oxide nanoparticle films can be obtained by self-assembly after the hydrophobization by appropriate ligand functionalization.[41] Similarly, the decoration of Au nanoparticles by self-assembly or other methods can enhance light assisted gas sensing.[187] Another way self-assembly can enhance sensing is by making highly porous nanostructures by the clustering of nanoparticles in three dimensions. As shown by Suematsu *et al*., SnO_2 nanoparticle clusters exhibit considerably higher sensitivity in H_2 and CO sensing as compared to isolated nanoparticles, **Figure 15 (b)**. The sensitivity is then further enhanced by the incorporation of Pd.[188]

Plasmonic nanostructures are well-known for their application in SERS (Surface Enhanced Raman Spectroscopy) based sensing, where the inelastic Raman scattering signal of probe molecules is enhanced by the near-field enhancement or the light concentration effect of the nanostructures. It has been shown that in self-assembled periodic plasmonic nanoparticles/nanostructures, the near-field enhancement is stronger than for isolated nanoparticles due to the inter-particle coupling.[145] As shown by Shin *et al.,* interparticle gaps of desired dimensions can be obtained by subsequent etching steps to remove the SiO_2 shell over the Au nanoparticles in the self-assembled film, **Figure 15 (c)**.[189] Importantly, for Raman enhancement, the etching step is important as the probe molecules are exposed to the near-field enhancement only if the silica shells are removed. For certain cases, to shift the SERS enhancement to longer wavelengths, the plasmon resonance must be red shifted. For this, supercrystals of Au nanoparticle clusters can be obtained by combining self-assembly and lithography resulting in resonances in the infrared region, **Figure 15 (d)**. On the other hand, with magnetic-plasmonic bi-functional nanoparticles, self-assembled clusters of nanoparticles for SERS enhancement can be obtained by the application of magnetic fields.[190] While SERS application of self-assembled plasmonic nanoparticles has been studied quite extensively,[191] some recent developments have shown new applications in biosensing. Self-assembled plasmonic Au nanoparticle clusters combined with metal organic frameworks are excellent platforms for SERS based detection of VOCs (volatile organic compounds) in human breath that are indicators of certain diseases like cancer.[192] [193] For example, among different VOCs, certain aldehydes in breath have been identified as biomarkers of lung cancer [194] The combination of MOFs with self-assembled plasmonic nanoparticles facilitates high absorption of the probe molecules in the porous MOF, where their SERS intensity is amplified by the strong near-field enhancement of coupled plasmonic response of the nanoparticles, **Figure 15 (e)**. Recently, Borah *et al*. [195] have shown an alternative strategy for the detection of VOCs by self-assembled Au nanoparticle films in the Kretschmann (*i.e*. Attenuated Total Reflection, ATR) configuration, where the adsorbed VOCs on the nanoparticles can be detected by the change in the optical intensities due to the change in refractive index, **Figure 15 (f)**. In the ATR configuration, the plasmon resonance is excited by the evanescent field due to the total internally reflected incident beam.[196] The evanescent field is strongly dependent on the direction of polarization of the incoming light. It is shown that further improvement in sensitivity can be achieved by the use of ellipsometry instead of intensity based optical spectroscopy.[195] Refractive index based sensing by plasmonic nanostructures is based on the change in the optical intensities or plasmon resonance positions (usually a red shift) due to the change in the refractive index in the surrounding medium of the nanoparticles after interaction with the analyte. Naturally, the adsorption of biomolecules (in liquid phase), gases, VOCs, *etc*., on the plasmonic nanostructure leads to this change in the refractive index. Plasmonic nanoparticle films have a very short-range evanescent field (or near-field enhancement) that senses the changing refractive index. Thus, self-assembled plasmonic nanoparticle films can selectively probe only the molecules that are in the immediate vicinity of the film. This can facilitate higher selectivity as compared to planar thin films which have long range evanescent fields that can interact with distant molecules (or resulting refractive index changes). Naturally, refractive index-based sensing itself is not selective as the adsorption of any

molecule can lead to the change in the refractive index. Thus, the selectivity in this case can be achieved by selective adsorption of the probe molecules on the sensing platform. In this regard, combining metal organic frameworks (MOFs) with plasmonic nanoparticles reappears as a promising approach as the adsorption of molecules in MOFs can be highly selective.[197] [198] For example, $CHCl_3$ shows preference in adsorption to CH_2Cl_2 from a mixture, in the adsorption to a Cu(II)-metal organic framework, which is linked to the hydrophobic nature of the pores.[199] Such trends have also been demonstrated for aromatic molecules.

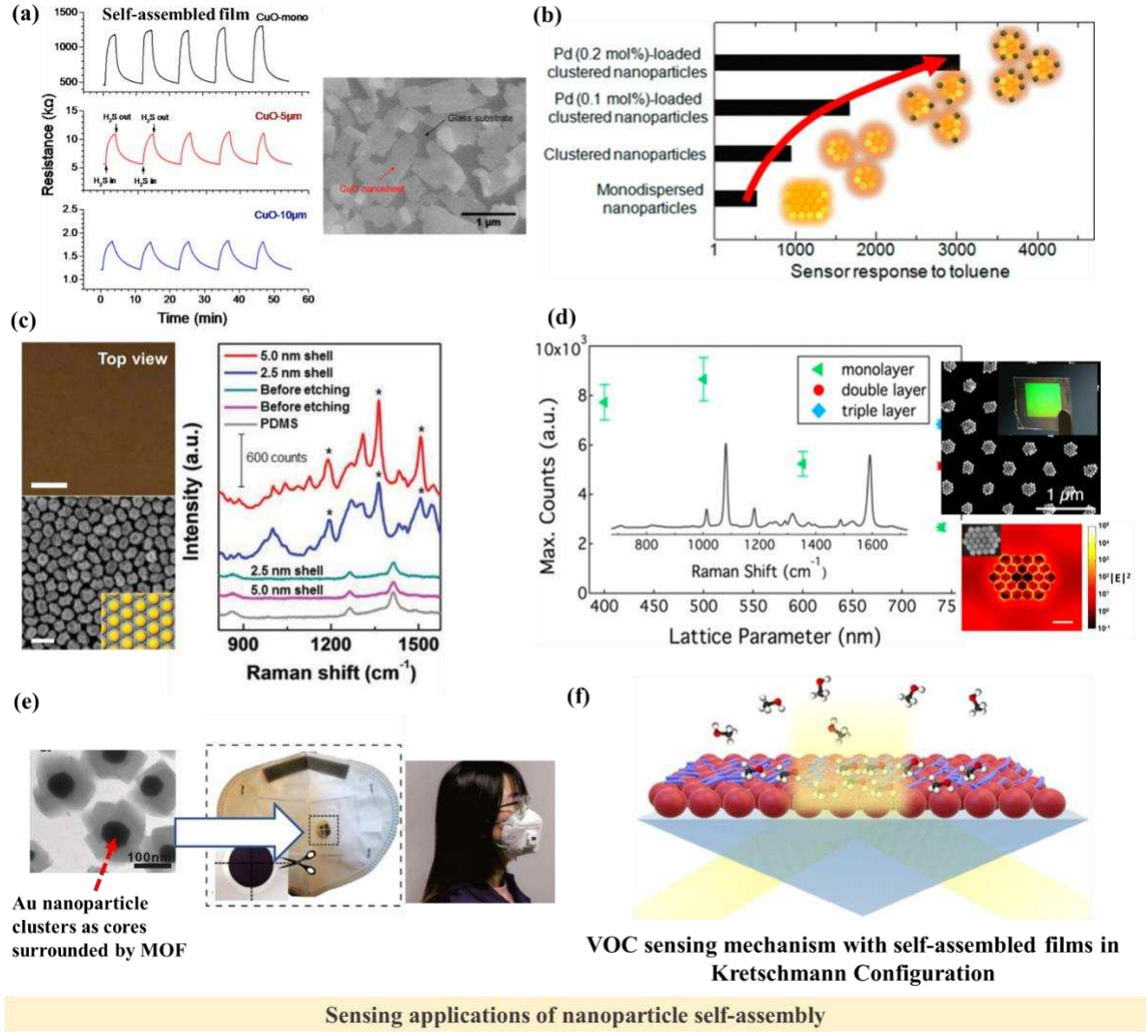

Figure 15. (a) Self-assembled CuO nanosheets for H_2S gas sensing applications. A monolayer film yields higher sensitivity than multilayer due to low thickness with high surface area. Reprinted with permission[186] © 2019, American Chemical Society (b) Self-assembled SnO_2 nanoparticle clusters have stronger sensitivity than isolated nanoparticles in H_2 and CO gas sensing due to higher porosity resulting from clustering. Reprinted with permission[188] © 2014, American Chemical Society (c) Self-assembled Au@SiO_2 core-shell nanoparticle films with controlled interparticle gap for SERS applications. Reprinted with permission[189] © 2015 John Wiley & Sons. (d) Self-assembled supercrystals of Au nanoparticle clusters can shift SERS enhancement to infrared wavelengths due to the red-shifted lattice plasmon resonance. Reprinted with permission[68] © 2018, American Chemical Society (e) Demonstration of a SERS based biosensing device: self-assembled Au nanoparticle clusters combined with MOF facilitates SERS signal enhancement of cancer biomarker VOCs from breath that adsorb onto the MOF in high concentration. Reprinted with permission[193] © 2022 John Wiley & Sons. (f) Schematic of ellipsometric VOC sensing by self-assembled Au nanoparticle films in the Kretschmann

(or ATR) configuration: the optical response is driven by the evanescent field (varies with the polarization) that interacts with the nanoparticles and the surrounding environment (not to scale).Reprinted with permission[195] © 2022, American Chemical Society.

Another common sensing technique that is ubiquitous nowadays is colorimetric sensing. The lateral flow assay (LFA) test strips became quite common during the COVID19 pandemic. The colors of the control line and the test line in LFA tests originate from plasmonic (commonly Au nanoparticles) nanoparticles that show a strong color contrast against the cellulosic background. Since it has been shown that in plasmonic nanoparticle clusters, the plasmonic coupling increases the optical cross section of the individual nanoparticles, self-assembled nanoparticle clusters can be interesting for LFA tests. Chen *et al*. showed that Au nanoparticle clusters obtained by emulsion directed self-assembly provide ~40 times higher sensitivities than isolated 40 nm Au nanoparticles. With increasing cluster size, the sensitivity increases up to a maximum before dropping again, **Figure 16 (a)**[200]. Similarly, Oh *et al*. reported higher sensitivities with even smaller assemblies of several Au nanoparticles for SARS-CoV-2 sensing with LFA tests, **Figure 16 (b)**[201]. It is important to note that while increasing size leads to the increase in the optical intensities, the surface area also increases. For a fixed amount of analyte or biomarkers, more analyte per nanoparticle may be required with increasing size. Thus, the ideal situation is where high optical cross sections (or intensities) are combined with small nanostructures. Recently, there have been several studies that have shown significant sensitivity enhancement in LFA tests by self-assembled nanoparticles.[201] [202] [203] Apart from LFA, other colorimetric sensing methods can also make use of self-assembled nanoparticle clusters or the process of clustering itself. As clustering comes with a change in color compared to individual nanoparticles, the process of self-assembly itself can be directly useful in colorimetric sensing in general.[204] For example, Mirkin and co-workers showed back in 1997 the possibility of colorimetric detection of DNA in liquid phase by self-assembly or aggregation of Au nanoparticles, **Figure 16 (c)**.[205] Such plasmonic coupling mediated colorimetric sensing has since been studied extensively and further enhancement by the incorporation of modern optical sensors still holds great promise.[206] Similar to how clustering of plasmonic nanoparticles affects the overall optical properties, the clustering of magnetic nanoparticle also leads to changes in the magnetic resonance (MR) signal. It has been shown that during the self-assembly of magnetic nanoparticles, the nanoparticles act as magnetic relaxation switches by causing extensive spin-spin relaxation time changes (δT2) of surrounding water molecules.[207] Thus, clustering of superparamagnetic iron oxide nanoparticles labelled with antibodies specific to antigens presented on specific viral capsids result in detectable perturbations of the T2 magnetic relaxation times. This strategy by self-assembly of magnetic nanoparticles can be used to detect viruses up to concentrations as few as five viral particles in 10 μL of 25% protein solution without the need of PCR amplification, **Figure 16 (d)**. Another recent yet fast developing field is the sensing with chiral plasmonic nanostructures. These chiral structures can also be obtained by self-assembly of nanoparticles, especially by DNA directed techniques to achieve high control over the structure.[56] A number of other review articles have specifically addressed chiral sensing in great detail already.[208] [209] [210] [211]

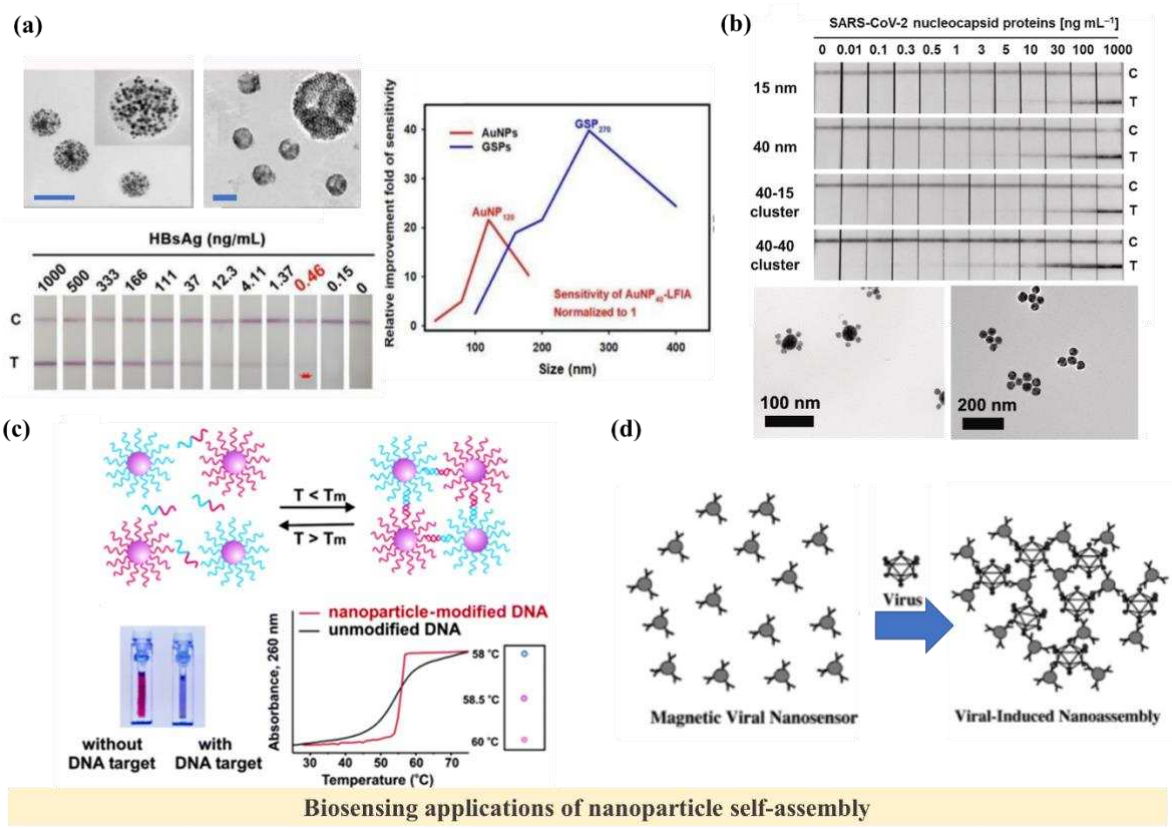

Figure 16. (a) Sensitivity enhancement in lateral flow assay (LFA) device by the use of self-assembled Au nanoparticle clusters.[200] Reprinted with permission © CC-BY 4.0. (b) Sensitivity in LFA can be further enhanced by the use of larger Au nanoparticles for SARS-CoV-2 sensing. The comparison between 15 and 40 nm nanoparticles shows that 40 nm nanoparticles have a stronger color due to stronger plasmonic coupling.[201] © CC-BY 4.0. (c) In solution phase, colorimetric detection of DNA in liquid phase is possible by self-assembly or aggregation of Au nanoparticles that changes the color of the colloid.[211] Reprinted with permission © 2005, American Chemical Society. (d) Superparamagnetic iron oxide nanoparticles (brown spheres) labelled with antibodies (green) specific to antigens (blue) presented on viral capsids (red) will form aggregates in the presence of target viruses, which result in detectable perturbations of the T2 magnetic relaxation times of protons in the surrounding media. Reprinted with permission[207] © 2003, American Chemical Society.

3.1.5 ***Drug delivery*****.** For drug delivery applications, drug carrying polymeric nanoparticles formed by the self-assembly of polymeric blocks have been studied by different groups.[212] [213] Such systems facilitate the delivery of hydrophobic drugs to the target cells by encapsulation of the drug in a hydrophobic core surrounded by a hydrophilic shell. In a similar way, nanoparticle assemblies can also encapsulate drug molecules to be delivered and released in the target cells. As shown by Wang *et al*., ligand-capped 4 nm Au nanoparticles can efficiently encapsulate poorly water soluble molecules from the dispersing solvent with high uptake.[214] Considerable uptake of different molecules such as bisphenol A (BPA), azulene, para-dichlorobenzene (p-DCB), Alachlor, *etc*. is demonstrated in this procedure. The molecules could also be released easily by the dissolution of the nanoparticle clusters in CD_2Cl_2 environment, **Figure 17 (a)**. The release of the drug can similarly be triggered by for instance changing the pH of the solvent. Song *et al*. showed that Au nanoparticle assemblies forming vesicles can be used as drug carriers for controlled drug release inside cells by changing the pH from 7.4 to 5.0, **Figure 17 (b)**.[215] Nanoparticle clusters can further facilitate the incorporation of multiple functionalities. For example, the encapsulation of photosensitizer Ce6 in Au nanoparticle clusters

enables three functionalities: strong fluorescence, photoacoustic signal and photothermal effect, for imaging-guided synergistic photothermal/photodynamic therapy (PTT/PDT).

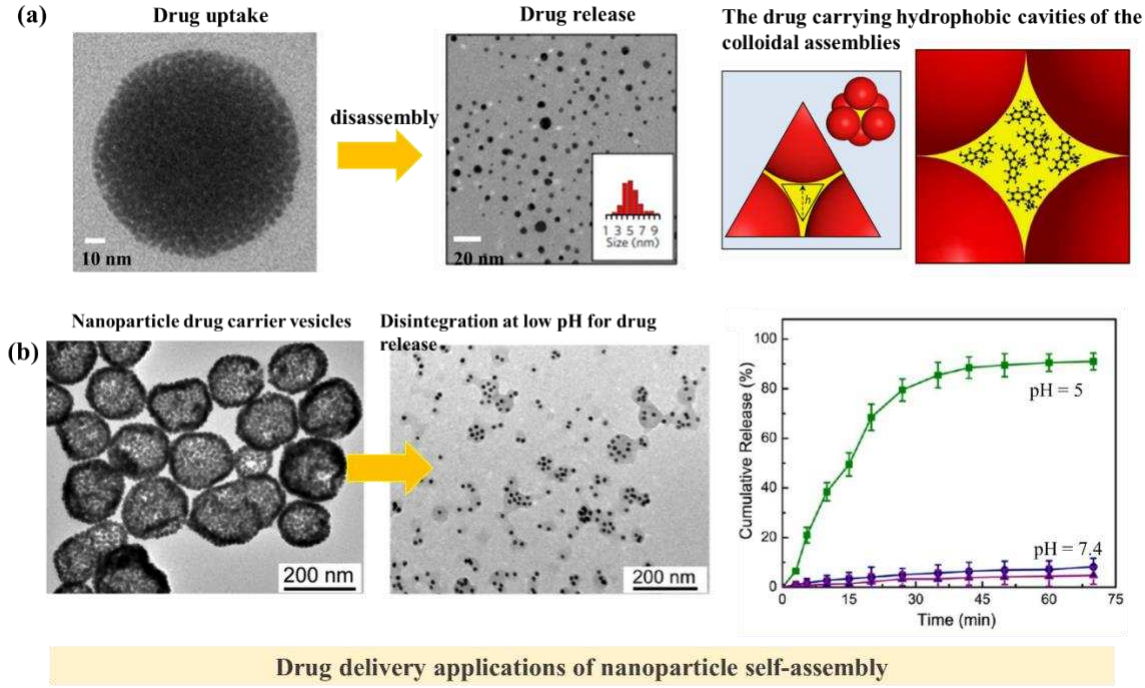

Figure 17. (a) Self-assembled Au nanoparticles can take up drug molecules from the solvent phase which can later be released upon disassembly by the change in solvent from water to CD_2Cl_2. Rightmost: interstitial pores of the assembles that carry the hydrophobic drug molecules. Reprinted with permission[214] © 2017 Nature Publishing Group. (b) pH sensitive Au nanoparticle vesicles as drug carriers. The drug is released by the disassembly of the vesicles by changing the pH from 7.4 to 5.0. Reprinted with permission[215] © 2012, American Chemical Society.

3.1.6 ***Self-assembled nanoparticle clusters for micro/nano reactors.*** The utilization of the self-assembly concept to form nanoreactors originates from molecular self-assembly of different functional molecules into one molecular unit.[216] In **Figure 13 (d)** it is illustrated how self-assembly facilitates the combination of different functional nanoparticles *i.e*. Au and CdSe nanoparticles into one unit. Apart from creating multiple functionalities, the process of self-assembly can also allow the formation of nano or micro reactor units. A straightforward example of this is the self-assembly of nanoparticles to form Pickering emulsions. In Pickering emulsions, nanoparticles encapsulate an oil phase in a continuous aqueous phase and in that way they can facilitate catalytic reactions in either phase. Such a system can be advantageous in different circumstances. For examples, as shown by Burdyny *et al*., self-assembled TiO_2 nanoparticles forming oil-in-water Pickering emulsions are excellent for continuously running photocatalytic reactors as 100% photocatalyst retention can be achieved with 96% conversion efficiency, in contrast to simple nanoparticle suspensions with complete loss of photocatalyst to the outlet stream, **Figure 18 (a)**.[217] Such biphasic systems become even more interesting with Janus nanoparticles, that have different functionalities or constitutions on different sides of a single nanoparticle. Cho *et al*. showed that Janus nanoparticles with a catalytic hemisphere assemble at the reactant-water interfaces to form Pickering emulsions, **Figure 18 (b)**. In the self-assembly, the catalytic side decorated with catalytic nanoparticles, Ag or Pd, remains in the oil phase to accelerate a specific reaction. As shown in **Figure 18 (b)**, the conversion from 4-nitrophenol (indicated by UV-Vis band at 400 nm) to 4-aminophenol (UV-Vis band at 250 nm) inside these microreactors takes place efficiently. It is also shown that by further incorporation of magnetic Fe_2O_3 nanoparticles into the nanostructure facilitates fast and easy separation of the micro-reactors for product separation. Thus, complex

separation and purification processes can be simplified to a great extent. In the same line of developments, Zhang *et al*. recently proposed a biomimetic Pickering emulsion based microreactor concept inspired by multi-compartmental living cells, **Figure 18 (c)**.[218] While hydrophobic silica nanoparticles (60 to 80 nm) are used as the emulsifier, mesoporous silica nanoparticles (80–90 nm) that are encapsulated in an ionic liquid (interior medium) act as the support for the metal complex catalysts or enzymes. The as-obtained biomimetic microreactors are then packed in a fixed-bed reactor for continuous flow cascade catalysis, exhibiting 5- to 420-fold enhancement in catalytic efficiency (CE), 99% ee (enantiomeric excess) as well as durability of 240 h in continuous operation. Similarly, Huang *et al*. demonstrated Pickering emulsions of self-assembled lead sulfide Janus quantum dots with ligand shells as nanoreactors for photocatalytic reactions.[219] Another example is palladium/graphitic carbon nitride (g-C_3N_4) stabilized emulsions as microreactor for storing hydrogen from ammonia borane for the use in alkene hydrogenation[220] Copper nanoparticles loaded polymer vesicles have also been demonstrated as environmentally amicable nanoreactors for the synthesis of benzimidazole via a cascade reaction. The vesicles exhibited a uniform size distribution, spherical morphology, excellent stability and efficient Cu loading.[221] As in Pickering emulsions the nanoparticles at the interface are in partial contact with two different media *i.e*. the dispersed and the solvent medium, functionalization or additional formation on any of these two sides can lead to the formation of Janus nanoparticles. Self-assembly of nanoparticles in Pickering emulsions is thus a convenient strategy for the synthesis of such multi-faceted Janus nanoparticles.[222]

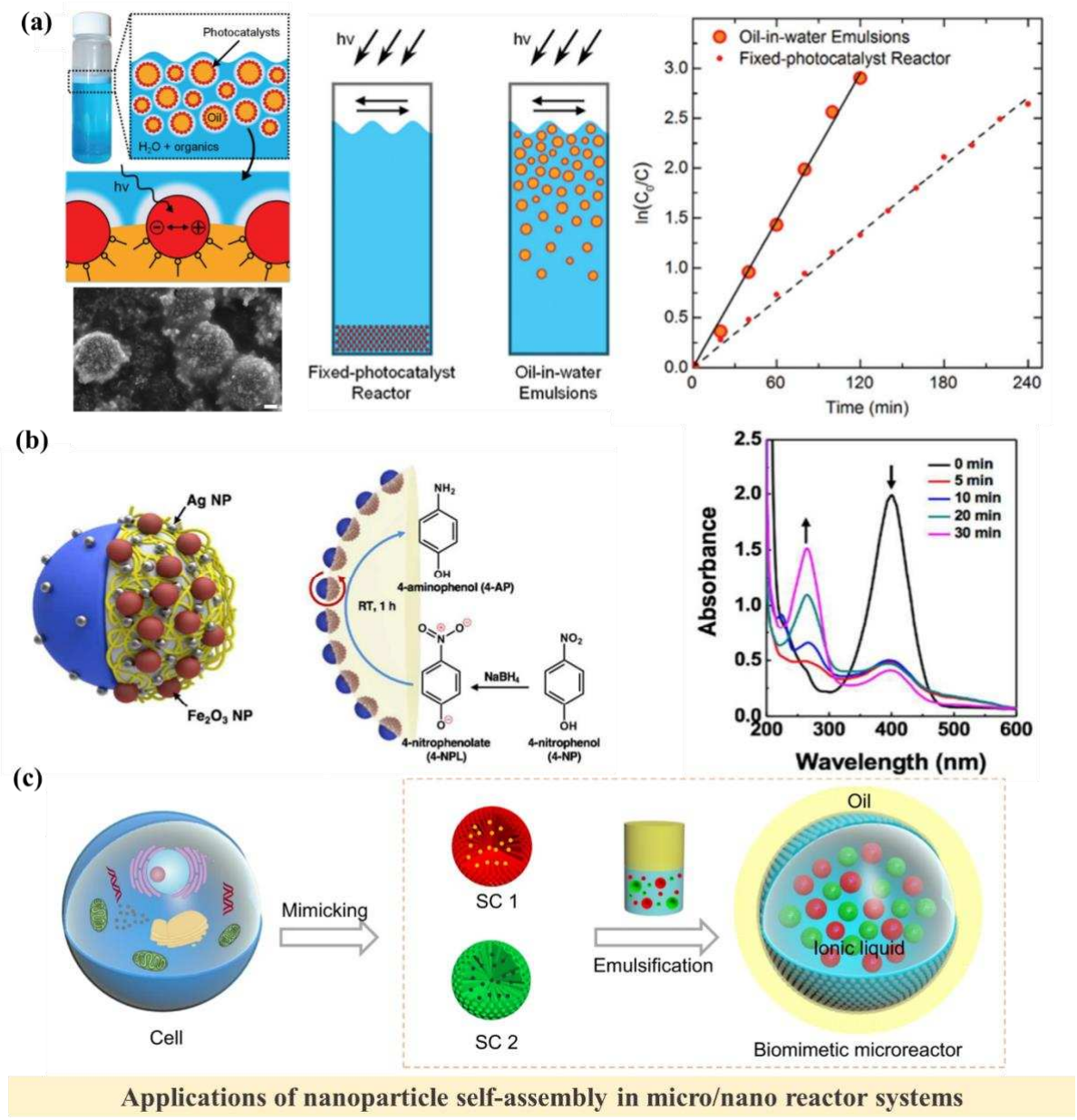

Figure 18. (a) Self-assembled TiO_2 nanoparticles forming oil-in-water Pickering emulsions are excellent for high catalyst retention (100%) while continuous operation photocatalytic reactors. Reprinted with permission[217] © 2016 Royal Society of Chemistry (b) Janus nanoparticles with a catalytic hemisphere assemble at the reactant-water interfaces to form Pickering emulsions with the catalytic nanoparticles, Ag or Pd, remaining in the oil phase to accelerate a specific reaction: 4-nitrophenol (indicated by UV-Vis band at 400 nm) to 4-aminophenol (UV-Vis band at 250 nm). Incorporation of magnetic Fe_2O_3 nanoparticles facilitates fast and easy separation of the micro-reactors for product separation. Reprinted with permission[223] © 2018 Royal Society of Chemistry. (c) A biomimetic Pickering emulsion based microreactor concept inspired by multi-compartmental living cells, exhibiting 5- to 420-fold enhancement in catalysis efficiency (CE).[218] © 2022 CC-BY 4.0.

3.1.7 ***Nanomachines***. Another interesting application of self-assembled systems of nanoparticles is the performance mechanical tasks at the nanoscale. For example, colloidal magnetic nanoparticles can be moved easily by the application of an external magnetic field. It has been shown that linear assembly of magnetic nanoparticles can be used like magnetic stirring bars, but then at nanoscale. Yang *et al.* demonstrated that the hydrogenation of methylene blue can be achieved efficiently in microdroplets by

using self-assembled magnetic nanoparticle (Fe_3O_4-NC-PZS-Pd) linear arrays as stirrers, **Figure 19 (a)**.[224] Similarly, Chong *et al.* showed that nano-stirring by self-assembled chains of magnetic nanoparticles prevents the settling of the reaction suspension unlike larger micron sized stirrers, **Figure 19 (b)**[45]. Such nano-stirring systems are remarkable as the mass transfer resistance at nanoscale inside micro-droplets can be overcome without breaking of the droplets. A similar magnetically driven concept was demonstrated by Dong *et al.*, where nanomotors were obtained by the self-assembly of different nanoparticles (Au, Pt, Fe_3O_4) over polymer single crystal (PSC) nanoplatforms[225]. In this system the Fe_3O_4 nanoparticles respond to the magnetic field. Interestingly, the same self-assembled nanoparticle system can be moved by a catalytic reaction in 15% H_2O_2 solution due to the Pt nanoparticles that give rise to oxygen bubbles. The oxygen bubbles depart from the assembly pushing the assembly in the opposite direction by momentum exchange. Such catalytic propulsion has also been shown by others.[226] [227]

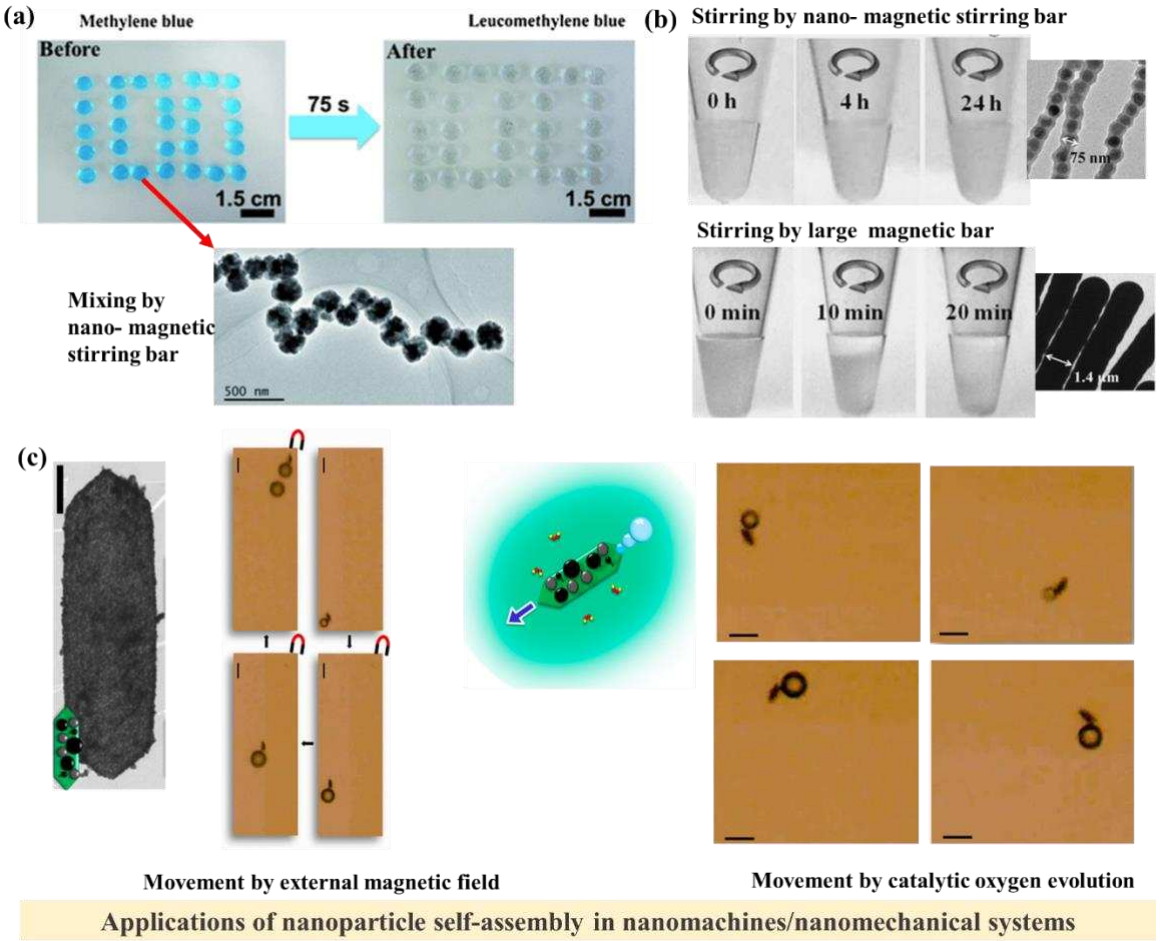

Figure 19. (a) Linearly self-assembled Fe_3O_4-NC-PZS-Pd nanoparticles as nano-magnetic stirring bar for methylene blue hydrogenation in microdroplets. Reprinted with permission[224] © 2015 John Wiley & Sons (b) Nanostirring bars of 75 nm wide keep the reaction suspension of 30 μL well mixed in contrast to larger magnetic bars. Reprinted with permission[45] © 2013 John Wiley & Sons (c) Self-assembled system of Au, Pt, Fe_3O_4 nanoparticles on polymer single crystal nanoplatforms that can be moved in the solution phase by external magnetic field and catalytic oxygen evolution (in H_2O_2 solution).Reprinted with permission[225] © 2013, American Chemical Society.

3.1.8 *Other miscellaneous applications*

The scope of applications of self-assembled nanoparticle structures is widening. New fields of application are rapidly emerging in different disciplines. In this section, some of these other applications

of self-assembled structures are briefly highlighted. One specific class of nanostructures whose fabrication is particularly compatible with self-assembly techniques is that of photonic crystals, which are an interesting class of material for the manipulation of light at the nanoscale. In fact, three dimensional photonic crystals in most cases cannot be fabricated by thin film techniques.[228] In the particular case of soft matter based photonic applications, self-assembly is extremely useful.[229] Photonic crystals as antireflective or antiglare coating and their application for the light management in photovoltaic systems has already been discussed.[230] [231] [232] However, other applications of metal or dielectric photonic crystals also include all-optical switching, optoelectronics, energy-harvesting, and even the future generation of electro-optical devices, such as lab-on-a-chip with all-integrated optical spectroscopy techniques.[233] [234] The slow light effect in photonic-crystals is especially attractive for on-chip integration and room temperature operation, and can offer wide-bandwidth and dispersion-free propagation.[235] Due to the enhanced color phenomena of self-assembled plasmonic nanostructures or their hybrids, emerging color based applications such as full-spectrum displays, active coatings, and rewritable papers are also being extensively investigated.[236] Alike MOFs, self-assembled films of other inherently porous materials like COFs (covalent organic framework) can be interesting for different applications. Self-assembled films of COFs nanoparticles have been shown to have excellent nanomechanical properties[237]. Such films are generally useful for applications requiring porous thin films or membranes. Due to high surface area and dense surface coverage, self-assembled films or structures can be also be promising as antimicrobial interfaces.[238] Self-assembly is also particularly interesting for the synthesis of chiral plasmonic structures with colloidal nanoparticles.[239] Obviously, the possibilities for the application of self-assembly and self-assembled nanoparticle structures are countless. New reports demonstrating novel innovative applications are therefore being published in great numbers.

4. Challenges and future outlook

As the colloidal synthesis techniques of functional nanostructures are advancing at a fast pace, the systematic organization of these nanostructures for their optimal activity is also becoming equally important. Thus, in the last decades, self-assembly of nanostructures has been developing as an independent sub-field of colloidal synthesis methods. However, many challenges still remain to be solved for self-assembly to be a mature nanofabrication technology. The primary challenge is posed by the surface chemistry of the nanostructures. The wet chemical methods for colloidal nanostructure synthesis usually involve intricate chemistry of organic and inorganic reagents for shape and size control, and stabilization in the following chemical/physical processes. Colloidal nanostructures are often stabilized by organic ligands, surfactants, polymers, *etc*., that determine the surface chemistry. As most self-assembly techniques involve surface functionalization for hydrophobization, surface-charge/pH control, further reactions, and so on, the surface molecules carried over from the wet-chemical synthesis should facilitate the chemistry. For example, citrate capped Au nanoparticles can be easily replaced by thiol ligands. However, these thiol ligands once grafted onto the nanoparticle surface cannot be replaced by an amine ligand. For a certain material, it is not possible to define a fixed chemistry as different shapes and sizes of nanoparticles require different surface molecules in the synthesis process. The invention of compatible chemistry for different surface functionalization of different nanostructures synthesized via different routes remains the biggest challenge in the self-assembly techniques. This challenge is further compounded for hybrid nanostructures such as Janus structures, core-shell structures and so on. On this front, significant attention has been given to click-chemistry driven processes as a versatile route for joining nanoparticles with desired functionalizing molecules/groups. On a final note, self-assembly is a powerful technique complementary to wet-chemical synthesis techniques towards functional interfaces. With the desired progress in this field, one can foresee a new paradigm in nanofabrication techniques which will enable tailor-made nanostructures to be used as building blocks of large-scale functional interfaces as well as bulk phases.

Acknowledgment

R.B. acknowledges financial support from the University of Antwerp Special Research Fund (BOF) for a DOCPRO4 doctoral scholarship.

References

[1] L. R. Harriott, *Proceedings of the IEEE* **2001**, *89*, 366.
[2] J. T. Fourkas, J. Gao, Z. Han, H. Liu, B. Marmiroli, M. J. Naughton, J. S. Petersen, Y. Sun, A. Vagilio Pret, Y. Zheng, *Frontiers in Nanotechnology* **2021**, *3*.
[3] T. Siegfried, Y. Ekinci, O. J. F. Martin, H. Sigg, *ACS Nano* **2013**, *7*, 2751.
[4] P. R. Sajanlal, T. S. Sreeprasad, A. K. Samal, T. Pradeep, *Nano Reviews* **2011**, *2*, 5883.
[5] N. Baig, I. Kammakakam, W. Falath, *Materials Advances* **2021**, *2*, 1821.
[6] M. A. Boles, M. Engel, D. V. Talapin, *Chem. Rev.* **2016**, *116*, 11220.
[7] A. Rao, S. Roy, V. Jain, P. P. Pillai, *ACS Appl. Mater. Interfaces* **2022**.
[8] S. Li, X. Guo, M. Sun, A. Qu, C. Hao, X. Wu, J. Guo, C. Xu, H. Kuang, L. Xu, *Nanoscale* **2021**, *13*, 2302.
[9] E. Piccinini, D. Pallarola, F. Battaglini, O. Azzaroni, *Mol. Syst. Des. Eng.* **2016**, *1*, 155.
[10] Z. Nie, A. Petukhova, E. Kumacheva, *Nature Nanotech* **2010**, *5*, 15.
[11] R. Borah, S. W. Verbruggen, *J. Phys. Chem. C* **2019**, *123*, 30594.
[12] Y. A. D. Fernandez, T. A. Gschneidtner, C. Wadell, L. H. Fornander, S. L. Avila, C. Langhammer, F. Westerlund, K. Moth-Poulsen, *Nanoscale* **2014**, *6*, 14605.
[13] D. F. Swearer, H. Zhao, L. Zhou, C. Zhang, H. Robatjazi, J. M. P. Martirez, C. M. Krauter, S. Yazdi, M. J. McClain, E. Ringe, E. A. Carter, P. Nordlander, N. J. Halas, *PNAS* **2016**, *113*, 8916.
[14] S. Shrestha, B. Wang, P. Dutta, *Advances in Colloid and Interface Science* **2020**, *279*, 102162.
[15] T. Missana, A. Adell, *Journal of Colloid and Interface Science* **2000**, *230*, 150.
[16] E. M. Hotze, T. Phenrat, G. V. Lowry, *Journal of Environmental Quality* **2010**, *39*, 1909.
[17] N. Carl, S. Prévost, J. P. S. Fitzgerald, M. Karg, *Phys. Chem. Chem. Phys.* **2017**, *19*, 16348.
[18] V. N. Kuzovkov, E. A. Kotomin, *Phys. Chem. Chem. Phys.* **2014**, *16*, 25449.
[19] M. Yang, G. Chen, Y. Zhao, G. Silber, Y. Wang, S. Xing, Y. Han, H. Chen, *Phys. Chem. Chem. Phys.* **2010**, *12*, 11850.
[20] D. Hu, K. Ogawa, M. Kajiyama, T. Enomae, *Royal Society Open Science 7*, 200296.
[21] W. Wei, F. Bai, H. Fan, *iScience* **2019**, *11*, 272.
[22] J. Schmitt, S. Hajiw, A. Lecchi, J. Degrouard, A. Salonen, M. Impéror-Clerc, B. Pansu, *J. Phys. Chem. B* **2016**, *120*, 5759.
[23] L. Leclercq, A. Mouret, S. Renaudineau, V. Schmitt, A. Proust, V. Nardello-Rataj, *J. Phys. Chem. B* **2015**, *119*, 6326.
[24] J. Wang, C. F. Mbah, T. Przybilla, B. Apeleo Zubiri, E. Spiecker, M. Engel, N. Vogel, *Nat Commun* **2018**, *9*, 5259.
[25] B. de Nijs, S. Dussi, F. Smallenburg, J. D. Meeldijk, D. J. Groenendijk, L. Filion, A. Imhof, A. van Blaaderen, M. Dijkstra, *Nature Mater* **2015**, *14*, 56.
[26] J. Park, D. R. Hickey, S. Jun, S. Kang, X. Hu, X.-J. Chen, S.-J. Park, *Advanced Functional Materials* **2016**, *26*, 7791.
[27] E. Glogowski, R. Tangirala, J. He, T. P. Russell, T. Emrick, *Nano Lett.* **2007**, *7*, 389.
[28] Y. Lin, H. Skaff, T. Emrick, A. D. Dinsmore, T. P. Russell, *Science* **2003**, *299*, 226.
[29] M. E. Leunissen, A. van Blaaderen, A. D. Hollingsworth, M. T. Sullivan, P. M. Chaikin, *PNAS* **2007**, *104*, 2585.
[30] S. Jiang, S. Granick, *Langmuir* **2008**, *24*, 2438.
[31] Y.-S. Cho, S.-H. Kim, G.-R. Yi, S.-M. Yang, *Colloids and Surfaces A: Physicochemical and Engineering Aspects* **2009**, *345*, 237.
[32] P. Qiu, C. Jensen, N. Charity, R. Towner, C. Mao, *J. Am. Chem. Soc.* **2010**, *132*, 17724.

[33] C. S. Wagner, A. Fortini, E. Hofmann, T. Lunkenbein, M. Schmidt, A. Wittemann, *Soft Matter* **2012**, *8*, 1928.
[34] D. Liu, F. Zhou, C. Li, T. Zhang, H. Zhang, W. Cai, Y. Li, *Angewandte Chemie International Edition* **2015**, *54*, 9596.
[35] R. Koike, Y. Iwashita, Y. Kimura, *Langmuir* **2018**, *34*, 12394.
[36] D. Wang, T. Dasgupta, E. B. van der Wee, D. Zanaga, T. Altantzis, Y. Wu, G. M. Coli, C. B. Murray, S. Bals, M. Dijkstra, A. van Blaaderen, *Nat. Phys.* **2021**, *17*, 128.
[37] H. Puliyalil, U. Cvelbar, *Nanomaterials* **2016**, *6*, 108.
[38] P. Mohapatra, S. Shaw, D. Mendivelso-Perez, J. M. Bobbitt, T. F. Silva, F. Naab, B. Yuan, X. Tian, E. A. Smith, L. Cademartiri, *Nat Commun* **2017**, *8*, 1.
[39] S. Shaw, X. Tian, T. F. Silva, J. M. Bobbitt, F. Naab, C. L. Rodrigues, E. A. Smith, L. Cademartiri, *Chemistry of Materials* **2018**.
[40] L. Lu, B. Lou, S. Zou, H. Kobayashi, J. Liu, L. Xiao, J. Fan, *ACS Catal.* **2018**, *8*, 8484.
[41] R. Borah, R. Ninakanti, G. Nuyts, H. Peeters, A. Pedrazo-Tardajos, S. Nuti, C. V. Velde, K. D. Wael, S. Lenaerts, S. Bals, S. W. Verbruggen, *Chemistry – A European Journal* **2021**, *27*, 9011.
[42] S. Singamaneni, V. N. Bliznyuk, C. Binek, E. Y. Tsymbal, *J. Mater. Chem.* **2011**, *21*, 16819.
[43] G. Singh, H. Chan, A. Baskin, E. Gelman, N. Repnin, P. Král, R. Klajn, *Science* **2014**, *345*, 1149.
[44] S. M. Taheri, M. Michaelis, T. Friedrich, B. Förster, M. Drechsler, F. M. Römer, P. Bösecke, T. Narayanan, B. Weber, I. Rehberg, S. Rosenfeldt, S. Förster, *PNAS* **2015**, *112*, 14484.
[45] W. H. Chong, L. K. Chin, R. L. S. Tan, H. Wang, A. Q. Liu, H. Chen, *Angewandte Chemie International Edition* **2013**, *52*, 8570.
[46] L. Ye, T. Pearson, Y. Cordeau, O. T. Mefford, T. M. Crawford, *Sci Rep* **2016**, *6*, 23145.
[47] A. F. Demirörs, P. P. Pillai, B. Kowalczyk, B. A. Grzybowski, *Nature* **2013**, *503*, 99.
[48] R. M. Erb, H. S. Son, B. Samanta, V. M. Rotello, B. B. Yellen, *Nature* **2009**, *457*, 999.
[49] J. A. Johnson, A. Dehankar, A. Robbins, P. Kabtiyal, E. Jergens, K. Ho Lee, E. Johnston-Halperin, M. Poirier, C. E. Castro, J. O. Winter, *Materials Science and Engineering: R: Reports* **2019**, *138*, 153.
[50] N. C. Seeman, *Journal of Theoretical Biology* **1982**, *99*, 237.
[51] H. Yan, S. H. Park, G. Finkelstein, J. H. Reif, T. H. LaBean, *Science* **2003**.
[52] W. B. Rogers, W. M. Shih, V. N. Manoharan, *Nat Rev Mater* **2016**, *1*, 1.
[53] J. J. Storhoff, R. Elghanian, C. A. Mirkin, R. L. Letsinger, *Langmuir* **2002**, *18*, 6666.
[54] C. A. Mirkin, R. L. Letsinger, R. C. Mucic, J. J. Storhoff, *Nature* **1996**, *382*, 607.
[55] H. Yao, C. Yi, C.-H. Tzang, J. Zhu, M. Yang, *Nanotechnology* **2006**, *18*, 015102.
[56] A. Kuzyk, R. Schreiber, Z. Fan, G. Pardatscher, E.-M. Roller, A. Högele, F. C. Simmel, A. O. Govorov, T. Liedl, *Nature* **2012**, *483*, 311.
[57] J. Sharma, R. Chhabra, A. Cheng, J. Brownell, Y. Liu, H. Yan, *Science* **2009**, *323*, 112.
[58] P. Wang, S. Gaitanaros, S. Lee, M. Bathe, W. M. Shih, Y. Ke, *J. Am. Chem. Soc.* **2016**, *138*, 7733.
[59] P. Wang, J.-H. Huh, H. Park, D. Yang, Y. Zhang, Y. Zhang, J. Lee, S. Lee, Y. Ke, *Nano Lett.* **2020**, *20*, 8926.
[60] J. S. Kahn, O. Gang, *Angewandte Chemie International Edition* **2022**, *61*, e202105678.
[61] M. Xie, Y. Hu, J. Yin, Z. Zhao, J. Chen, J. Chao, *Research* **2022**, *2022*.
[62] A. Peil, L. Xin, S. Both, L. Shen, Y. Ke, T. Weiss, P. Zhan, N. Liu, *ACS Nano* **2022**, *16*, 5284.
[63] J. Kim, S. Lee, J. Choi, K. Baek, T. S. Shim, J. K. Hyun, S.-J. Park, *Advanced Materials* **2022**, *34*, 2109091.
[64] E. Auyeung, W. Morris, J. E. Mondloch, J. T. Hupp, O. K. Farha, C. A. Mirkin, *J. Am. Chem. Soc.* **2015**, *137*, 1658.

[65] Y. Liu, L. Ma, S. Jiang, C. Han, P. Tang, H. Yang, X. Duan, N. Liu, H. Yan, X. Lan, *ACS Nano* **2021**, *15*, 16664.
[66] R. A. Hughes, E. Menumerov, S. Neretina, *Nanotechnology* **2017**, *28*, 282002.
[67] C. Hanske, G. González-Rubio, C. Hamon, P. Formentín, E. Modin, A. Chuvilin, A. Guerrero-Martínez, L. F. Marsal, L. M. Liz-Marzán, *J. Phys. Chem. C* **2017**, *121*, 10899.
[68] C. Matricardi, C. Hanske, J. L. Garcia-Pomar, J. Langer, A. Mihi, L. M. Liz-Marzán, *ACS Nano* **2018**, *12*, 8531.
[69] V. Flauraud, M. Mastrangeli, G. D. Bernasconi, J. Butet, D. T. L. Alexander, E. Shahrabi, O. J. F. Martin, J. Brugger, *Nature Nanotech* **2017**, *12*, 73.
[70] C. Hanske, E. H. Hill, D. Vila-Liarte, G. González-Rubio, C. Matricardi, A. Mihi, L. M. Liz-Marzán, *ACS Appl. Mater. Interfaces* **2019**, *11*, 11763.
[71] D. Xia, D. Li, Y. Luo, S. R. J. Brueck, *Advanced Materials* **2006**, *18*, 930.
[72] X. Zeng, Y. Nyquist, Q. Zhang, H.-J. Butt, S. Wu, *Supramolecular Materials* **2022**, *1*, 100004.
[73] S. Das, P. Ranjan, P. S. Maiti, G. Singh, G. Leitus, R. Klajn, *Advanced Materials* **2013**, *25*, 422.
[74] P. K. Kundu, D. Samanta, R. Leizrowice, B. Margulis, H. Zhao, M. Börner, T. Udayabhaskararao, D. Manna, R. Klajn, *Nature Chem* **2015**, *7*, 646.
[75] H. He, J.-E. Ostwaldt, C. Hirschhäuser, C. Schmuck, J. Niemeyer, *Small* **2020**, *16*, 2001044.
[76] J. Vialetto, M. Anyfantakis, S. Rudiuk, M. Morel, D. Baigl, *Angewandte Chemie International Edition* **2019**, *58*, 9145.
[77] E. Jaquay, L. J. Martínez, C. A. Mejia, M. L. Povinelli, *Nano Lett.* **2013**, *13*, 2290.
[78] C. A. Mejia, A. Dutt, M. L. Povinelli, *Opt. Express, OE* **2011**, *19*, 11422.
[79] C. M. Jin, W. Lee, D. Kim, T. Kang, I. Choi, *Small* **2018**, *14*, 1803055.
[80] H. Han, J. Y. Lee, X. Lu, *Chem. Commun.* **2013**, *49*, 6122.
[81] K. B. Blodgett, *J. Am. Chem. Soc.* **1935**, *57*, 1007.
[82] S. A. Hussain, B. Dey, D. Bhattacharjee, N. Mehta, *Heliyon* **2018**, *4*, e01038.
[83] A. Tao, P. Sinsermsuksakul, P. Yang, *Nature Nanotech* **2007**, *2*, 435.
[84] X. Ye, J. Chen, M. Engel, J. A. Millan, W. Li, L. Qi, G. Xing, J. E. Collins, C. R. Kagan, J. Li, S. C. Glotzer, C. B. Murray, *Nature Chem* **2013**, *5*, 466.
[85] A. Dong, J. Chen, P. M. Vora, J. M. Kikkawa, C. B. Murray, *Nature* **2010**, *466*, 474.
[86] M. Cargnello, A. C. Johnston-Peck, B. T. Diroll, E. Wong, B. Datta, D. Damodhar, V. V. T. Doan-Nguyen, A. A. Herzing, C. R. Kagan, C. B. Murray, *Nature* **2015**, *524*, 450.
[87] N. S. Mueller, Y. Okamura, B. G. M. Vieira, S. Juergensen, H. Lange, E. B. Barros, F. Schulz, S. Reich, *Nature* **2020**, *583*, 780.
[88] Y. Liu, K. Deng, J. Yang, X. Wu, X. Fan, M. Tang, Z. Quan, *Chem. Sci.* **2020**, *11*, 4065.
[89] S. D. Griesemer, S. S. You, P. Kanjanaboos, M. Calabro, H. M. Jaeger, S. A. Rice, B. Lin, *Soft Matter* **2017**, *13*, 3125.
[90] H.-L. Nie, X. Dou, Z. Tang, H. D. Jang, J. Huang, *J. Am. Chem. Soc.* **2015**, *137*, 10683.
[91] A. Morag, L. Philosof-Mazor, R. Volinsky, E. Mentovich, S. Richter, R. Jelinek, *Advanced Materials* **2011**, *23*, 4327.
[92] F. Dumur, S. Reculusa, M. Mruczkiewicz, M. Perrin, L. Vignau, S. Fasquel, *Opt. Express, OE* **2016**, *24*, 27184.
[93] F. Schulz, O. Pavelka, F. Lehmkühler, F. Westermeier, Y. Okamura, N. S. Mueller, S. Reich, H. Lange, *Nat Commun* **2020**, *11*, 3821.
[94] F. Kim, S. Kwan, J. Akana, P. Yang, *J. Am. Chem. Soc.* **2001**, *123*, 4360.
[95] H. Song, F. Kim, S. Connor, G. A. Somorjai, P. Yang, *J. Phys. Chem. B* **2005**, *109*, 188.
[96] M. N. Martin, J. I. Basham, P. Chando, S.-K. Eah, *Langmuir* **2010**, *26*, 7410.
[97] G. D. Moon, T. I. Lee, B. Kim, G. Chae, J. Kim, S. Kim, J.-M. Myoung, U. Jeong, *ACS Nano* **2011**, *5*, 8600.

[98] S. Xiong, D. R. Dunphy, D. C. Wilkinson, Z. Jiang, J. Strzalka, J. Wang, Y. Su, J. J. de Pablo, C. J. Brinker, *Nano Lett.* **2013**, *13*, 1041.
[99] D. YOGEV, S. EFRIMA, *J. phys. chem. (1952)* **1988**, *92*, 5754.
[100] Y.-J. Li, W.-J. Huang, S.-G. Sun, *Angewandte Chemie International Edition* **2006**, *45*, 2537.
[101] L. Isa, F. Lucas, R. Wepf, E. Reimhult, *Nat Commun* **2011**, *2*, 438.
[102] F. Reincke, S. G. Hickey, W. K. Kegel, D. Vanmaekelbergh, *Angewandte Chemie* **2004**, *116*, 464.
[103] F. Reincke, W. K. Kegel, H. Zhang, M. Nolte, D. Wang, D. Vanmaekelbergh, H. Möhwald, *Phys. Chem. Chem. Phys.* **2006**, *8*, 3828.
[104] Y.-K. Park, S.-H. Yoo, S. Park, *Langmuir* **2007**, *23*, 10505.
[105] M. Mao, B. Zhou, X. Tang, C. Chen, M. Ge, P. Li, X. Huang, L. Yang, J. Liu, *Chemistry – A European Journal* **2018**, *24*, 4094.
[106] B. Jia, Q. Wang, W. Zhang, B. Lin, N. Yuan, J. Ding, Y. Ren, F. Chu, *RSC Adv.* **2014**, *4*, 34566.
[107] E. Smirnov, P. Peljo, M. D. Scanlon, H. H. Girault, *ACS Nano* **2015**, *9*, 6565.
[108] P.-P. Fang, S. Chen, H. Deng, M. D. Scanlon, F. Gumy, H. J. Lee, D. Momotenko, V. Amstutz, F. Cortés-Salazar, C. M. Pereira, Z. Yang, H. H. Girault, *ACS Nano* **2013**, *7*, 9241.
[109] Y. Ren, M. Chen, L. Hu, X. Fang, L. Wu, *J. Mater. Chem.* **2011**, *22*, 944.
[110] L. Velleman, D. Sikdar, V. A. Turek, A. R. Kucernak, S. J. Roser, A. A. Kornyshev, J. B. Edel, *Nanoscale* **2016**, *8*, 19229.
[111] Y. Chai, A. Lukito, Y. Jiang, P. D. Ashby, T. P. Russell, *Nano Lett.* **2017**, *17*, 6453.
[112] H. B. Sebastian, R. M. Mayall, V. I. Birss, S. Bryant, *Langmuir* **2017**, *33*, 10125.
[113] R. G. Larson, *Nature* **2017**, *550*, 466.
[114] R. D. Deegan, O. Bakajin, T. F. Dupont, G. Huber, S. R. Nagel, T. A. Witten, *Nature* **1997**, *389*, 827.
[115] Y. Xie, S. Guo, C. Guo, M. He, D. Chen, Y. Ji, Z. Chen, X. Wu, Q. Liu, S. Xie, *Langmuir* **2013**, *29*, 6232.
[116] D. Mampallil, H. B. Eral, *Advances in Colloid and Interface Science* **2018**, *252*, 38.
[117] E. He, D. Guo, Z. Li, *Advanced Materials Interfaces* **2019**, *6*, 1900446.
[118] T. P. Bigioni, X.-M. Lin, T. T. Nguyen, E. I. Corwin, T. A. Witten, H. M. Jaeger, *Nature Mater* **2006**, *5*, 265.
[119] K. N. Al-Milaji, R. R. Secondo, T. N. Ng, N. Kinsey, H. Zhao, *Advanced Materials Interfaces* **2018**, *5*, 1701561.
[120] S. Watanabe, M. T. Miyahara, *Advanced Powder Technology* **2013**, *24*, 897.
[121] S. Watanabe, K. Inukai, S. Mizuta, M. T. Miyahara, *Langmuir* **2009**, *25*, 7287.
[122] S. Watanabe, Y. Mino, Y. Ichikawa, M. T. Miyahara, *Langmuir* **2012**, *28*, 12982.
[123] E. V. Shevchenko, D. V. Talapin, C. B. Murray, S. O'Brien, *J. Am. Chem. Soc.* **2006**, *128*, 3620.
[124] N. Arai, S. Watanabe, M. T. Miyahara, *Langmuir* **2019**, *35*, 11533.
[125] C. Xing, D. Liu, J. Chen, Y. Fan, F. Zhou, K. Kaur, W. Cai, Y. Li, *Chem. Mater.* **2021**, *33*, 310.
[126] P. Jiang, J. F. Bertone, K. S. Hwang, V. L. Colvin, *Chem. Mater.* **1999**, *11*, 2132.
[127] J. Ku, D. M. Aruguete, A. P. Alivisatos, P. L. Geissler, *J. Am. Chem. Soc.* **2011**, *133*, 838.
[128] M. Mueller, M. Tebbe, D. V. Andreeva, M. Karg, R. A. Alvarez Puebla, N. Pazos Perez, A. Fery, *Langmuir* **2012**, *28*, 9168.
[129] P. Li, Y. Li, Z.-K. Zhou, S. Tang, X.-F. Yu, S. Xiao, Z. Wu, Q. Xiao, Y. Zhao, H. Wang, P. K. Chu, *Advanced Materials* **2016**, *28*, 2511.
[130] Y. Li, Q. Yang, M. Li, Y. Song, *Sci Rep* **2016**, *6*, 24628.
[131] A. S. Dimitrov, K. Nagayama, *Langmuir* **1996**, *12*, 1303.
[132] D. Chowdhury, *Current Science* **2009**, *96*, 923.

[133] S. Liu, T. Zhu, R. Hu, Z. Liu, *Phys. Chem. Chem. Phys.* **2002**, *4*, 6059.
[134] F. L. Yap, P. Thoniyot, S. Krishnan, S. Krishnamoorthy, *ACS Nano* **2012**, *6*, 2056.
[135] X. Ling, X. Zhu, J. Zhang, T. Zhu, M. Liu, L. Tong, Z. Liu, *J. Phys. Chem. B* **2005**, *109*, 2657.
[136] S. Liu, R. Maoz, J. Sagiv, *Nano Lett.* **2004**, *4*, 845.
[137] S. Hoeppener, R. Maoz, S. r. Cohen, L. f. Chi, H. Fuchs, J. Sagiv, *Advanced Materials* **2002**, *14*, 1036.
[138] Y. K. Ryu, A. W. Knoll, In *Electrical Atomic Force Microscopy for Nanoelectronics* (Ed.: Celano, U.), Springer International Publishing, Cham, **2019**, pp. 143–172.
[139] R. Borah, S. W. Verbruggen, *J. Phys. Chem. C* **2020**, *124*, 12081.
[140] L. Zhu, M. Gao, C. K. N. Peh, G. W. Ho, *Mater. Horiz.* **2018**, *5*, 323.
[141] J. Liang, H. Liu, J. Yu, L. Zhou, J. Zhu, *Nanophotonics* **2019**, *8*, 771.
[142] S. Luo, X. Ren, H. Lin, H. Song, J. Ye, *Chemical Science* **2021**, *12*, 5701.
[143] J. E. Lemaster, J. V. Jokerst, *WIREs Nanomedicine and Nanobiotechnology* **2017**, *9*, e1404.
[144] M. Kim, J.-H. Lee, J.-M. Nam, *Advanced Science* **2019**, *6*, 1900471.
[145] C. Kuttner, *Plasmonics in Sensing: From Colorimetry to SERS Analytics*, IntechOpen, **2018**.
[146] B. Ciraulo, J. Garcia-Guirado, I. de Miguel, J. Ortega Arroyo, R. Quidant, *Nat Commun* **2021**, *12*, 2001.
[147] H. Tan, H. Hu, L. Huang, K. Qian, *Analyst* **2020**, *145*, 5699.
[148] Y. Yang, X. Yang, L. Fu, M. Zou, A. Cao, Y. Du, Q. Yuan, C.-H. Yan, *ACS Energy Lett.* **2018**, *3*, 1165.
[149] L. Zhou, Y. Tan, J. Wang, W. Xu, Y. Yuan, W. Cai, S. Zhu, J. Zhu, *Nature Photon* **2016**, *10*, 393.
[150] M. Dhiman, A. Maity, A. Das, R. Belgamwar, B. Chalke, Y. Lee, K. Sim, J.-M. Nam, V. Polshettiwar, *Chem. Sci.* **2019**, *10*, 6594.
[151] Y. Mantri, J. V. Jokerst, *ACS Nano* **2020**, *14*, 9408.
[152] R. Zhu, L. Su, J. Dai, Z.-W. Li, S. Bai, Q. Li, X. Chen, J. Song, H. Yang, *ACS Nano* **2020**, *14*, 3991.
[153] C. L. Bayer, S. Y. Nam, Y.-S. Chen, S. Y. Emelianov, *JBO* **2013**, *18*, 016001.
[154] Y. Liu, J. He, K. Yang, C. Yi, Y. Liu, L. Nie, N. M. Khashab, X. Chen, Z. Nie, *Angewandte Chemie International Edition* **2015**, *54*, 15809.
[155] S. J. Yoon, S. Mallidi, J. M. Tam, J. O. Tam, A. Murthy, K. P. Johnston, K. V. Sokolov, S. Y. Emelianov, *Opt. Lett., OL* **2010**, *35*, 3751.
[156] S. Han, R. Bouchard, K. V. Sokolov, *Biomed. Opt. Express, BOE* **2019**, *10*, 3472.
[157] L. Song, N. Qiu, Y. Huang, Q. Cheng, Y. Yang, H. Lin, F. Su, T. Chen, *Advanced Optical Materials* **2020**, *8*, 1902082.
[158] Y. Sun, B. Xu, Q. Shen, L. Hang, D. Men, T. Zhang, H. Li, C. Li, Y. Li, *ACS Appl. Mater. Interfaces* **2017**, *9*, 31897.
[159] A. D. Utyushev, V. I. Zakomirnyi, I. L. Rasskazov, *Reviews in Physics* **2021**, *6*, 100051.
[160] S. Deng, B. Zhang, P. Choo, P. J. M. Smeets, T. W. Odom, *Nano Lett.* **2021**, *21*, 1523.
[161] D. Kim, J. Resasco, Y. Yu, A. M. Asiri, P. Yang, *Nat Commun* **2014**, *5*, 4948.
[162] M. Wu, J. Jin, J. Liu, Z. Deng, Y. Li, O. Deparis, B.-L. Su, *J. Mater. Chem. A* **2013**, *1*, 15491.
[163] J. Liu, H. Zhao, M. Wu, B. Van der Schueren, Y. Li, O. Deparis, J. Ye, G. A. Ozin, T. Hasan, B.-L. Su, *Advanced Materials* **2017**, *29*, 1605349.
[164] R. Shi, Y. Cao, Y. Bao, Y. Zhao, G. I. N. Waterhouse, Z. Fang, L.-Z. Wu, C.-H. Tung, Y. Yin, T. Zhang, *Advanced Materials* **2017**, *29*, 1700803.
[165] K. Zhu, D. Wang, J. Liu, *Nano Res.* **2009**, *2*, 1.
[166] F. Zhang, R. Liu, Y. Wei, J. Wei, Z. Yang, *J. Am. Chem. Soc.* **2021**, *143*, 11662.

[167] Z. Wang, A. VahidMohammadi, L. Ouyang, J. Erlandsson, C.-W. Tai, L. Wågberg, M. M. Hamedi, *Small* **2021**, *17*, 2006434.
[168] K.-P. Lee, A. I. Gopalan, P. Santhosh, K. M. Manesh, J. H. Kim, K. S. Kim, *Journal of Nanoscience and Nanotechnology* **2006**, *6*, 1575.
[169] Y.-C. Lin, S. Liao, T. Huang, G.-J. Wang, *J. Electrochem. Soc.* **2019**, *166*, B349.
[170] N. Mohamad Nor, S. Arivalakan, N. D. Zakaria, N. Nilamani, Z. Lockman, K. Abdul Razak, *ACS Omega* **2022**, *7*, 3823.
[171] S. Rej, L. Mascaretti, E. Y. Santiago, O. Tomanec, Š. Kment, Z. Wang, R. Zbořil, P. Fornasiero, A. O. Govorov, A. Naldoni, *ACS Catal.* **2020**, *10*, 5261.
[172] S. Lee, H. Hwang, W. Lee, D. Schebarchov, Y. Wy, J. Grand, B. Auguié, D. H. Wi, E. Cortés, S. W. Han, *ACS Energy Lett.* **2020**, *5*, 3881.
[173] W. Wang, L. Qi, *Advanced Functional Materials* **2019**, *29*, 1807275.
[174] H. Shimomura, Z. Gemici, R. E. Cohen, M. F. Rubner, *ACS Appl. Mater. Interfaces* **2010**, *2*, 813.
[175] N. Shanmugam, R. Pugazhendhi, R. Madurai Elavarasan, P. Kasiviswanathan, N. Das, *Energies* **2020**, *13*, 2631.
[176] C. K. Huang, H. H. Lin, J. Y. Chen, K. W. Sun, W.-L. Chang, *Solar Energy Materials and Solar Cells* **2011**, *95*, 2540.
[177] T.-H. Chang, P.-H. Wu, S.-H. Chen, C.-H. Chan, C.-C. Lee, C.-C. Chen, Y.-K. Su, *Opt. Express, OE* **2009**, *17*, 6519.
[178] J. E. Allen, B. Ray, M. R. Khan, K. G. Yager, M. A. Alam, C. T. Black, *Appl. Phys. Lett.* **2012**, *101*, 063105.
[179] S. Guldin, S. Hüttner, M. Kolle, M. E. Welland, P. Müller-Buschbaum, R. H. Friend, U. Steiner, N. Tétreault, *Nano Lett.* **2010**, *10*, 2303.
[180] X. Chen, J. Ye, S. Ouyang, T. Kako, Z. Li, Z. Zou, *ACS Nano* **2011**, *5*, 4310.
[181] K. A. Arpin, M. D. Losego, A. N. Cloud, H. Ning, J. Mallek, N. P. Sergeant, L. Zhu, Z. Yu, B. Kalanyan, G. N. Parsons, G. S. Girolami, J. R. Abelson, S. Fan, P. V. Braun, *Nat Commun* **2013**, *4*, 2630.
[182] Y. H. Jang, Y. J. Jang, S. Kim, L. N. Quan, K. Chung, D. H. Kim, *Chem. Rev.* **2016**, *116*, 14982.
[183] A. Yadav, B. Gerislioglu, A. Ahmadivand, A. Kaushik, G. J. Cheng, Z. Ouyang, Q. Wang, V. S. Yadav, Y. K. Mishra, Y. Wu, Y. Liu, S. RamaKrishna, *Nano Today* **2021**, *37*, 101072.
[184] P. Reineck, G. P. Lee, D. Brick, M. Karg, P. Mulvaney, U. Bach, *Advanced Materials* **2012**, *24*, 4750.
[185] Y.-F. Sun, S.-B. Liu, F.-L. Meng, J.-Y. Liu, Z. Jin, L.-T. Kong, J.-H. Liu, *Sensors (Basel)* **2012**, *12*, 2610.
[186] J. Miao, C. Chen, L. Meng, Y. S. Lin, *ACS Sens.* **2019**, *4*, 1279.
[187] P. Chen, J. Hu, M. Yin, W. Bai, X. Chen, Y. Zhang, *ACS Appl. Nano Mater.* **2021**, *4*, 5981.
[188] K. Suematsu, Y. Shin, Z. Hua, K. Yoshida, M. Yuasa, T. Kida, K. Shimanoe, *ACS Appl. Mater. Interfaces* **2014**, *6*, 5319.
[189] Y. Shin, J. Song, D. Kim, T. Kang, *Advanced Materials* **2015**, *27*, 4344.
[190] C. Wang, M. M. Meloni, X. Wu, M. Zhuo, T. He, J. Wang, C. Wang, P. Dong, *AIP Advances* **2019**, *9*, 010701.
[191] R. Liu, S. Li, J.-F. Liu, *TrAC Trends in Analytical Chemistry* **2017**, *97*, 188.
[192] X. Qiao, B. Su, C. Liu, Q. Song, D. Luo, G. Mo, T. Wang, *Advanced Materials* **2018**, *30*, 1702275.
[193] A. Li, X. Qiao, K. Liu, W. Bai, T. Wang, *Advanced Functional Materials n/a*, 2202805.
[194] P. Fuchs, C. Loeseken, J. K. Schubert, W. Miekisch, *International Journal of Cancer* **2010**, *126*, 2663.

[195] R. Borah, J. Smets, R. Ninakanti, M. L. Tietze, R. Ameloot, D. N. Chigrin, S. Bals, S. Lenaerts, S. W. Verbruggen, *ACS Appl. Nano Mater.* **2022**, *5*, 11494.
[196] R. Borah, R. Ninakanti, S. Bals, S. W. Verbruggen, *Sci Rep* **2022**, *12*, 15738.
[197] X. Qiao, B. Su, C. Liu, Q. Song, D. Luo, G. Mo, T. Wang, *Advanced Materials* **2018**, *30*, 1702275.
[198] A. Li, X. Qiao, K. Liu, W. Bai, T. Wang, *Advanced Functional Materials n/a*, 2202805.
[199] F. Yang, Q.-K. Liu, J.-P. Ma, Y.-A. Li, K.-X. Wang, Y.-B. Dong, *CrystEngComm* **2015**, *17*, 4102.
[200] X. Chen, Y. Leng, L. Hao, H. Duan, J. Yuan, W. Zhang, X. Huang, Y. Xiong, *Theranostics* **2020**, *10*, 3737.
[201] H.-K. Oh, K. Kim, J. Park, H. Im, S. Maher, M.-G. Kim, *Biosensors and Bioelectronics* **2022**, *205*, 114094.
[202] J. Hwang, D. Kwon, S. Lee, S. Jeon, *RSC Adv.* **2016**, *6*, 48445.
[203] Y. Li, X. Chen, J. Yuan, Y. Leng, W. Lai, X. Huang, Y. Xiong, *Journal of Dairy Science* **2020**, *103*, 6940.
[204] H. Rao, H. Ge, X. Wang, Z. Zhang, X. Liu, Y. Yang, Y. Liu, W. Liu, P. Zou, Y. Wang, *Microchim Acta* **2017**, *184*, 3017.
[205] R. Elghanian, J. J. Storhoff, R. C. Mucic, R. L. Letsinger, C. A. Mirkin, *Science* **1997**, *277*, 1078.
[206] P. Gaviña, M. Parra, S. Gil, A. M. Costero, *Red or Blue? Gold Nanoparticles in Colorimetric Sensing*, IntechOpen, **2018**.
[207] J. M. Perez, F. J. Simeone, Y. Saeki, L. Josephson, R. Weissleder, *J. Am. Chem. Soc.* **2003**, *125*, 10192.
[208] Y. Luo, C. Chi, M. Jiang, R. Li, S. Zu, Y. Li, Z. Fang, *Advanced Optical Materials* **2017**, *5*, 1700040.
[209] S. Yoo, Q.-H. Park, *Nanophotonics* **2019**, *8*, 249.
[210] N. John, A. T. Mariamma, *Microchim Acta* **2021**, *188*, 424.
[211] N. L. Rosi, C. A. Mirkin, *Chem. Rev.* **2005**, *105*, 1547.
[212] L. Zhang, J. M. Chan, F. X. Gu, J.-W. Rhee, A. Z. Wang, A. F. Radovic-Moreno, F. Alexis, R. Langer, O. C. Farokhzad, *ACS Nano* **2008**, *2*, 1696.
[213] R. Dahiya, S. Dahiya, In *Handbook on Nanobiomaterials for Therapeutics and Diagnostic Applications* (Eds.: Anand, K.; Saravanan, M.; Chandrasekaran, B.; Kanchi, S.; Jeeva Panchu, S.; Chen, Q.), Elsevier, **2021**, pp. 297–339.
[214] Y. Wang, O. Zeiri, M. Raula, B. Le Ouay, F. Stellacci, I. A. Weinstock, *Nature Nanotech* **2017**, *12*, 170.
[215] J. Song, J. Zhou, H. Duan, *J. Am. Chem. Soc.* **2012**, *134*, 13458.
[216] D. M. Vriezema, M. Comellas Aragonès, J. A. A. W. Elemans, J. J. L. M. Cornelissen, A. E. Rowan, R. J. M. Nolte, *Chem. Rev.* **2005**, *105*, 1445.
[217] T. Burdyny, J. Riordon, C.-T. Dinh, E. H. Sargent, D. Sinton, *Nanoscale* **2016**, *8*, 2107.
[218] M. Zhang, R. Ettelaie, L. Dong, X. Li, T. Li, X. Zhang, B. P. Binks, H. Yang, *Nat Commun* **2022**, *13*, 475.
[219] Z. Huang, J. T. Koubek, A. Sellinger, M. C. Beard, *ACS Appl. Nano Mater.* **2022**, *5*, 3183.
[220] C. Han, P. Meng, E. R. Waclawik, C. Zhang, X.-H. Li, H. Yang, M. Antonietti, J. Xu, *Angewandte Chemie International Edition* **2018**, *57*, 14857.
[221] F. Shukla, M. Das, S. Thakore, *Journal of Molecular Liquids* **2021**, *336*, 116217.
[222] A. Walther, A. H. E. Müller, *Chem. Rev.* **2013**, *113*, 5194.
[223] J. Cho, J. Cho, H. Kim, M. Lim, H. Jo, H. Kim, S.-J. Min, H. Rhee, J. W. Kim, *Green Chem.* **2018**, *20*, 2840.
[224] S. Yang, C. Cao, Y. Sun, P. Huang, F. Wei, W. Song, *Angewandte Chemie* **2015**, *127*, 2699.
[225] B. Dong, T. Zhou, H. Zhang, C. Y. Li, *ACS Nano* **2013**, *7*, 5192.

[226] I. Santiago, L. Jiang, J. Foord, A. J. Turberfield, *Chem. Commun.* **2018**, *54*, 1901.
[227] L. Hu, N. Wang, K. Tao, *Catalytic Micro/Nanomotors: Propulsion Mechanisms, Fabrication, Control, and Applications*, IntechOpen, **2020**.
[228] A.-P. Hynninen, J. H. J. Thijssen, E. C. M. Vermolen, M. Dijkstra, A. van Blaaderen, *Nature Mater* **2007**, *6*, 202.
[229] S. Cho, M. Takahashi, J. Fukuda, H. Yoshida, M. Ozaki, *Commun Mater* **2021**, *2*, 1.
[230] K. Katagiri, S. Yamazaki, K. Inumaru, K. Koumoto, *Polym J* **2015**, *47*, 190.
[231] S. E. Yancey, W. Zhong, J. R. Heflin, A. L. Ritter, *Journal of Applied Physics* **2006**, *99*, 034313.
[232] K. Askar, B. M. Phillips, X. Dou, J. Lopez, C. Smith, B. Jiang, P. Jiang, *Opt. Lett., OL* **2012**, *37*, 4380.
[233] Z. Cai, Z. Li, S. Ravaine, M. He, Y. Song, Y. Yin, H. Zheng, J. Teng, A. Zhang, *Chem. Soc. Rev.* **2021**, *50*, 5898.
[234] K. Zhong, L. Liu, X. Xu, M. Hillen, A. Yamada, X. Zhou, N. Verellen, K. Song, S. Van Cleuvenbergen, R. Vallée, K. Clays, *ACS Photonics* **2016**, *3*, 2330.
[235] T. Baba, *Nature Photon* **2008**, *2*, 465.
[236] V. T. Tran, J. Kim, S. Oh, K.-J. Jeong, J. Lee, *Small* **2022**, *18*, 2200317.
[237] K. Dey, S. Bhunia, H. S. Sasmal, C. M. Reddy, R. Banerjee, *J. Am. Chem. Soc.* **2021**, *143*, 955.
[238] A. M. Carmona-Ribeiro, *International Journal of Environmental Research and Public Health* **2018**, *15*, 1408.
[239] Q. Lei, R. Ni, Y. Ma, *ACS Nano* **2018**, *12*, 6860.